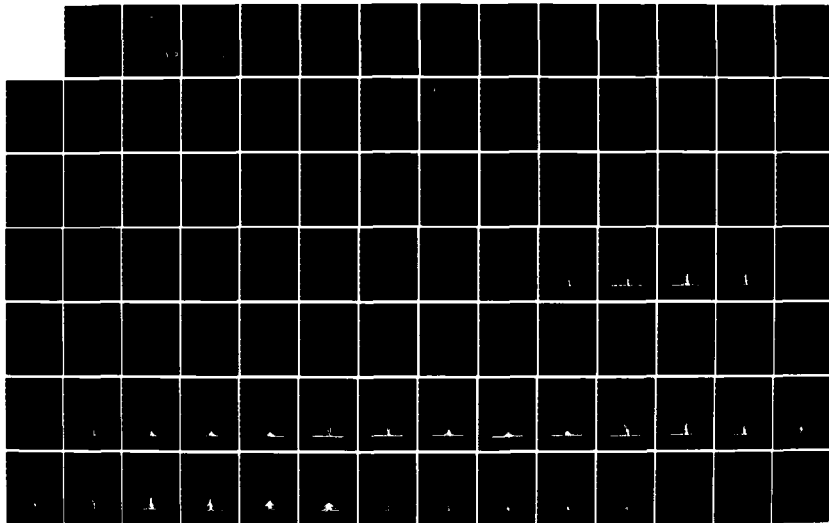
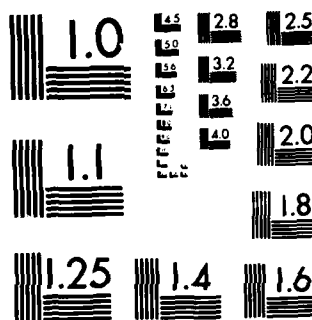


AD-A151 855 INFLUENCE OF SURFACE ROUGHNESS ON COMPRESSOR BLADES AT 1/2
HIGH REYNOLDS NUMB. (U) AIR FORCE INST OF TECH
WRIGHT-PATTERSON AFB OH SCHOOL OF ENGI. G P MOE
UNCLASSIFIED DEC 84 AFIT/GAE/AA/84D-19 F/G 20/4 NL





MICROCOPY RESOLUTION TEST CHART
NATIONAL BUREAU OF STANDARDS-1963-A

①

AD-A151 855



INFLUENCE OF SURFACE ROUGHNESS ON COMPRESSOR
BLADES AT HIGH REYNOLDS NUMBER IN A
TWO-DIMENSIONAL CASCADE

THESIS

Gary P. Moe, B.S.
Captain, USAF

AFIT/CAP/11/ORD-10

DISTRIBUTION STATEMENT A

Approved for public release;
Distribution Unlimited

DTIC
ELECTE
S D
MAR 28 1985
B

DTIC FILE COPY

DEPARTMENT OF THE AIR FORCE
AIR UNIVERSITY
AIR FORCE INSTITUTE OF TECHNOLOGY

Wright-Patterson Air Force Base, Ohio

85 03 13 096

AFIT/GAE/AA/84D-19

INFLUENCE OF SURFACE ROUGHNESS ON COMPRESSOR
BLADES AT HIGH REYNOLDS NUMBER IN A
TWO-DIMENSIONAL CASCADE

THESIS

Gary P. Moe, B.S.
Captain, USAF

AFIT/GAE/AA/84D-19

DTIC
ELECTE
MAR 28 1985
S D
B

Approved for public release; distribution unlimited

AFIT/GAE/AA/84D-19

INFLUENCE OF SURFACE ROUGHNESS ON COMPRESSOR
BLADES AT HIGH REYNOLDS NUMBER IN A
TWO-DIMENSIONAL CASCADE

THESIS

Presented to the Faculty of the School of Engineering
of the Air Force Institute of Technology

Air University

In Partial Fulfillment of the
Requirements for the Degree of
Master of Science in Aeronautical Engineering

Gary P. Moe, B.S.

Captain, USAF

December 1984

Approved for public release; distribution unlimited

Acknowledgments

I appreciate this opportunity to express my thanks to the many people whose contributions were invaluable in completing this project. I thank Dr. Milton Franke and Capt. Wesley Cox, my committee members, for their insight and suggestions regarding this work.

I am especially grateful for guidance given me by my principal thesis advisor, Dr. William C. Elrod. My thanks also go to Lt. Frederick Tanis Jr. who, though no longer a student at AFIT, gave of his time to help me become acquainted with the Cascade Test Facility.

This work could not have been accomplished without the excellent support of the men of the fabrication shop and the laboratory technicians; especially John Brohas, who in five days completed a job that would normally take three times as long, and Harley Linville, who was always willing to help the students.

Finally, I give my heartfelt thanks to my wife, Phyllis, for her encouragement throughout my schooling and her many hours spent typing this report.



Accession For	
NTIS	<input checked="checked" type="checkbox"/>
DTIC	<input type="checkbox"/>
Unpublished	<input type="checkbox"/>
Justification	
Distribution/	
Availability Codes	
Dist	Avail and/or Special
A-1	

Table of Contents

	Page
Acknowledgments	ii
List of Figures	v
List of Symbols	vii
List of Tables	ix
Abstract	x
I. Introduction	1
Objectives and Scope	3
II. Experimental Apparatus	4
Cascade Test Facility	4
Test Section	5
Blade Roughness Configurations	7
Boundary Layer Control Mechanism	8
Test Section Exit Diffuser	9
X-Y Traversing Mechanism	9
Instrumentation	10
Data Acquisition and Analysis System	12
III. Procedure	13
Test Procedure	13
IV. Results and Discussion	15
Loss Coefficient	15
Preliminary Tests	16
Establishing Two-Dimensional Flow	17
Two-Dimensional Flow and Blade Profile Efficiency . .	19
Non-Dimensional Total Pressure Loss Maps	20
Effect of Roughness on Blade Performance	29
Total Pressure Loss Coefficient	30
Exit Velocity and Turbulence Intensity Profiles . . .	37
V. Conclusions and Recommendations	47
Conclusions	47
Recommendations	48

Appendix A: Roughness Definitions	49
Appendix B: Development of Adiabatic Efficiency of the Cascade . .	50
Appendix C: Non-Dimensional Total Pressure Loss Data for NACA 65-A506 Airfoils	53
Appendix D: Velocity and Turbulence Intensity Profiles	56
Bibliography	97
Vita	99

List of Figures

Figure	Page
1. Test Section	6
2. Test Blade Profiles	8
3. Hot Film Probe Calibration Curves	11
4. Loss Coefficient Contours (Percent of Dynamic Head) for NACA 65-Series Blades With No Suction Applied - .63 Chord Behind Blades	21
5. Loss Coefficient Contours (Percent of Dynamic Head) for NACA 65-Series Blades With Suction Applied - .63 Chord Behind Blades	24
6. Loss Coefficient Contours (Percent of Dynamic Head) for NACA 64-Series Blades With Suction Applied - .63 Chord Behind Blades 4 and 5	27
7. Logarithmic Plot of Performance Loss With Relative Sand Roughness for NACA 64-Series Blades	31
8. Linear Plot of Performance Loss With Relative Sand Roughness for NACA 64-Series Blades	32
9. Logarithmic Plot of Performance Loss With Relative Sand Roughness for NACA 65-Series Blades	33
10. Linear Plot of Performance Loss With Relative Sand Roughness for NACA 65-Series Blades	34
11. Velocity and Turbulence Intensity Profile Conf No. 1 Traverse No. 2: $Ks/l=0.088 \times 10^{-3}$	38
12. Velocity and Turbulence Intensity Profile Conf No. 2 Traverse No. 2: $Ks/l=0.473 \times 10^{-3}$	39
13. Velocity and Turbulence Intensity Profile Conf No. 3 Traverse No. 2: $Ks/l=3.47 \times 10^{-3}$	40
14. Velocity and Turbulence Intensity Profile Conf No. 4 Traverse No. 2: $Ks/l=4.71 \times 10^{-3}$	41
15. Turbulence Intensity With Relative Sand Roughness For NACA 64-Series Airfoil	43

16.	Turbulence Intensity With Relative Sand Roughness For NACA 65-Series Airfoil	44
17.	Arithmetic Average Roughness	49
18.	Temperature-Entropy Plot Of Compression Process	50
19.	Velocity and Turbulence Intensity Profile Conf No. 1	57
20.	Velocity and Turbulence Intensity Profile Conf No. 2	62
21.	Velocity and Turbulence Intensity Profile Conf No. 3	67
22.	Velocity and Turbulence Intensity Profile Conf No. 4	72
23.	Velocity and Turbulence Intensity Profile Conf No. 11	77
24.	Velocity and Turbulence Intensity Profile Conf No. 12	82
25.	Velocity and Turbulence Intensity Profile Conf No. 13	87
26.	Velocity and Turbulence Intensity Profile Conf No. 14	92

List of Symbols

<u>Symbol</u>	<u>Name</u>	<u>Units</u>
A	Area	in ²
C _p	Specific Heat at Constant Pressure	B/lbm-F
dA	Differential Area	in ²
dy	Differential Length	in
h	Specific Enthalpy	B/lbm
K _s	Equivalent Sand Roughness	micrometers
L	Sample Length	micrometers
l	Chord Length	in
P	Pressure	psia
P	Mass-Averaged Pressure	psia
1q2	Heat Transfer Per Unit Mass Between Stations One And Two	B/lbm
R _a	Arithmetic Average Roughness	micrometers
Re	Reynolds Number	none
S	Entropy	B/lbm R
T	Temperature	F
Tu	Turbulence Intensity	Percent
V	Velocity	ft/sec
W	Inlet Relative Velocity	ft/sec
1w2	Specific Work Between Stations One And Two	B/lbm
α	Flow Angle	deg
Y	Ratio Of Specific Heats	None
η _a	Adiabatic Efficiency	None
μ	Micro	None
ν	Kinematic Viscosity	ft ² /sec
ω	Total Pressure Loss Coefficient	None
ρ	Density	lbm/ft ³

Subscripts

adm	Admissable Value
mean	Mean Value
rms	Root Mean Square
trans	Transition Value
o	Total
z	Axial
1	Inlet
2	Exit

Superscripts

' Isentropic Value

Acronyms

AFIT	Air Force Institute of Technology
AVDR	Axial Velocity Density Ratio
CTF	Cascade Test Facility
HP	Hewlett Packard
NACA	National Advisory Committee on Aeronautics
TSI	Thermo Systems International

List of Tables

Table	Page
I. Airfoil Data	5
II. Airfoil Roughness Data	30
III. Comparison Of Adiabatic Efficiency	52

Abstract

A cascade test facility has been established which incorporates sidewall boundary layer control, permitting two-dimensional flow investigation over the center span (about $2/3$ the width of the blade) of an airfoil in cascade, and an investigation has been conducted to determine the influence of roughness on the airfoil. Two representative compressor profiles, the NACA 64-A905 and 65-A506, with two inch chords and aspect ratios of one were tested at airflow inlet velocities comparable to those in axial flow compressors. An Axial Velocity Density Ratio of unity was the criterion used to determine when two-dimensional flow was achieved.

Test results indicate that initial small increases of roughness have a much greater effect on blade total pressure loss than do subsequent larger roughness values. A small increase in roughness produces a substantial increase in free stream turbulence with practically no effect on the wake. Further increase in roughness produces a substantial effect on the wake but little effect on the free stream turbulence. Surface roughness is shown to have a much greater influence on blade wake turbulence intensity for the higher camber airfoils tested than for lower camber airfoils.

INFLUENCE OF SURFACE ROUGHNESS ON COMPRESSOR

BLADES AT HIGH REYNOLDS NUMBER IN A

TWO-DIMENSIONAL CASCADE

I. Introduction

Modern military aircraft are required to operate in a variety of flight regimes, from cruise at high altitude to the high speed, low-level dash. To power these aircraft, turbine engines operate with flow conditions in the last stages of the high pressure compressor ranging from low Reynolds number based on blade chord ($Re < 1.0 \times 10^5$) to Reynolds numbers in excess of 1.1×10^6 . The engines are also subjected to extreme environmental conditions which may include concentrations of particulate matter from explosions and dust, or salt ingestion inherent in naval operations.

Operation in these types of environments causes the engine efficiency to decrease over time. Among the chief factors affecting efficiency is the mechanical or corrosive pitting of blades in the compressor and turbine sections. The surfaces of the compressor and turbine blades may also be roughened by the formation of deposits. In compressors, the behavior of the blade boundary layer varies with the blade chord Reynolds number. Three separate flow regions can be identified, each by particular characteristics. At low Reynolds numbers

($Re < 1.0 \times 10^5$) the boundary layer is laminar and is much more prone to separation in an adverse pressure gradient than the turbulent boundary layer. Large losses accompany the laminar separation (Ref. 3).

Schaffler, in his study of surface roughness effects on axial flow compressors, described the boundary layer in the intermediate range of Reynolds numbers (based on blade chord) as being turbulent over much of the blade and the surface as hydrodynamically smooth (Ref. 11). That is, the boundary layer over the blade begins as laminar, but in a short distance transitions to turbulent with the peaks of the roughness totally submerged in the laminar sublayer of the turbulent boundary layer. The blade losses are proportional to Reynolds number raised to an appropriate power which depends on camber and incidence (Ref 18:150). At high Reynolds numbers the boundary layer is turbulent and the peaks of the roughness may be high enough to protrude through the laminar sublayer making the blade surface hydrodynamically rough. Blade losses in this range do not depend on chord Reynolds number but are a function of the roughness itself (Ref 11:9). Fottner and Schaffler report that "increasing pressure ratios and flow velocities in modern gas turbine compressors increase the Reynolds Number over chord length ratio at the back end of the compression system to an extent that even with the best presently available manufacturing methods, noticeable losses of potentially achievable efficiency gains must be accepted." (Ref. 5:171)

This investigation was primarily concerned with the high Reynolds number flow regime ($Re > 4 \times 10^5$). The work was conducted in a two-dimensional cascade test facility used for testing compressor and turbine airfoils. Research began in 1981 with several investigators

studying roughness effects in cascade flow (Ref. 6,14,17). The results of those previous experiments were overshadowed by the solid endwall/blade boundary layer interaction to the extent that two-dimensional flow was not established.

Objective and Scope

The objectives of this investigation were twofold.

1. Establish a facility that would permit two-dimensional flow investigations of a cascade of compressor blades.
2. Determine the effect of surface roughness on blade losses using a non-dimensional total pressure loss coefficient to characterize the effect.

To accomplish these objectives a sidewall boundary layer control system was built and installed on the cascade test section to reduce secondary flow and airfoil/sidewall boundary layer interaction to the degree that two-dimensional flow is attained. Total pressure surveys were made in the exit plane to evaluate the effectiveness of the boundary layer control. Once two-dimensional flow was established, exit wake surveys were run on smooth and roughened blades to determine flow losses due to roughness through the test section. A non-dimensional total pressure loss parameter was used as a measure of the losses. Average Blade Roughness, R_a , and Equivalent Sand Roughness, K_s , were used in this investigation to characterize the blade surfaces. The roughness parameters are defined in Appendix A.

II. Experimental Apparatus

The investigation of effects of blade roughness on compressor blade cascade performance was conducted in the Cascade Test Facility (CTF) at the Air Force Institute of Technology Aeronautics Laboratory. The system, which is described in detail by Allison (Ref. 1), is a cascade wind tunnel with a computerized data acquisition system. A brief description follows along with modifications made specifically for this research.

Cascade Test Facility

The cascade test facility is built around a two-inch by eight-inch test section containing seven airfoils. The flow unit Reynolds number based on blade chord and inlet velocity is in excess of two million per foot. A suction system has been added to control the boundary layer within the test section by drawing off the sidewall boundary layer prior to, and throughout, the blade row.

To run the CTF, source air is supplied by a blower rated at 3000 cfm with a discharge head of 26 ounces. Cool air is drawn in from the outside and mixed with warmer recirculated air to stabilize operating temperatures. Particles which may damage a hot film sensor are trapped by a series of fiber and electrostatic filters ahead of the blower and in the stilling chamber.

After passing through the blower the airflow is straightened and conditioned by several screens and a honeycomb lattice located in the stilling chamber. This system provides air to the test section with turbulence intensities of generally less than one percent.

Test Section

The two dimensional cascade test section used in the present investigation is shown in Figure 1. Two different sets of airfoils were studied. The first was a cascade containing seven NACA 64-A905 airfoils (including the two that form the end walls) with a two-inch chord and aspect ratio of 1.0. A second test section had seven NACA 65-A506 airfoils installed also with a two-inch chord and aspect ratio of 1.0. The profile of the NACA 64-A905 blade is similar to that of a compressor exit guide vane while the NACA 65-A506 profile approximates that of a blade in the latter stages of a high pressure compressor. The parameters describing the two test sections are listed in Table I.

TABLE I
Airfoil Data

Airfoil	NACA 64-A905	NACA 65-A506
Chord	2 in	2 in
Aspect Ratio	1.0	1.0
Row Inlet Angle	31 deg	31 deg
Angle of Attack	25 deg	13 deg
Stagger Angle	6 deg	18 deg
Turning Angle	33 deg	18 deg

A blade spacing of 1.333 inches was used in each test section. With these dimensions the solidity, defined as

$$\text{solidity} = \text{chord/spacing} \quad (1)$$

was 1.5.

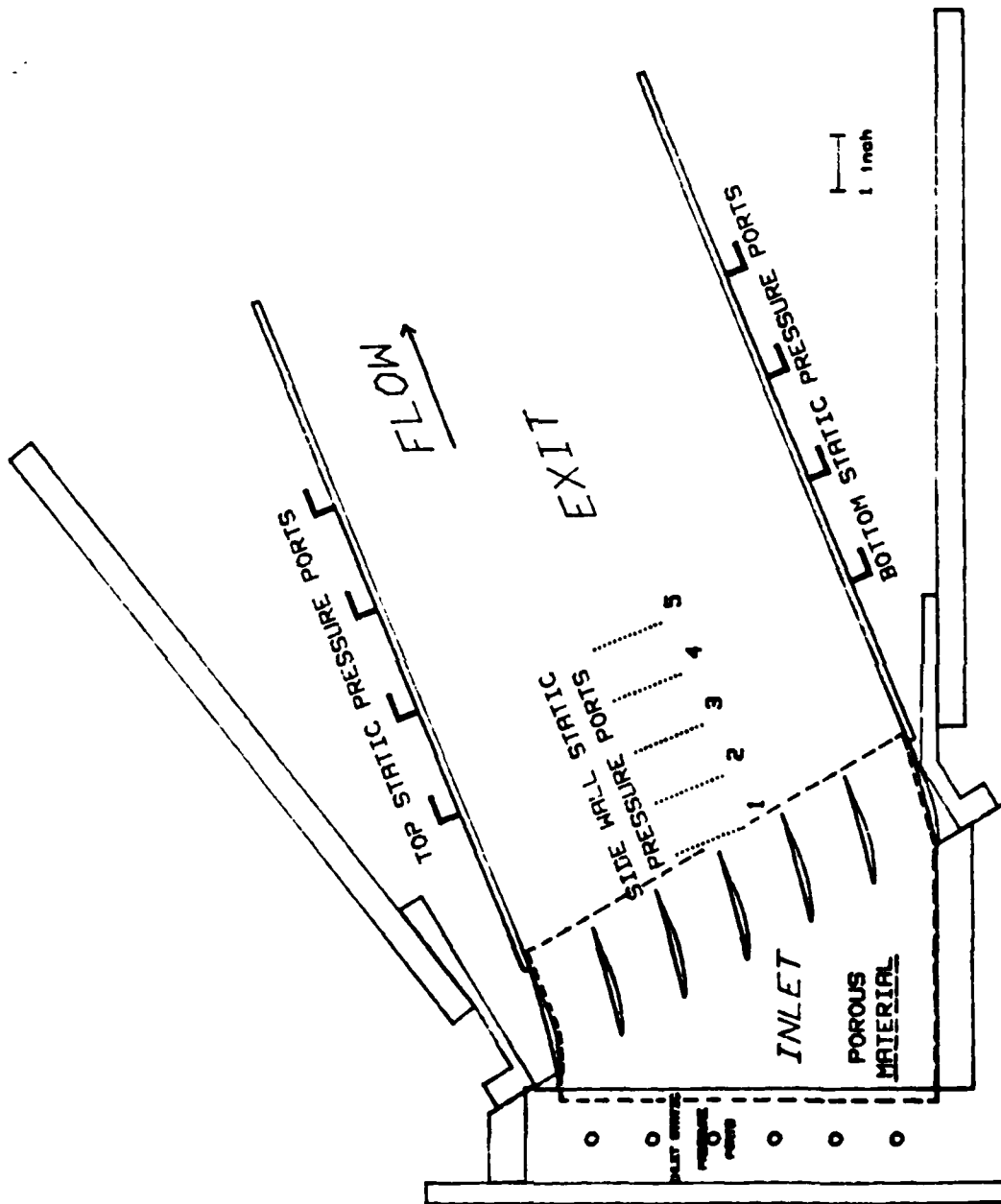


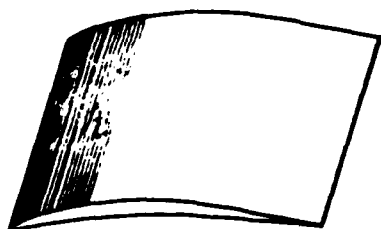
Figure 1: Test section

Blade Roughness Configurations

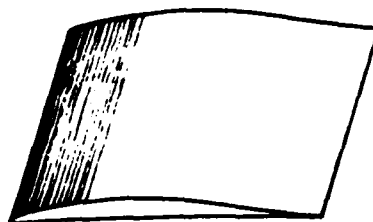
The two different airfoil shapes tested for roughness effects are shown in Figure 2. Tanis (Ref. 14) determined that suction side roughness on the first quarter chord had the greatest influence on the efficiency of the cascade since the roughness magnitude relative to the local boundary layer was greatest near the leading edge. For this reason several sets of airfoils were roughened on the suction side by either sand blasting or applying various sizes of grit to the first quarter chord.

The blades were cast from Fiber-Resin FR-44 casting resin using the 5595 cure, then aged at an elevated temperature to increase the resistance to bending in the airflow. Some of the blades were then sandblasted to the desired roughness. The others were coated with a thin film of ceramic acrylic sealer and carborundum grit was blown on. A final coating of acrylic sealer was then applied to these blades. Much care had to be taken not to alter the shape of the leading edge.

After the blades were modified, a Rank Taylor Hobson Surtronic 3 profilometer with recorder and parameter units attached was used to measure roughness values of R_a (Ref. 15). The roughened surface, though very uniform, was measured at several locations and the average of these measurements was recorded as characterizing the roughness.



NACA 64-A905



NACA 65-A506

Figure 2: Test Blade Profiles

Boundary Layer Control Mechanism

Several investigators have used a combination of an upstream suction slot and sidewalls which were porous across the blade row to effect boundary layer control (Ref. 2, 4). For this investigation a continuous porous sidewall which extended from at least one-half chord up stream to just past the trailing edges of the blades was added to the cascade test section (see Figure 1). With this system the boundary layer can be continuously drawn off from the sidewalls before reaching the blades and also throughout the blade passage.

One sixteenth-inch thick metallic walls of Pall corporation PSS 316L Porous Stainless Steel were used. This particular material is normally used in filtering applications and is capable of trapping particles 11 micrometers in size. Because of the dense construction, the porous stainless steel provided adequate flow resistance to give uniform suction flow in the blade passages.

Panels of perforated plexiglass backing supported the porous sidewalls. The rest of the boundary layer control mechanism consisted of two aluminum manifolds, one on each side of the test section, and an industrial vacuum cleaner with a measured flow rate capacity of about 60 cfm through the sidewall suction system. This is about 4.3 lbm/min mass flow at 110 F.

Test Section Exit Diffuser

A 13-inch channel with adjustable endwalls was incorporated into the test section to enable simulation of either nozzle, diffuser, or neutral exit conditions. Static pressure taps in the endwalls and sidewalls were used to determine when the exit channel was set in the proper configuration. Since an ambient exit pressure was desired, the endwalls were adjusted until all pressure readings were essentially atmospheric. Additional static pressure taps were located in the test section inlet throat to aid in positioning the endwalls for uniform flow conditions and for measuring inlet velocity.

X-Y Traversing Mechanism

A computer controlled traversing mechanism which is described in Ref. 14 was used to position the hot film anemometer sensor in the exit flow. The traverser would locate the probe at any downstream (X) or crosstream (Y) point with an accuracy of 0.002-inch in the X direction and 0.001-inch in the Y direction. Locating the probe in the spanwise (Z) direction was accomplished manually by using a thumb screw and dial indicator. For this investigation a normal run would include five traverses in the Y direction at 1-inch intervals along the X direction.

The data window began at 0.25-inch behind the blade and contained 133 data points in each traverse. These points were spaced 0.01-inch apart and began 0.6-inch below the center blade. In this way good resolution was achieved across the 1.333-inch blade spacing. All data were taken on the blade centerline except that taken to determine quality of flow in the test section.

Instrumentation

The AFIT Cascade Test Facility is instrumented with a variety of devices. Fifteen 30-inch U-tube manometers, four Statham Laboratories P6TC-2D-350 pressure transducers, a hot film X-wire anemometer sensor, and two "T-type" thermocouples are all used to monitor the system. Manometers were used for balancing the test section and setting the suction flow. Tank total, throat and exit static, and ambient pressure were measured by pressure transducers. The tank total temperature and ambient temperature were measured by the thermocouples. The hot film anemometer system was composed of a TSI model 1241-10 X-wire sensor operated by two TSI model 1050 constant temperature anemometers. The system measured both the mean and fluctuating velocity components in the X and Y directions. From this information the turbulence intensity and exit flow velocity was obtained.

The hot film sensor was calibrated using a scheme designed to account for the effect of elevated temperatures. This scheme permitted representing all calibration data for a particular sensor in the temperature range of interest with a single curve as shown in figure 3. A detailed description is given by Tanis (Ref. 14). Sensor error of less than one percent was obtained with the calibration. However, when

Hot Wire Probe Calibration

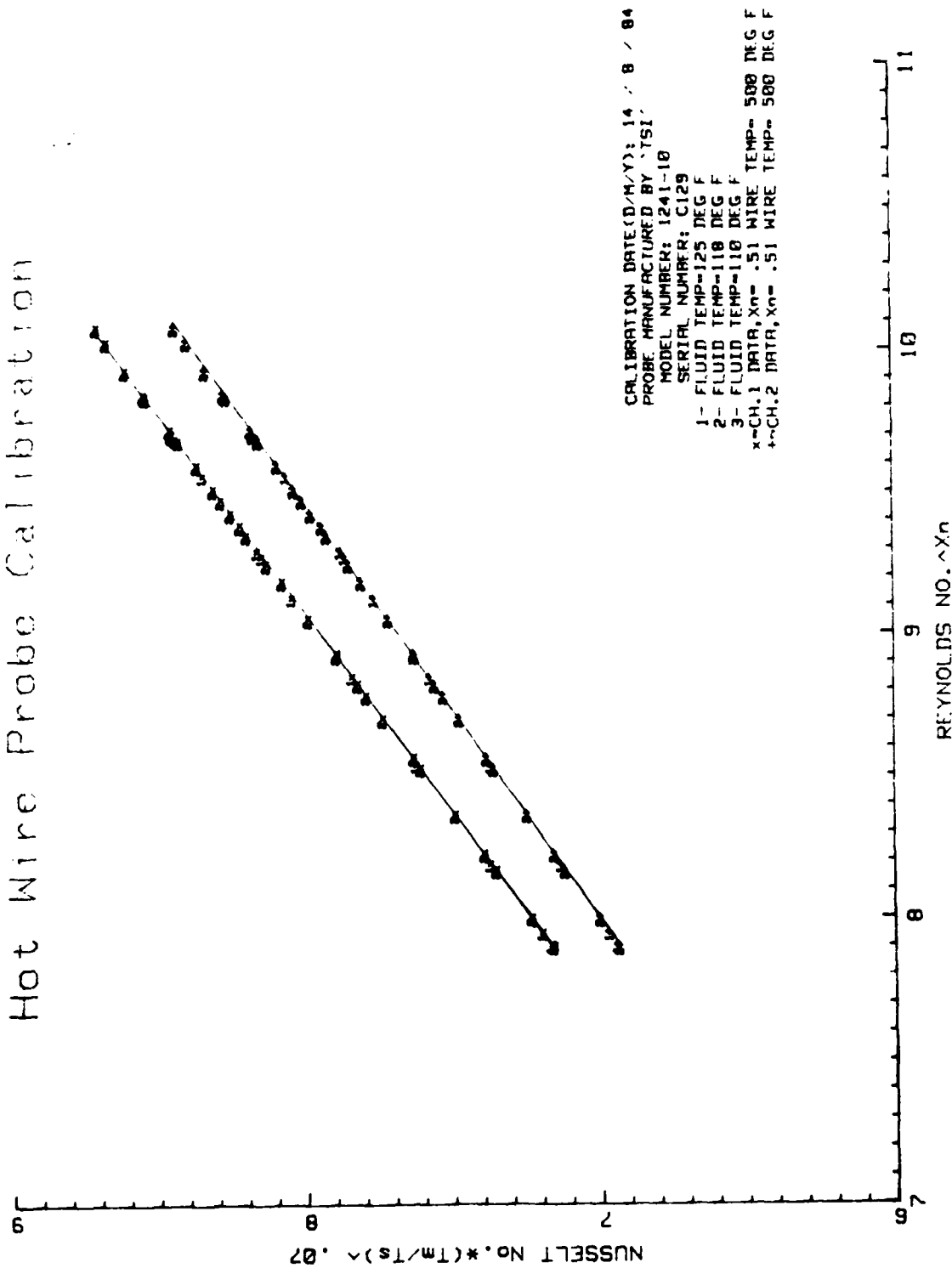


Figure 3. Hot Film Probe Calibration Curves

the sensor was used in the test apparatus the measured velocity was approximately five to seven percent greater than theoretically possible. The factors causing the increase are thought to be differences in flow humidity and probe support temperature between the calibration station and the test apparatus. To correct the velocity, continuity between two centerline planes located upstream and downstream of the blade row was used. The planes spanned the streamlines defining the channel between the two center blades of the cascade. The flow was two-dimensional through the cascade and, therefore, assumed uniform along the midspan of the blade. Inlet and exit mass flow rates were calculated from measured data. A comparison of the two was made and a correction factor, if required, applied to the exit velocity to maintain continuity through the cascade. Using this method, accuracies on the order of 99 percent were achieved.

Data Acquisition and Analysis System

The heart of the CTF is the data acquisition system controlled by an HP 9845B computer (Ref. 1). By using the appropriate software an investigator can specify the number and location of data points to be taken. The system positions the hot film probe at the desired positions and records the pertinent data (all pressures, temperatures, and anemometer readings). This data is then stored as voltages on magnetic disks. Subsequently, a data reduction program is used to convert the data into a useful form of pressures, temperatures and velocities, and again store the information on magnetic disks. The data in this form is then used to evaluate the various performance parameters.

III. Procedure

The general thrust of this investigation was to determine the effects of surface roughness on compressor blade performance in a two-dimensional cascade. To accomplish this, boundary layer control was incorporated in order to establish two-dimensional flow in the test section. This flow control was determined to be necessary as a result of a series of baseline test runs made in effort to reproduce data already taken from the NACA 64-A905 airfoils (Ref. 17).

Testing Procedure

In setting the test conditions, the sequence of actions was as follows: when the airflow through the test section reached the operating condition ($115 \text{ degrees F} < T_{01} < 120 \text{ degrees F}$), endwalls were adjusted until wall static pressure was ambient and uniform parallel to the cascade exit flow direction. A check was also made for uniform pressure across the inlet throat. The establishment of uniform pressure across the throat along with a stabilized temperature insured that uniform flow conditions existed upstream of the blade cascade. Once the test section was balanced, the measured turning angle was determined with the use of a protractor. A total pressure survey was subsequently made vertically across the exit channel of one blade at the 0.63 chord point downstream from the trailing edge. The survey consisted of 13 total pressure readings made with a pitot tube oriented parallel to the mean flow. The arithmetic average of the exit total pressure was used to calculate the outlet velocity, which was subsequently employed in

determining the flow conditions. The hot film sensor was then installed and adjusted for the particular measured turning angle. A test, containing 665 data points, was then run.

After completing the series of test runs on smooth blades without suction, boundary layer control was then used. Abbreviated runs were made at several suction rates to determine when two-dimensional flow was achieved. When two-dimensional flow was established, the blades were tested for the effects of surface roughness. Five traverses at one-inch intervals in the axial direction were made with 133 data positions in each traverse. The data were stored on magnetic disk then later reduced and analysed.

IV. Results and Discussion

The objectives of this study were to modify the cascade test section to give two-dimensional flow and to determine the effects of surface roughness on the efficiency, expressed as the total pressure loss coefficient, $\bar{\omega}$, of an airfoil in cascade. Two different test sections were used; each had porous sidewalls for boundary layer control and one had a set of solid sidewalls for comparing results without suction to those with the suction applied.

Loss Coefficient

Flow past a cascade of airfoils experiences a momentum deficit in the wake region of each airfoil. This deficit can be expressed mathematically as a loss in total pressure, P_o , where

$$P_o = P \left[1 + \frac{V^2}{2C_p T_o} \right]^{\gamma/(\gamma-1)} \quad (2)$$

For this investigation, the non-dimensional loss coefficient, $\bar{\omega}$, was used to characterize blade losses due to roughness. This coefficient is defined as (Ref. 8)

$$\bar{\omega} = \frac{P_{o1} - \bar{P}_{o2}}{1/2\rho V_1^2} \quad (3)$$

where P_{o1} is the stilling tank pressure, \bar{P}_{o2} is the downstream, mass-averaged total pressure, and $1/2\rho V_1^2$ is the upstream dynamic pressure. The mass-averaged total pressure was calculated using the following relation

$$\bar{P}_{o2} = \frac{\int_A P_{o2} \rho V_2 dA}{\int_A \rho V_2 dA} \quad (4)$$

where \bar{P}_{o2} is the mass-averaged value of the total pressure. Since the flow was two-dimensional and spanwise uniform at the blade centerline, the area integrals were replaced by single integrals. The relation for a blade of unit width is

$$\bar{P}_{o2} = \frac{\int P_{o2} \rho V_2 dy}{\int \rho V_2 dy} \quad (5)$$

where dy is an incremental length in the Y direction. The integrals were then numerically evaluated.

Preliminary Tests

Several preliminary tests were made on the NACA 64-series blades with no roughness applied in effort to reproduce data obtained in an earlier investigation by Vonada (Ref. 17). The total pressure loss coefficient, $\bar{\omega}$, for the tests was 0.1146 for the run with porous sidewalls installed but no suction applied. This value is 26 percent greater than the $\bar{\omega}$ of 0.0909 obtained in Vonada's work. The reason for this discrepancy is that the blade tip leakage through the porous wall and resulting secondary flow caused an increase in losses. Briggs (Ref. 2:4) ran similar tests without suction in a cascade with an aspect ratio of four and porous walls. He reasoned the results would be comparable with those of the solid wall cascades because the boundary layer control slot and porous walls would be submerged in the boundary layer. That

does not hold true for cascades with an aspect ratio of one because of the greater influence the wall/blade boundary layer interaction has on the centerline flow conditions.

-Establishing Two-Dimensional Flow

A series of tests were run on smooth NACA 65-series blades in order to establish the required suction for two-dimensional flow and determine the effects of suction on the flow. In order to be useful for engineering purposes, cascade data taken from several sources using the same flow conditions must be comparable. It is not uncommon for the data to differ from those of similar cascade tunnels which ran tests under nearly identical geometric settings. Physical characteristics of the different wind tunnels, such as aspect ratio and turbulence intensity, account for these differences in data (Ref. 2:2).

To give a common reference point at which cascade data is obtained, several criteria have been established. Erwin and Emery (Ref. 4) reported that the experimental pressure rise from existing cascades was usually substantially smaller than the value which theoretically corresponded to the measured turning angle. They also found disagreement between values of lift coefficients obtained from integrated experimental pressure distribution plots and those derived from the measured turning angle. As a result of such discrepancies, criteria for two-dimensional flow were given. A partial list follows:

- 1) Equal pressures, velocities, and directions exist at different spanwise positions.

- 2) The static pressure rise across the cascade equals the value associated with the measured turning angle and wake.
- 3) No region of low-energy flow other than the blade wakes exist and the wakes are constant in the spanwise direction.

An additional condition which must be met is an Axial Velocity Density Ratio (AVDR) of unity (Ref. 2, 13). Axial Velocity Density Ratio is defined as

$$AVDR = \frac{\rho_2 V_{z2}}{\rho_1 V_{z1}} \quad (6)$$

where

$$V_{z1} = V_1 \cos \alpha_1 \text{ and } V_{z2} = V_2 \cos \alpha_2$$

According to Briggs (Ref. 2) irrotational, momentum, and continuity conditions may be used to determine the deviation of the flow from two-dimensional. He also suggested that due to complexity and time constraints, satisfying continuity, that is, an AVDR of unity, on the tunnel centerline would be sufficient to establish two-dimensionality in a compressible flow.

A value of AVDR greater than unity is indicated when the flow is not two-dimensional. It is believed that interaction of the sidewall and test blade boundary layers causes premature separation at the wall-blade junction producing a large low energy region. This large wake causes a restricting of the flow and increases the exit velocity. With

sidewall suction applied the boundary layer is drawn off and the passage convergence is reduced. When $AVDR \approx 1$, two-dimensionality exists. Scholz (Ref. 13) gave a somewhat broader definition applicable to compressor units, where $0.3 < AVDR < 1.2$ defined a "quasi-two-dimensional" flow.

For this study, the amount of air removed by the suction system was a fairly constant 2.4 percent of the total inlet air. The range of values for other comparable tunnel cascade systems varies from 1.2 percent (Ref. 10) to 9 percent (Ref. 2). The AVDR measurements varied from 1.01 to 1.013 with suction applied. With no suction the values were generally about five percent larger. Although the magnitude of the change is not large, the flow improvements through boundary layer control were substantial.

Two-Dimensional Flow and Blade Profile Efficiency. An additional check of the flow two-dimensionality was made in this study by comparing the blade adiabatic efficiency obtained from cascade test results against blade profile losses. According to Vincent (Ref. 16) blade profile losses are about ten percent. Thus, if the flow in a cascade is actually two-dimensional, losses due to blade tip leakage or wall-blade interaction should be minimal, giving a blade profile efficiency on the order of 90 percent.

The blade adiabatic efficiency is defined as

$$\eta_a = \frac{h_2' - h_1}{h_2 - h_1} \quad (7)$$

where h_1 is the upstream static enthalpy, h_2 is the actual downstream static enthalpy, and h_2' is the downstream static enthalpy resulting from isentropic compression for the same pressure rise. For this study, the results indicated an increase in adiabatic efficiency from 0.727 without boundary layer control to 0.894 with boundary layer control applied. A detailed explanation is given in Appendix B.

Non-Dimensional Total Pressure Loss Maps. Exit plane surveys, from which the local total pressures were calculated were made at a distance of 0.63 chord downstream of the blades to evaluate the losses through the blade passage. Figures 4 and 5 present lines of constant value of $\bar{\omega}$ in percent for the NACA 65-series airfoils for three channels between blades. Figure 4 is for the test section with solid sidewalls and no suction applied and Figure 5 is for the same blade configuration but with boundary layer control in use. The effect of boundary layer control may be seen by a comparison of these two figures.

In each figure the horizontal axis represents the half-channel spanwise position in inches from the test section wall. The physical limit of the measuring probe was 0.125 inches from the wall. The vertical axis depicts the channel position between two blades in percent of channel height. Zero percent represents the pressure surface and 100 percent the suction surface.

A comparison of Figures 4 and 5 shows that for the flow with boundary layer suction the overall magnitude of losses is significantly smaller than for the section without suction. Two of the criteria mentioned by Erwin and Emery for two-dimensional flow were that no region of low energy flow other than the blade wake existed, and that

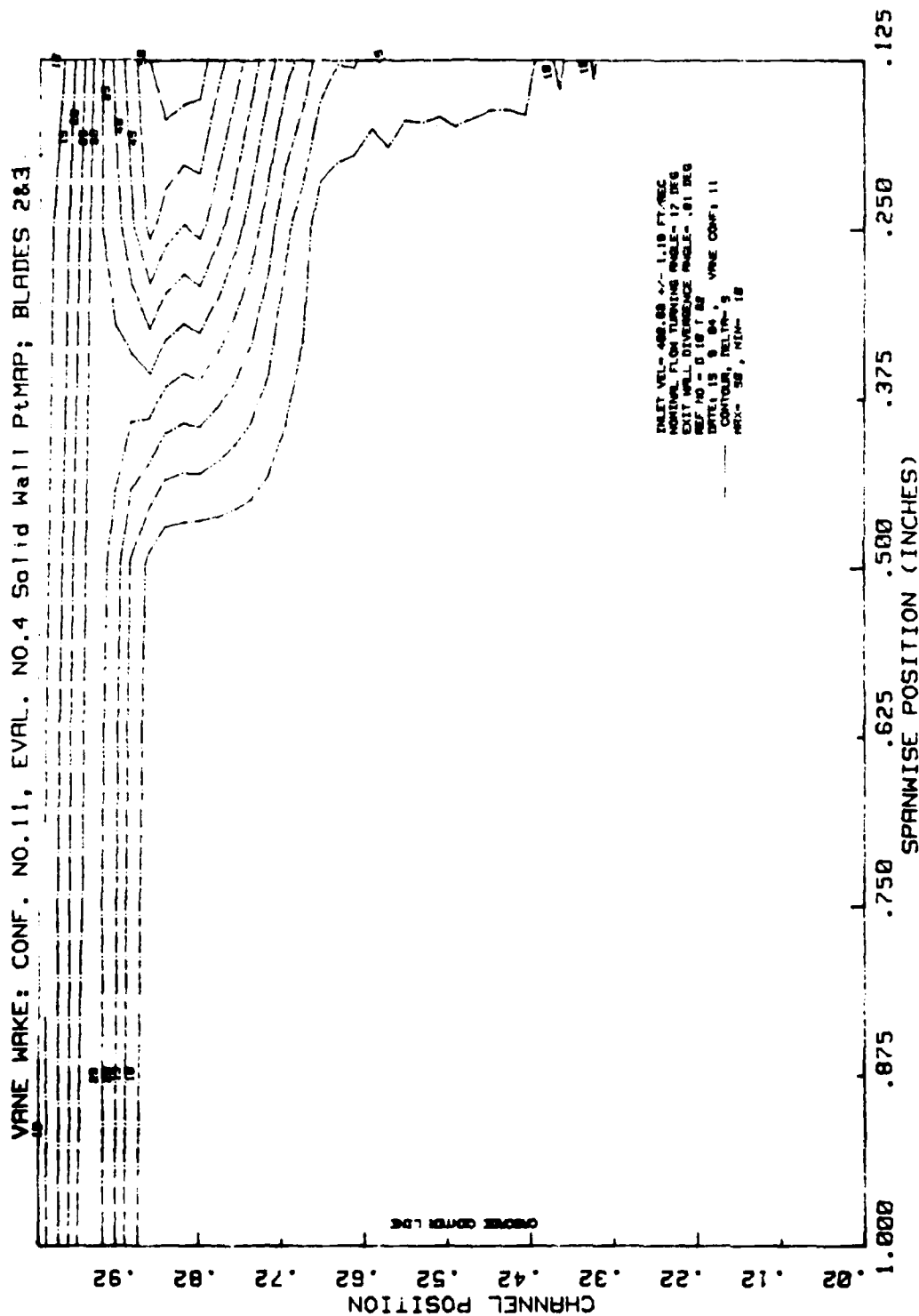


Figure 4a. Loss Coefficient Contours (Percent of Dynamic Head) for NACA 65-Series
 Blades With No Suction Applied - .63 Chord Behind Blades 2 and 3

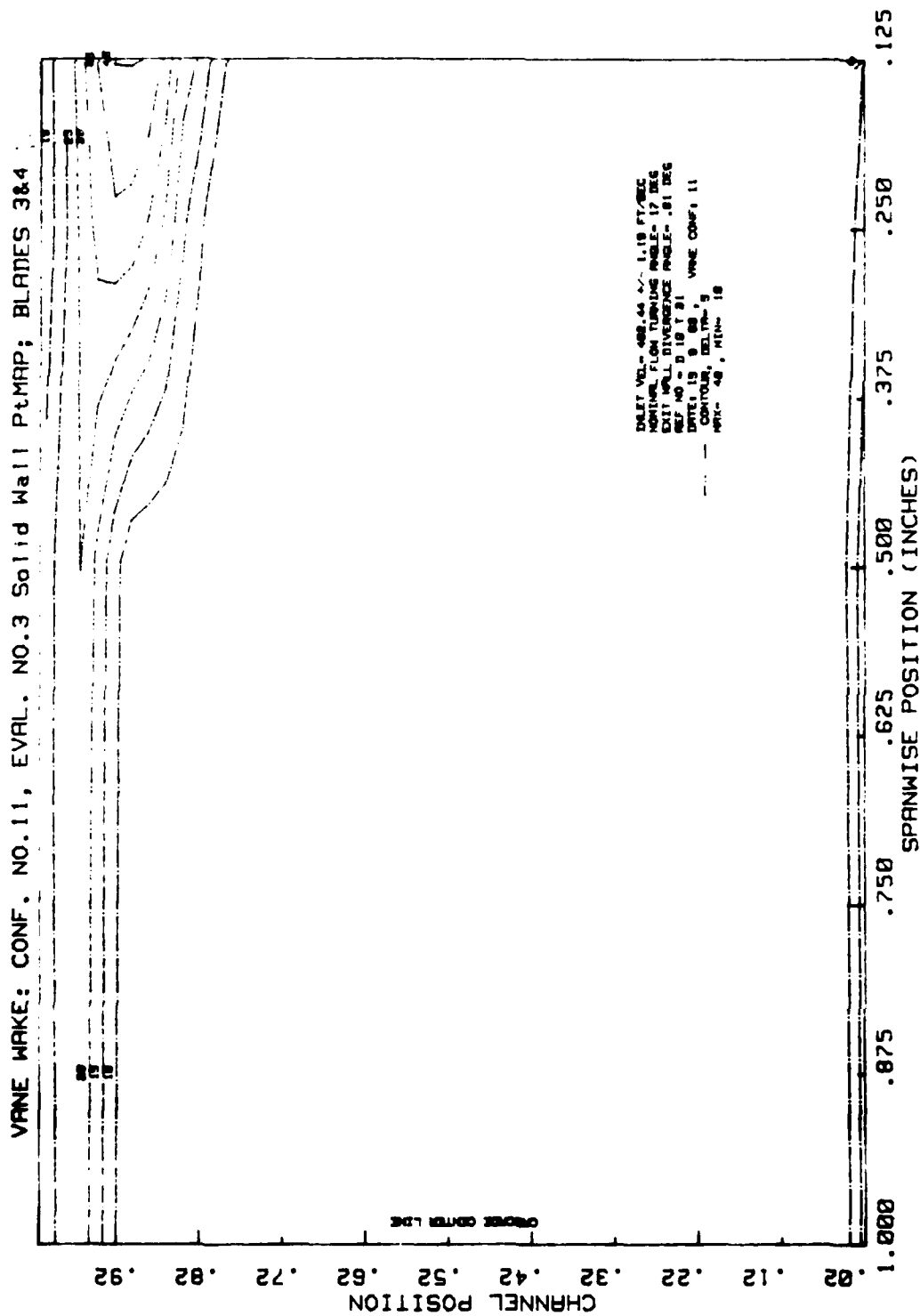


Figure 4b. Loss Coefficient Contours (Percent of Dynamic Head) for NACA 65-Series
 Blades With No Suction Applied - .63 Chord Behind Blades 3 and 4

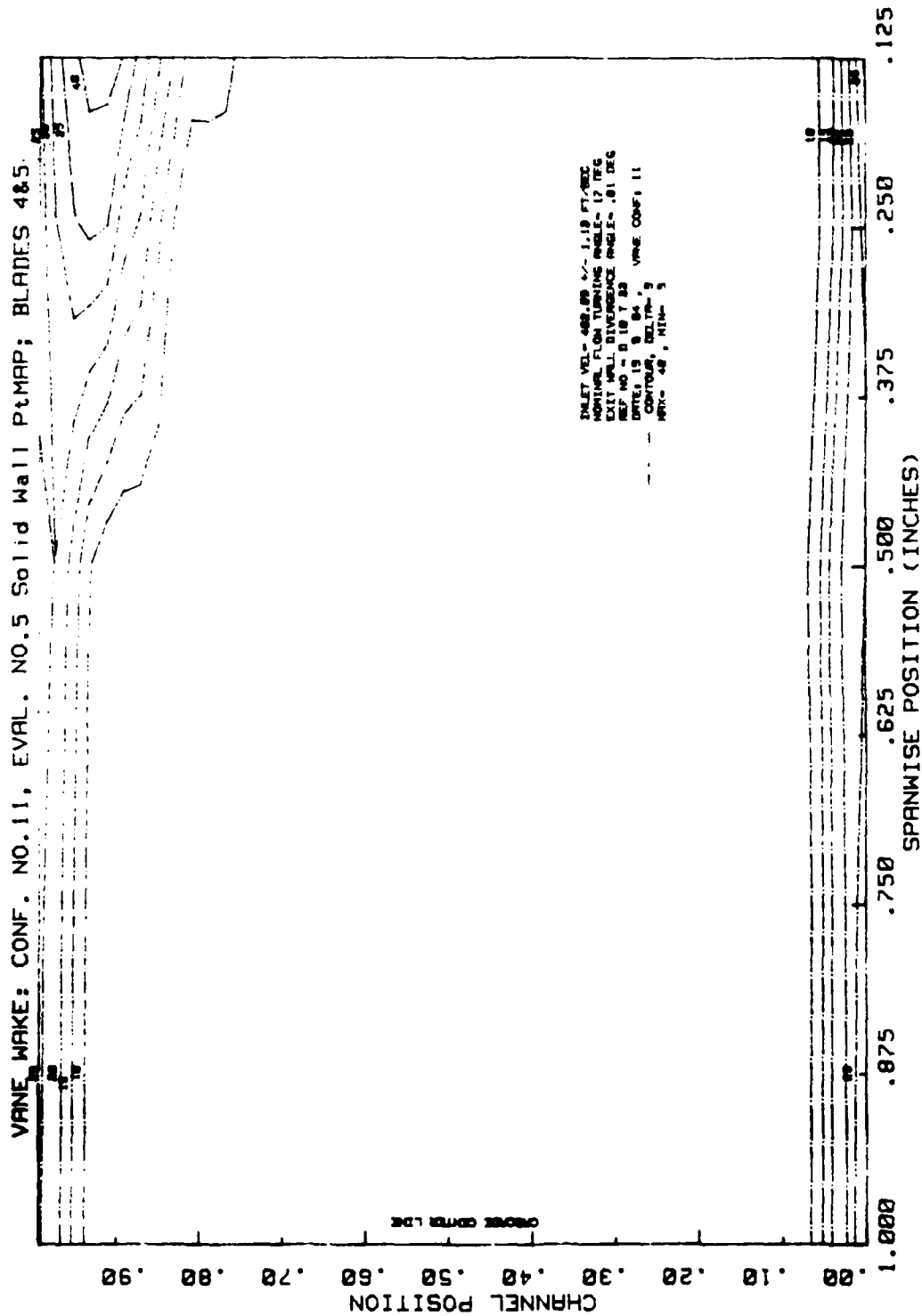


Figure 4c. Loss Coefficient Contours (Percent of Dynamic Head) for WACA 65-Series
 Blades With No Suction Applied - .63 Chord Behind Blades 4 and 5

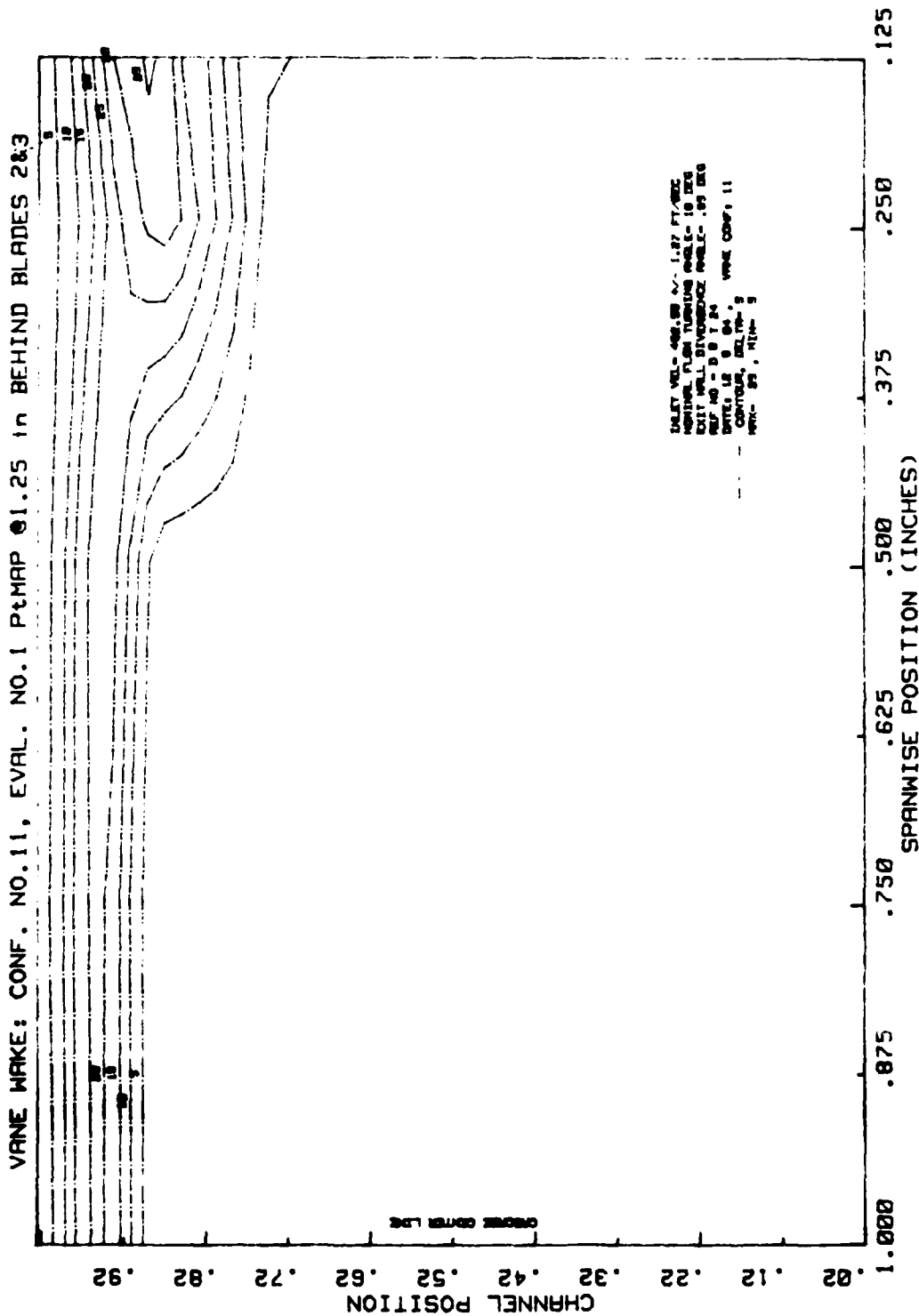


Figure 5a. Loss Coefficient Contours (Percent of Dynamic Head) for MACA 65-Series
 Blades With Suction Applied - .63 Chord Behind Blades 2 and 3

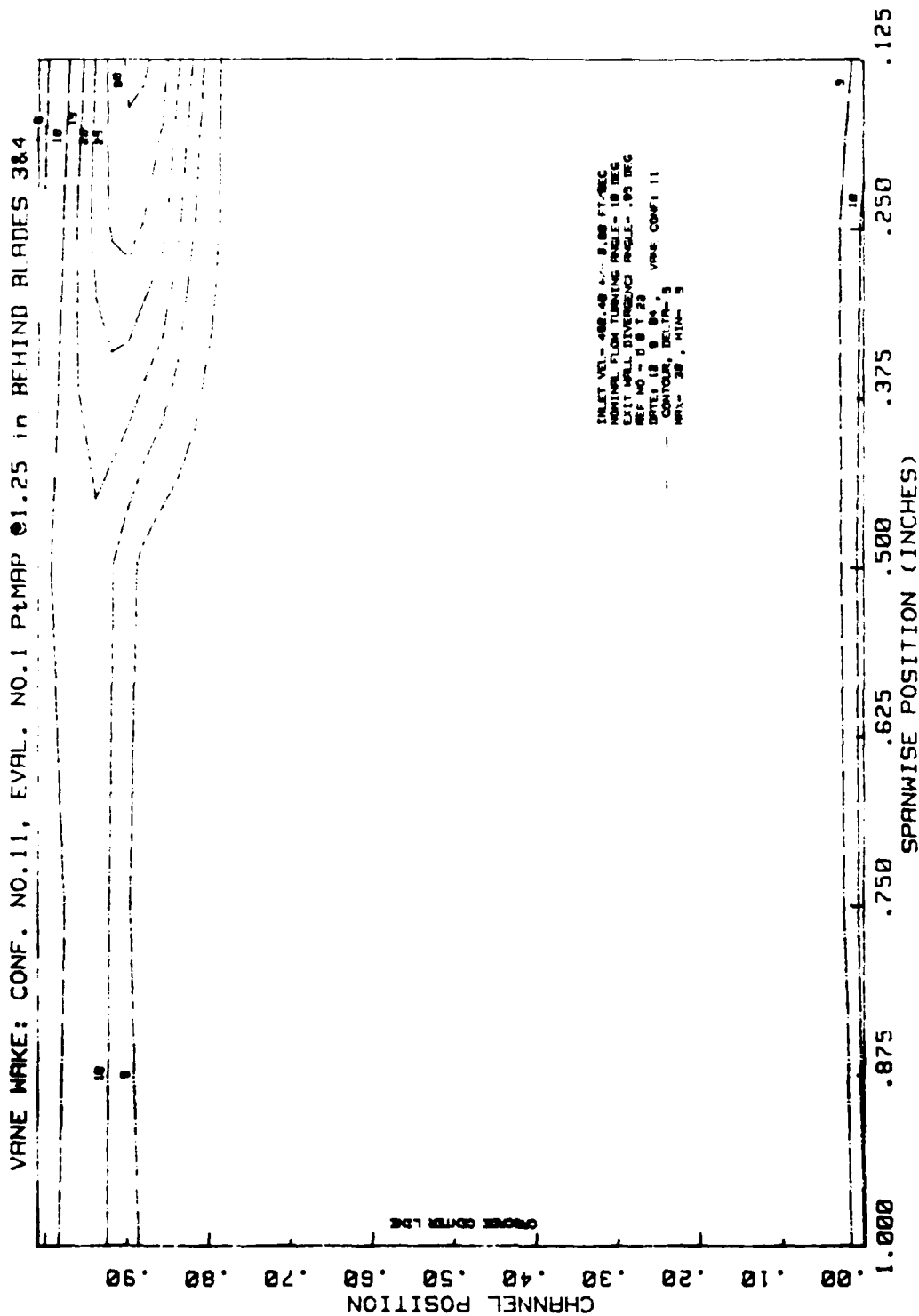


Figure 5b. Loss Coefficient Contours (Percent of Dynamic Head) for NACA 60-Series Blades With Suction Applied - .63 Chord Behind Blades 3 and 4

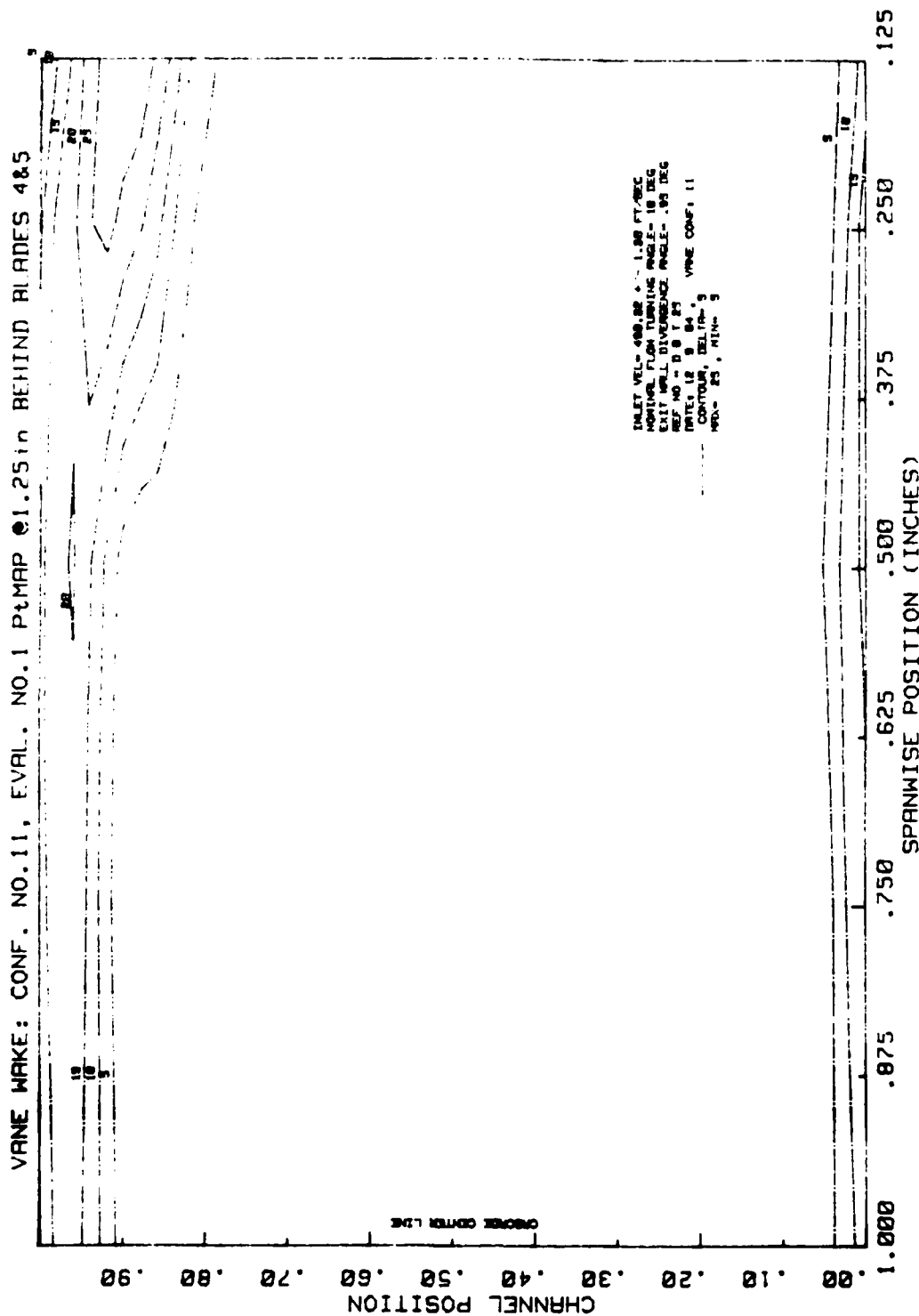


Figure 5c. Loss Coefficient Contours (Percent of Dynamic Head) for NACA 65-Series Blades With Suction Applied - .63 Chord Behind Blades 4 and 5

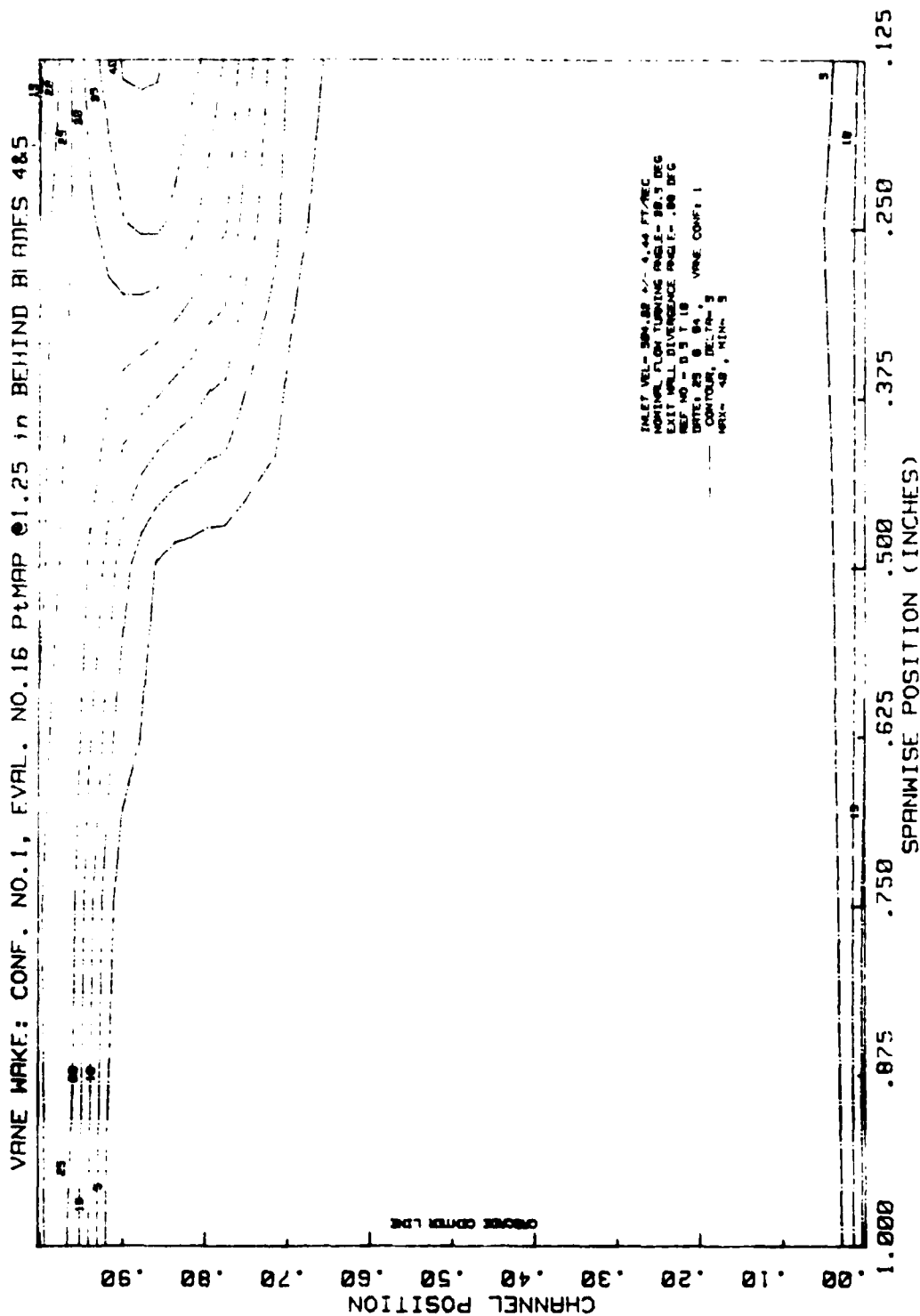


Figure 6. Loss Coefficient Contours (Percent of Dynamic Head) for HAPA 64-Series Blades With Suction Applied - .63 Chord Behind Blades 4 and 5

the wake be constant in the spanwise direction. One can see by inspection of the solid wall plots (Figure 4) that this is not the case. There are larger areas of loss and substantial differences in the losses from blade to blade (Figures 4a, b, c). For the blade row with suction (Figure 5), however, the areas with significant loss are small. Moreover, the uniformity of the flow from one blade channel to another is illustrated by the similarity of Figures 5a, b, and c.

Figure 6 shows the loss coefficient at the 0.63 chord exit plane behind the NACA 64-series airfoils. This plot shows a larger area of the channel with significant losses and larger loss magnitude. This is due to the greater diffusion which results from a higher turning angle. The higher flow turning angle gives rise to a steeper pressure gradient leading to a thicker blade boundary layer at the trailing edge.

It should be noted that, whether or not boundary layer control is used, there is a large region about the blade midspan (about two-thirds blade width) where the flow is very uniform. However, with suction applied, the large areas of undisturbed flow in both the 64-series and 65-series test sections had losses on the order of 1.5 to 3.0 percent, while flow losses approached 7.5 percent in the section with solid sidewalls, as indicated by the data in Appendix C. It is concluded that, in accordance with the criteria given in References 2 and 4, and from the results of this study, the test section with boundary layer control applied is adequate for two-dimensional compressor blade cascade studies.

Effect of Roughness on Blade Performance

The effects of roughness on blade performance in cascade may be illustrated in two ways:

- - (1) by considering the overall performance in terms of a total pressure loss coefficient and
- (2) by an examination of the more specific effect of roughness on the turbulence and velocity profile characteristics (in the wake vs. free stream).

To study the effects of roughness, investigations of the NACA 64 and 65-series airfoils were made at different roughness levels:

1. Smooth blades (configuration 1 and 11),
2. Blades with the first quarter chord sandblasted (configurations 2 and 12),
3. Blades with 180 grit material applied to first quarter chord (configuration 3 and 13),
4. Blades with 80 grit material applied to first quarter chord (configuration 4 and 14).

A number of parameters have been used to characterize the quality of a surface finish. To follow convention, the average roughness, R_a , and equivalent sand roughness, K_s , were chosen as measures of surface roughness (see Appendix A for R_a and K_s definitions). The values for R_a were obtained by measuring the blade surfaces with a profilometer. Values for K_s were derived from R_a by the relation given by Schaffler (Ref. 11:10) where

$$K_s = 8.9 R_a. \quad (8)$$

Values of Ra and Ks for the cascades of this research are given in Table II.

TABLE II

Airfoil Roughness Data

Conf #	Ra, μm	Ks, μm	Ks/ $l \times 10^3$	Conf #	Ra, μm	Ks, μm	Ks/ $l \times 10^3$
1	0.5	4.45	0.088	11	0.09	0.80	0.016
2	2.7	24.03	0.473	12	1.86	16.55	0.326
3	19.8	122.22	3.47	13	17.95	159.76	3.14
4	26.9	239.41	4.71	14	25.52	227.13	4.47

Total Pressure Loss Coefficient. The total pressure loss coefficient, \bar{w} , was used to characterize the roughness effects for this study. In each case \bar{w} is plotted against the relative sand roughness, Ks/l , where l is the blade chord length. Figures 7 and 8 depict the results for the NACA 64-A905 blades. The loss factor, \bar{w} , varies from 0.0467 for the smooth blade to 0.0733 for the blade roughened with 80 grit abrasive. This is a 56 percent increase in losses for the 33 degree camber angle blades. Results for the NACA 65-A506 blades (Figures 9 and 10) range from 0.0387 to 0.0483 for \bar{w} . This is a 25 percent increase in losses for the blades with 18 degrees of camber.

Referring to Figures 7 and 9, a straight line can be drawn through the data points, indicating a logarithmic function. It can be seen that the losses and the increase in losses for a given increase in relative roughness are greater for the blades with the larger camber angle. One would expect this be the case since the pressure gradient is steeper for

LOSS OF PERFORMANCE WITH RELATIVE SAND ROUGHNESS

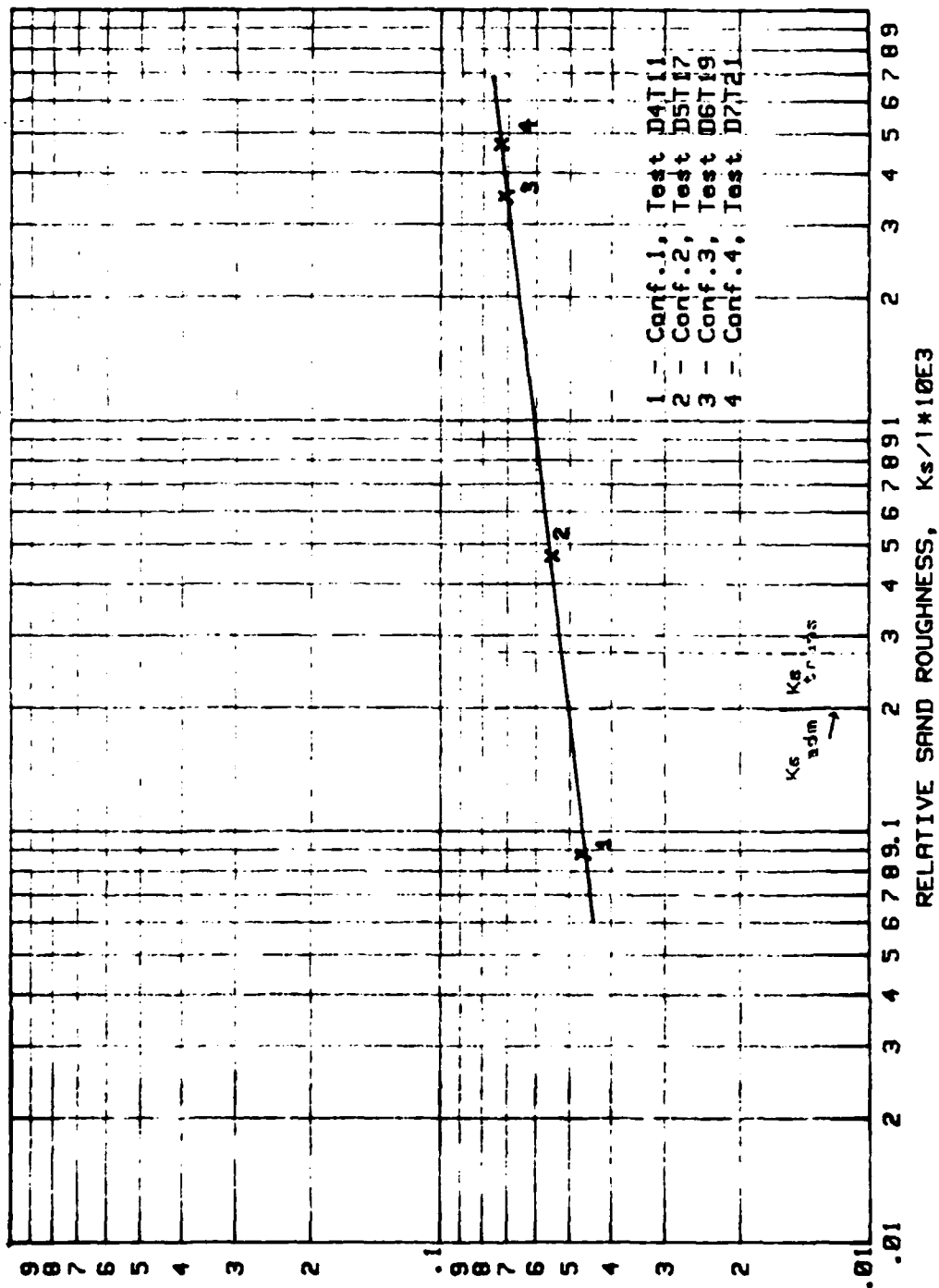


Figure 7. Logarithmic Plot of Performance Loss With Relative Sand Roughness for NACA 64-Series Blades

LOSS OF PERFORMANCE WITH RELATIVE SAND ROUGHNESS

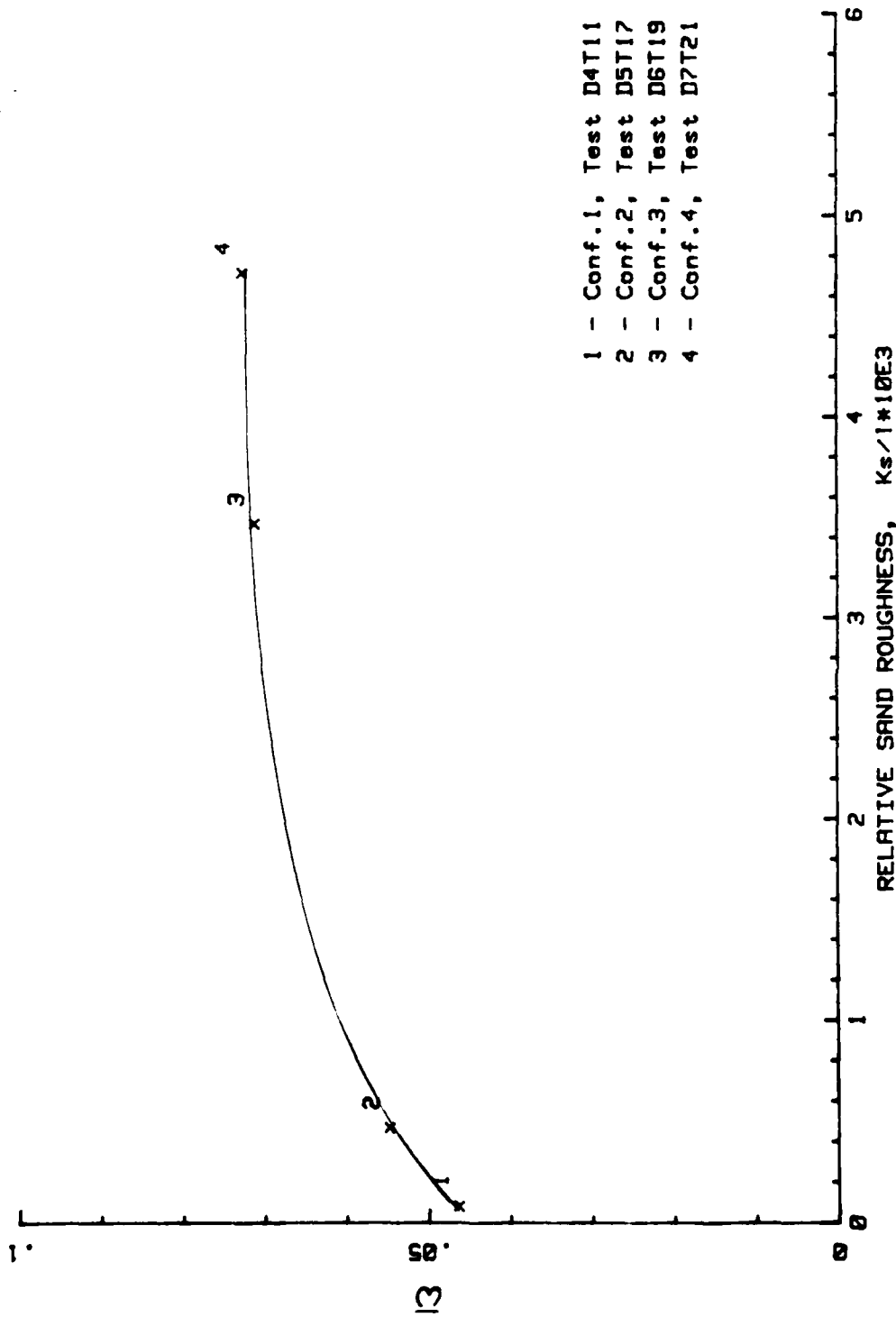


Figure 8. Linear Plot of Performance Loss With Relative Sand Roughness
for NACA 64-Series Blades

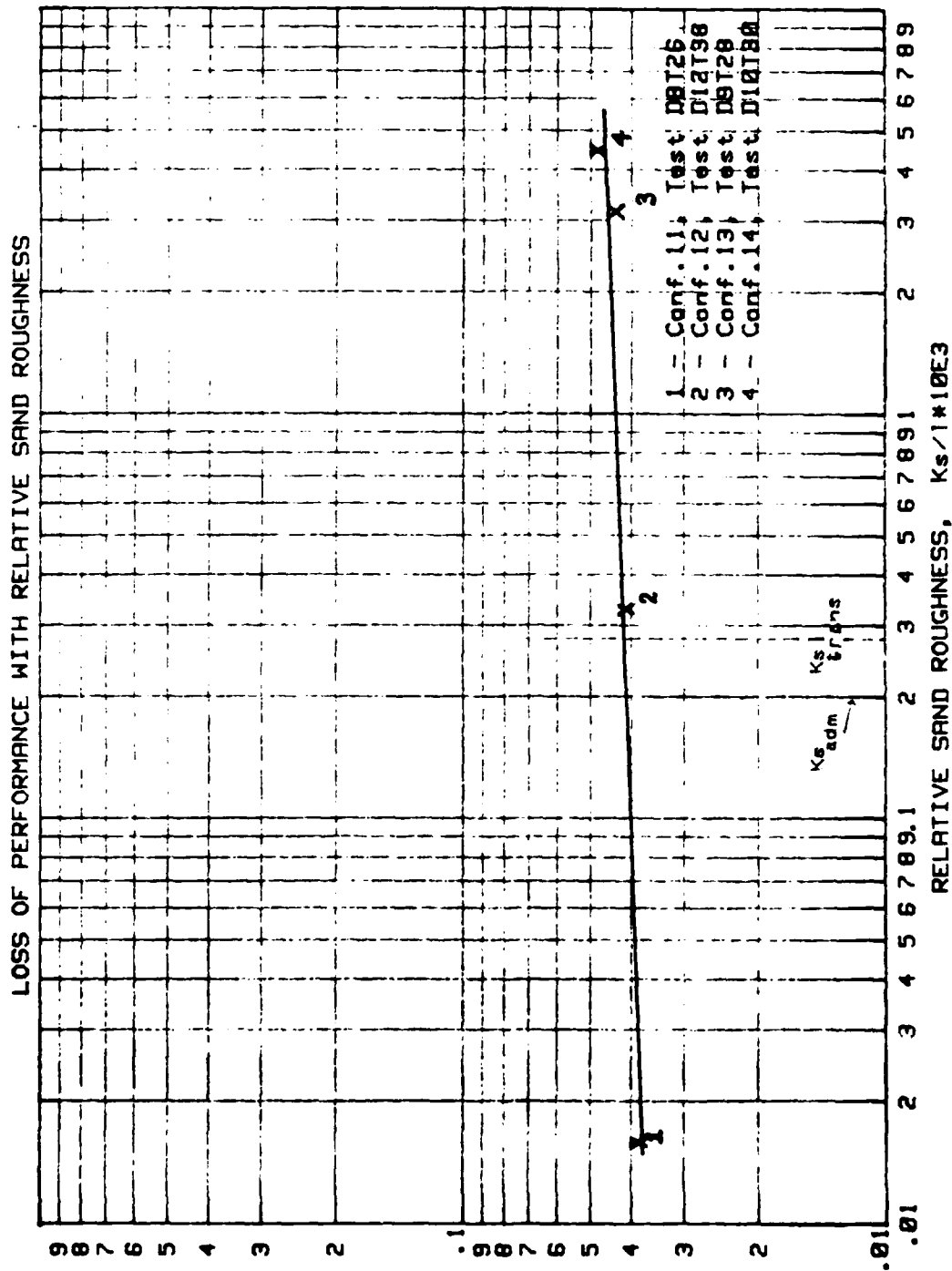


Figure 9. Logarithmic Plot of Performance Loss With Relative Sand Roughness
for NACA 65-Series Blades

LOSS OF PERFORMANCE WITH RELATIVE SAND ROUGHNESS

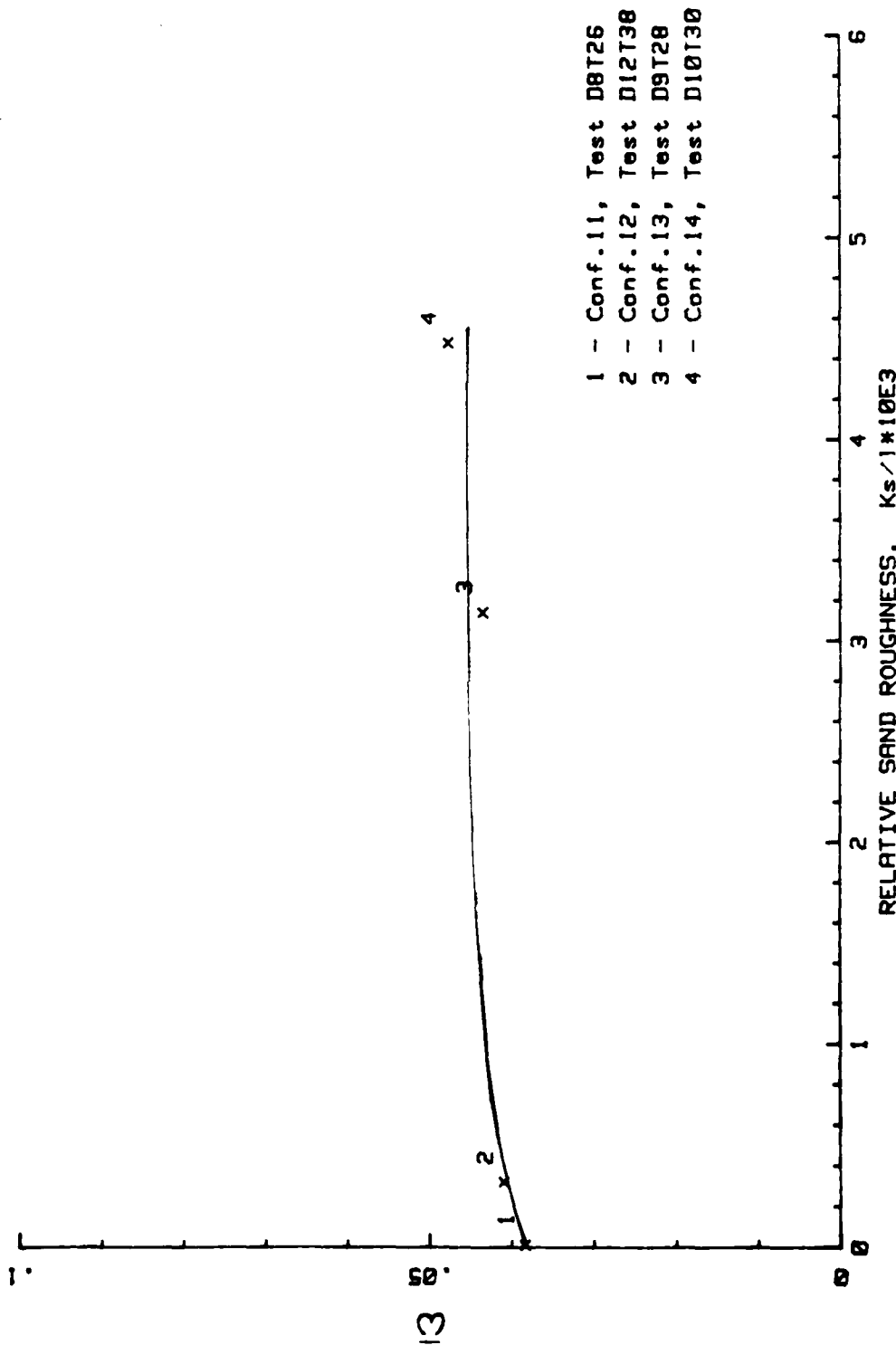


Figure 10. Linear Plot of Performance Loss With Relative Sand Roughness
for NACA 65-Series Blades

greater turning of the flow. The linearity suggests the boundary layer for configurations 2 through 4 is turbulent over much of the blade surface (Ref. 12:663).

Equations relating the loss coefficient to the equivalent sand roughness can be derived for the data obtained within the scope of this investigation. The two equations are:

$$\bar{w} = 0.0614(ks/1 \times 10^3)^{0.117} \quad (3)$$

for the 64 series airfoils with 33 degrees turning angle and

$$\bar{w} = 0.0439(ks/1 \times 10^3)^{0.034} \quad (10)$$

for the 65 series airfoils with 18 degrees turning angle. These relationships should be considered accurate only within the range of this study and should not be extrapolated arbitrarily for design purposes.

There are a number of factors which influence the boundary layer and resulting losses. The turbulence level of the free stream can compound the instability of the laminar boundary layer in the presence of an adverse pressure gradient and induce transition to turbulent flow. The boundary layer can also be disturbed from the inside by surface roughness. There is a limit below which the surface irregularities (specifically, equivalent sand roughness, K_s) do not affect the transition point. That limit is (Ref. 13:335)

$$\frac{W_1 K_{s,trans}}{v_1} < 120 \quad (11)$$

where W_1 is upstream relative velocity and ν_1 is the upstream kinematic viscosity.

Besides causing laminar-turbulent transition, surface roughness can also directly increase the frictional losses. In the turbulent boundary layer friction losses may become substantial once the size of the roughness reaches a particular value relative to the local boundary layer thickness. This value, known as admissible sand roughness, Ks_{adm} , can be approximated by (Ref. 5:174)

$$\frac{Ks_{adm} W_1}{\nu_1} < 90. \quad (12)$$

The values for ks_{trans}/l and ks_{adm}/l for the flow conditions in this investigation are 0.277×10^{-3} and 0.200×10^{-3} respectively and are located between data points one and two. One can see that both Ks_{trans} and Ks_{adm} are functions of the ratio between velocity and kinematic viscosity alone, that is, the Reynolds number per unit length (Ref. 11:10). That means above the limit of Ks_{trans} the losses are dependent only upon the size of the roughness elements. Schaffler (Ref. 11:6) called the flow in this region "turbulent attached flow with hydrodynamically rough surfaces."

Figures 8 and 10 illustrate that even surface roughness of small magnitude has a definite effect on blade losses. Minor deteriorations of the surface quality cause the total pressure losses to increase in greater measure than in the range of larger roughness. For example, the relative roughness, Ks/l , of the 33 degree camber blades, configurations 1 and 2, (Figure 8), increases from 0.088×10^{-3} to 0.479×10^{-3} . The

accompanying total pressure loss rises from 0.0467 to 0.0552, an 18.2 percent increase in losses. Between configurations 3 and 4 there is an increase in K_s/l from 3.469×10^{-3} to 4.713×10^{-3} . The total pressure loss in this case increases only 2.1 percent from 0.0718 to 0.0733. Results are similar, though smaller in magnitude, for the 18 degree camber blades. These results indicate that decreases in surface quality should be kept to a minimum to avoid significant increases in losses.

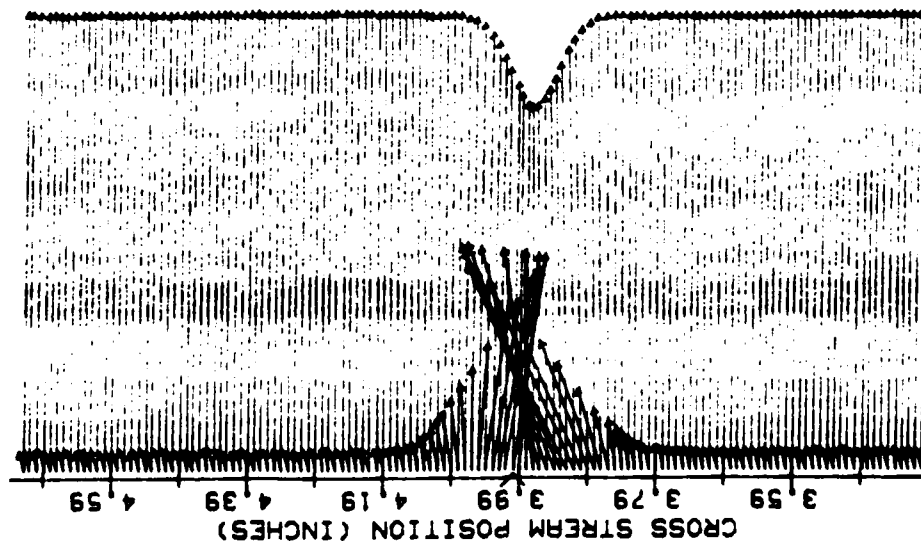
Exit Velocity and Turbulence Intensity Profiles. Velocity and turbulence intensity information at each traverse (cross stream) point was resolved into X and Y components and plotted vectorially as shown in Figures 11, 12, 13, and 14 for the NACA 64-A905 blade exit profiles obtained at the 1.25-inch (0.63 chord) traverse plane. A complete set of exit profiles at the five traverse planes is contained in Appendix D. The origin of each vector is the survey position and the length of each vector is proportional to the velocity or turbulence intensity. Scale factors are given for velocity (thin black lines) and turbulence (heavy black lines) as 167 (ft/sec)/inch and 8 percent/inch, respectively.

Turbulence intensity, Tu , as used in this study is defined as

$$Tu = \frac{V_{rms}}{V_{x_{mean}}} \quad (13)$$

where V_{rms} is the root mean square of the time varying velocity and $V_{x_{mean}}$ is the mean value of the streamwise velocity component. The effect of roughness on turbulence intensity (measured at 0.63 chord traverse plane) is plotted for the NACA 64-A905 blades in Figure 15 and for the NACA 65-A506 blades in Figure 16.

VANE WAKE: CONF. NO.1, EVAL. NO.11
 TRAVERSE NO. 2.00 AT 1.25 INCHES



0 1 2 3
 SCALE (INCHES)

--- VEL. SCALE=167.00 (FT/SEC)/INCH
 --- % TURB INT SCALE= 8.00 %/INCH

INLET VEL= 501.00 +/- 2.00 FT/SEC
 CORRECTED INLET VELOCITY= 500.00 FT/SEC
 NOMINAL FLUX TURNING ANGLE= 31.00 DEG
 EXIT WALL DIVERGENCE ANGLE= .00 DEG
 REF NO = 0 4.00 1 11.00
 DATE: 10.00 0.00 04.00 , VANE CONF: 1.00

Figure 11. Velocity and Turbulence Intensity Profile Conf No. 1 Traverse No. 2: $Ks/1-.088 \times 10^{-3}$

VANE WAKE: CONF. NO.2, EVAL. NO.1, SANDED BLADE
 TRAVERSE NO. 2.00 AT 1.25 INCHES

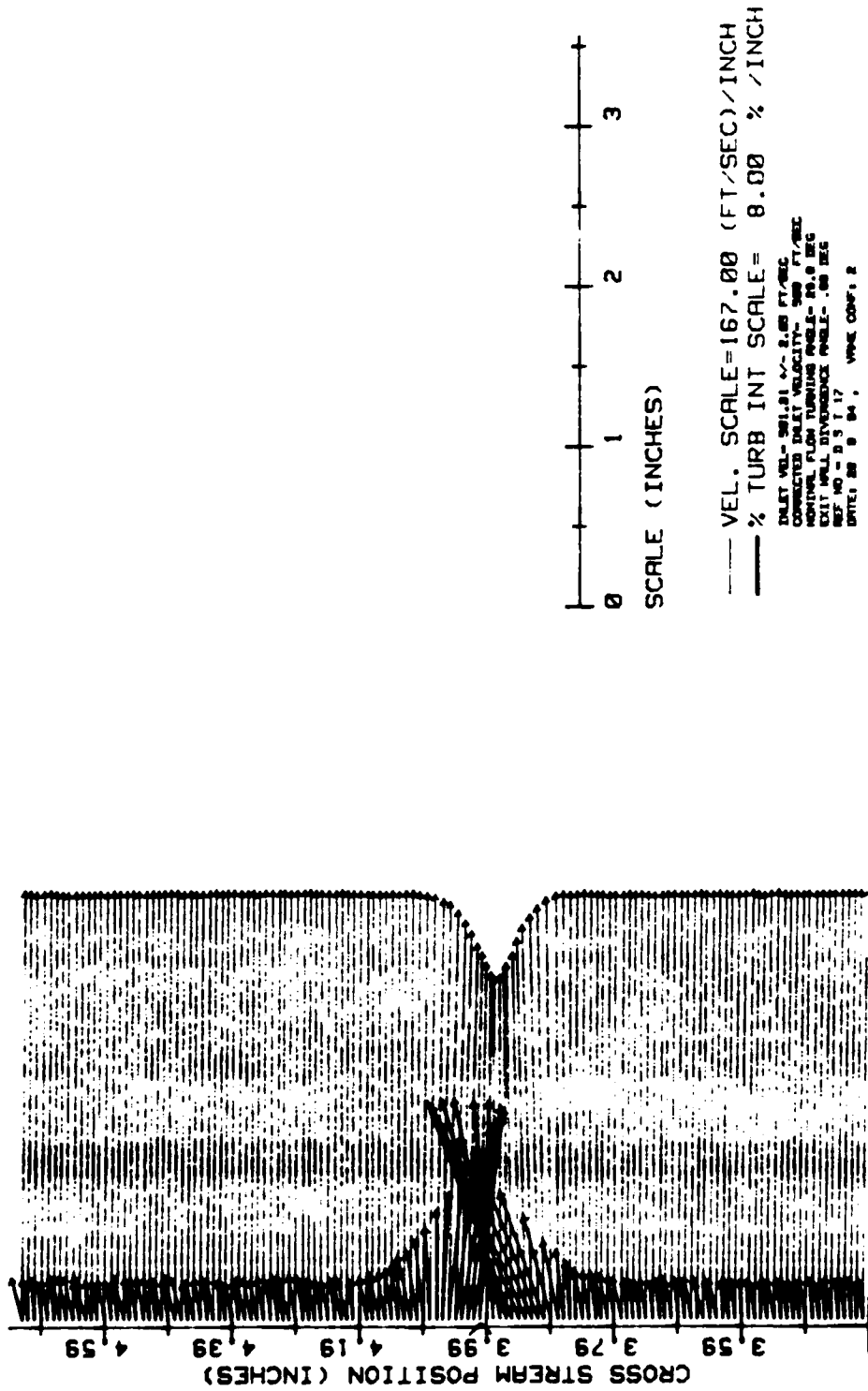
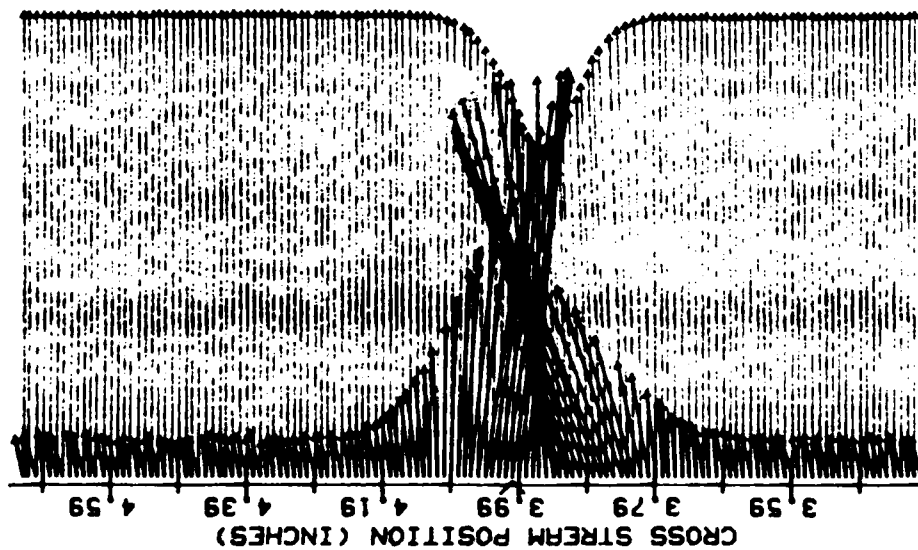


Figure 12. Velocity and Turbulence Intensity Profile Conf No. 2 Traverse No. 2: $Ks/1 = .473 \times 10^{-3}$

VRNE WAKE: CONF. NO.3, EVRL. NO.1 Ra-19.8 micrometers
TRAVERSE NO. 2.00 AT 1.25 INCHES



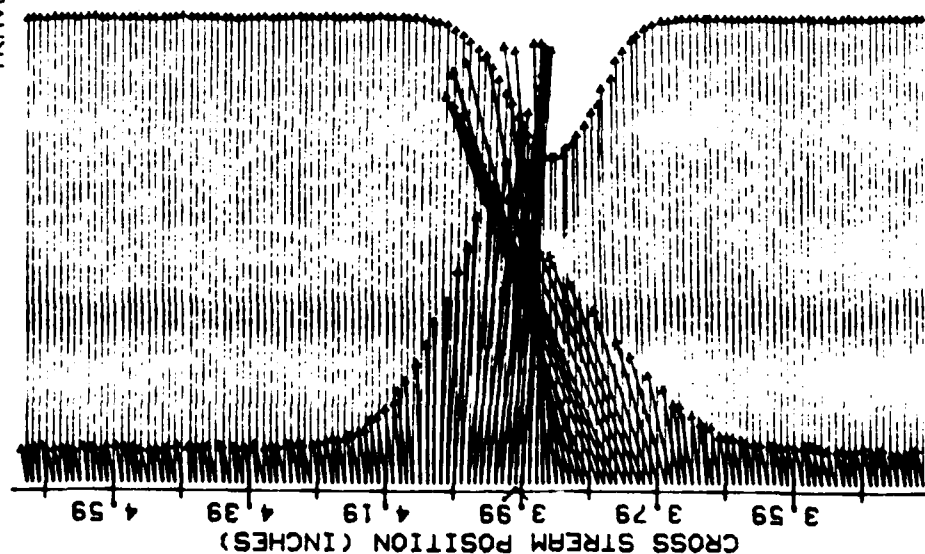
0 1 2 3
SCALE (INCHES)

— VEL. SCALE=167.00 (FT/SEC)/INCH
- - - % TURB INT SCALE= 8.00 % /INCH

INLET VEL= 490.48 +/- 1.00 FT/SEC
CORRECTED INLET VELOCITY= 500 FT/SEC
CORRECTION FACTOR= 1.02
INLET FLUX TURNING ANGLE= 25.5 DEG
INLET VELOCITY ANGLE= 174 DEG
INLET NO. 20 1.10
INLET 27 0.04, VRNE CONF. 8

Figure 13. Velocity and Turbulence Intensity Profile Conf No. 3 Traverse No. 2: $Ks/1-3.47 \times 10^{-3}$

VANE WAKE: CONF. NO. 4, EVAL. NO. 1 $Re=26.9$ micrometers
 TRAVERSE NO. 2.00 AT 1.25 INCHES



SCALE (INCHES)

VEL. SCALE=167.00 (FT/SEC)/INCH
 % TURB INT SCALE= 8.00 %/INCH

INLET VEL= 488.48 +/- 3.84 FT/SEC
 CORRECTED INLET VELOCITY= 500 FT/SEC
 CORRECTED FLOW RATE= 27.3 IN³/SEC
 EXIT WALL DISTANCE WAKE= 1.79 IN
 REF NO= 0.7 1.21 VANE CONF= 4
 DATE: 29 8 84

Figure 14. Velocity and Turbulence Intensity Profile Conf No. 4 Traverse No. 2: $Ks/1-4.71 \times 10^{-3}$

The effect of roughness on the velocity profiles is illustrated for configurations 1 through 4 in Figures 11 through 14, respectively. There is an overall deepening and broadening of the velocity decrement in the blade wake as the relative roughness increases. A slight decrease in wake width is evident between configurations 1 and 2 (Figures 11 and 12). At larger roughness levels, however, the wake again increases (Figures 12, 13, and 14).

It can be seen from Figures 11 through 16 that with increasing roughness there is an increase of Tu in both magnitude and affected wake area. There is an increase in the free stream turbulence intensity for configuration 2 in comparison to configuration 1 (Figures 11 and 12). The level of free stream turbulence then remains fairly constant, even though the relative roughness is further increased (Figures 12, 13, and 14).

Figures 15 and 16 illustrate the variation of Tu with relative roughness in another way. The two figures depict mass-averaged Tu values for the blade wake and entire blade channel (1.333 inches) plotted against relative roughness. Values of free stream Tu are also shown. For both cascade test sections, the mass-averaged turbulence intensity ("Channel Tu ") increases significantly for small increases in roughness (data points 1 and 2). Between points 2 and 4 values for blade channel and free stream Tu vary fairly linearly, but with a smaller incline, with increasing relative roughness. It is believed (Ref. 20) that the initial sharp increase in Tu is caused by the transition of the boundary layer over the blade from laminar to turbulent. As a result, turbulent fluctuations propagate across the

TURBULENCE INTENSITY LEVEL WITH RELATIVE SAND ROUGHNESS

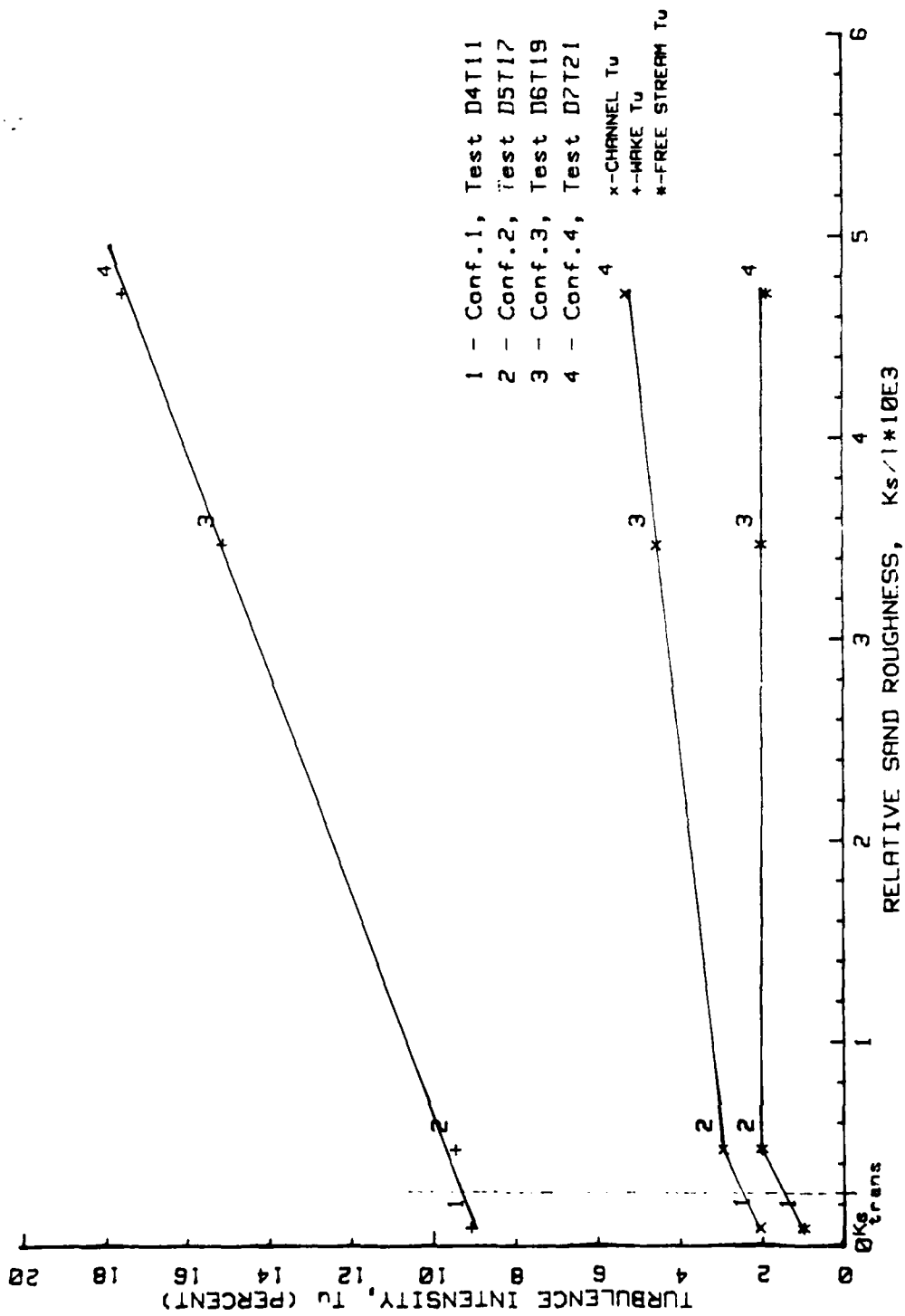


Figure 15. Turbulence Intensity With Relative Sand Roughness For NACA 64-Series Airfoil

TURBULENCE INTENSITY LEVEL WITH RELATIVE SAND ROUGHNESS

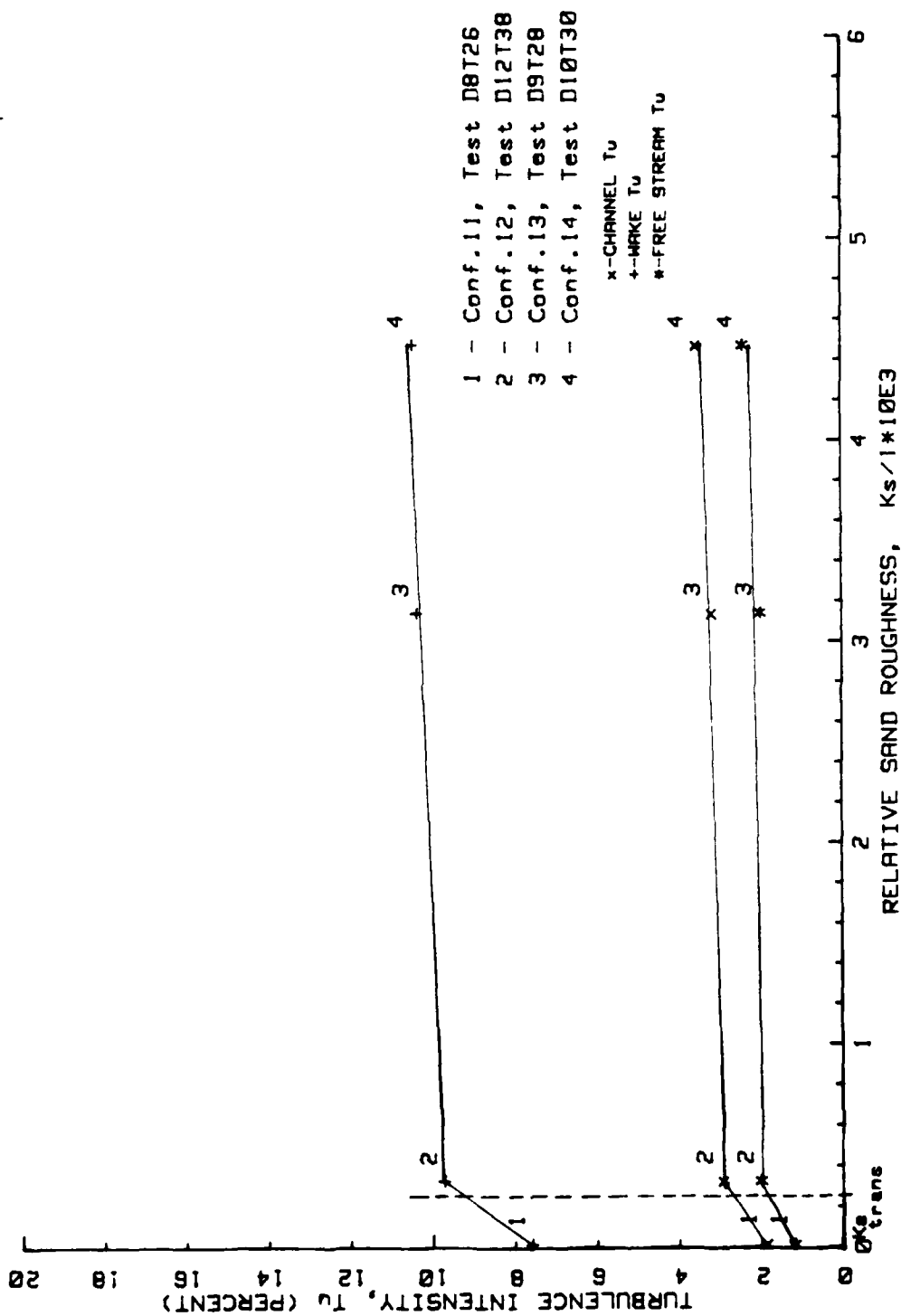


Figure 16. Turbulence Intensity With Relative Sand Roughness For NACA 65-Series Airfoil

blade passage at approximately the speed of sound causing the Tu in the mainstream to be higher than when much of the boundary layer was laminar. Once the free stream becomes turbulent because of the excitation of the boundary layer, further increases of roughness would make the boundary layer thicker but would not increase the free stream Tu .

By comparing the wake Tu of the 64-series blades (Figure 15) with that of the 65-series blades (Figure 16), it can be seen that surface roughness has a much greater effect on the wake Tu of the NACA 64-A905 airfoils. The wake Tu data for the 65-series blades increases in a manner similar to the channel and free stream Tu for that blade. There is a significant initial increase in Tu then almost no further increase of wake Tu even though there is a ten-fold increase in roughness. The wake Tu data for the 64-series blades continues to increase steadily with increasing roughness over the entire range. It appears that there is a relationship between the influence of roughness on the blade wake Tu and the camber of the airfoil. A possible explanation is that the flow over the more highly cambered blade is separated, whereas the flow over the lower cambered blade is not separated for any of the roughness configurations tested. As the degree of roughness is increased on the blade with the higher camber the boundary layer, which is already separated at some point on the blade, thickens and becomes more susceptible to earlier separation. This causes a shift in the separation point towards the blade leading edge. As the point of separation moves forward the wake continues to grow with an accompanying increase in wake Tu (Ref. 20).

A comparison of the plots of turbulence intensity, Tu , vs. relative sand roughness (Figures 15 and 16) and total pressure loss coefficient, $\bar{\omega}$, vs. relative roughness (Figures 8 and 10) suggests in the range of this investigation three effects of roughness are encountered:

- (1) A small increase in roughness produces a doubling of free stream turbulence with practically no effect on the wake. This effect might not be noticed at all if the free stream turbulence were higher, as in an actual turbomachine.
- (2) Further increase in surface roughness produces a substantial effect on the wake but little effect on the free stream turbulence. Both of these affect $\bar{\omega}$ since it is determined from mass-averaged values over the entire blade channel.
- (3) Surface roughness has a much greater influence on blade wake Tu over the entire range of roughness tested for the higher camber airfoils than for the lower camber airfoils.

V. Conclusions and Recommendations

Conclusions

This study was concerned with developing a facility to provide two-dimensional flow for investigations of compressor blade cascades and exploring the effects of roughness on different airfoils in cascade. Two blade profiles, the NACA 64-A905 and NACA 65-A506 were used. Existing criteria of Erwin and Emery (Ref. 4) and Briggs (Ref. 2) were used to determine when two-dimensional flow was achieved. As a result of this study, the following conclusions are drawn.

1. Through the use of sidewall boundary layer control, a facility has been established that permits two-dimensional flow investigation over the center span (about $2/3$ the width of the blade) of an airfoil in cascade.
2. The initial small increases of roughness have a much greater effect on blade total pressure loss than do subsequent larger roughness values.
3. A small increase in roughness produces a substantial increase in free stream turbulence (and $\bar{\omega}$) with practically no effect on the wake. This effect might not be noticed at all if the free stream turbulence were higher, as in an actual turbomachine.
4. Further increase in roughness produces a substantial effect on the wake but little effect on the free stream turbulence.

5. Surface roughness appears to have a much greater influence on blade wake Tu for the higher camber airfoils tested than for lower camber airfoils.

-Recommendations

The findings of this investigation suggest that compressor blade roughness should be kept as small as practicable. It is recommended that additional study on blade performance be accomplished as follows:

1. Investigate the influence of free stream turbulence on the blade wakes of roughened airfoils in cascade by varying the turbulence intensity in the test section upstream of the cascade,
2. Determine the existence of a relationship between the camber angle and blade wake Tu by making a series of tests on airfoils of increasing camber angles and,
3. Conduct a more detailed study of the pressure distribution and boundary layer over the blade over a range of roughness values.

APPENDIX A: ROUGHNESS DEFINITIONS

Surface roughness is defined as "the arithmetical average deviation expressed in microinches (or micrometers) measured normal to the centerline" (Ref. 7). The arithmetic average is denoted by the symbol, R_a and is shown to be

$$R_a = \int \frac{1}{L} |Y| dx \quad (14)$$

where the variables are defined as

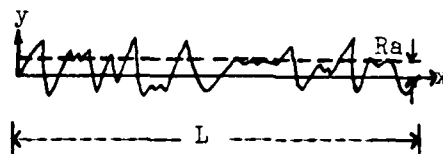


Figure 17: Arithmetic Average Roughness

Although this roughness definition does not totally characterize the surface quality, it is the definition most commonly used. For other definitions that may be used to characterize the surface, see Ref. 15.

The other definition for roughness used in this investigation is K_s , or equivalent sand roughness, the parameter which characterized the surface finishes in Nikuradse's roughness experiments (Ref. 9). Equivalent sand roughness describes a particular form of roughness which consists of tightly packed granules of sand of grain size K_s .

APPENDIX B

Development of Adiabatic Efficiency of the Cascade

Adiabatic efficiency for a compression process is defined in terms of static enthalpies as

$$\eta_a = \frac{h_2' - h_1}{h_2 - h_1} \quad (15)$$

In the above equation h_1 is upstream enthalpy, h_2 is the downstream enthalpy, and h_2' is the downstream enthalpy resulting from isentropic compression. The compression process may be seen in Figure 18.

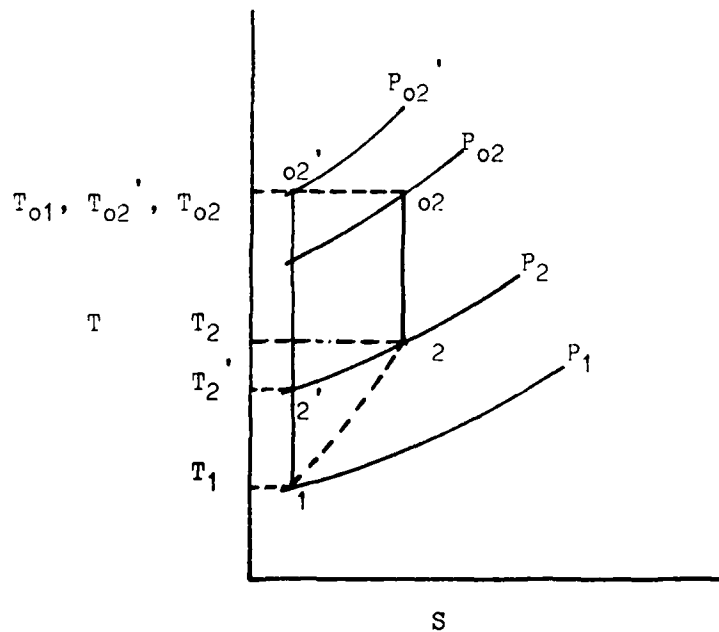


Figure 18: Temperature-Entropy Plot of Compression Process

One can see by the diagrams that the actual process, 1 to 2, produces a larger enthalpy rise.

The values for T_{01} , V_2 , P_1 , and P_2 are measured quantities. If the steady flow energy equation is written out as

$$1q_2 + h_1 + \frac{V_1^2}{2} = 1w_2 + h_2 + \frac{V_2^2}{2} \quad (16)$$

and $1q_2$ and $1w_2$ are both zero for a stationary, adiabatic blade row, then h_2 is

$$h_2 = h_1 + \frac{V_1^2}{2} - \frac{V_2^2}{2} \quad (17)$$

This can be rewritten as

$$h_2 = h_{01} - \frac{V_2^2}{2} \quad (18)$$

Isentropic equations are used to calculate T_2' , where

$$T_2' = T_1(P_2/P_1)^{(\gamma-1)/\gamma} \quad (19)$$

The enthalpy, h_2' , may then be determined from T_2' using the Gas Tables for air (Ref. 6). Finally, the adiabatic efficiency is calculated.

Two examples of the blade adiabatic efficiency are tabulated in Table III. The values are for NACA 64-A905 airfoils with and without boundary layer control applied.

TABLE III

Comparison of Adiabatic Efficiency

<u>Parameter</u>	<u>With B. L Control</u>	<u>Without B. L. Control</u>	(Ref. 17)
$T_1, ^\circ\text{F}$	97.73	96.21	
$T_{01}, ^\circ\text{F}$	118.7	116.3	
$h_1, \text{B/lbm}$	133.24	132.95	
$h_{01}, \text{B/lbm}$	138.28	137.73	
$V_2, \text{f/sec}$	420.65	414.7	
P_1, psia	13.84	14.12	
P_2, psia	14.33	14.49	
γ	1.4	1.4	

Calculated Values

$h_2, \text{B/lbm}$	134.75	134.31
$T_2, ^\circ\text{F}$	103.01	100.33
$h_2', \text{B/lbm}$	134.58	133.94
η_a	0.892	0.727

One can readily see the dramatic increase in blade efficiency when boundary control is used.

APPENDIX C: Non-dimensional Total Pressure Loss Data
For NACA 65-A506 Airfoils

***** TOTAL PRESSURE MAP AT 1.25 INCHES BEHIND BLADES 4 AND 5 *****
SOLID WALLS INSTALLED

Nominal Flow Turning Angle= 17 Deg., Exit Wall Divergence Angle= .61 Deg
Inlet Reynolds Number Per Foot= 2.66 Million

CHANNEL POSITION	SPANWISE POSITION IN INCHES				
	1.00	0.75	0.50	0.25	0.125
.992	.2771	.2812	.2893	.2426	.2602
.972	.2467	.2508	.271	.3251	.3593
.952	.1555	.1641	.1993	.3775	.4271
.932	.0901	.0938	.1152	.3967	.4572
.911	.0667	.0674	.0708	.3854	.4584
.891	.0676	.0642	.0583	.3001	.4379
.871	.0656	.0648	.0619	.2688	.3687
.851	.0673	.0649	.063	.1769	.2678
.83	.0662	.0639	.0601	.1094	.2208
.81	.0665	.0639	.0634	.0695	.1356
.79	.0681	.0655	.0619	.0585	.1451
.77	.0678	.0643	.0621	.0553	.1383
.749	.0671	.067	.0663	.0606	.0885
.729	.0662	.0653	.0646	.0524	.1005
.709	.0666	.0636	.0653	.0569	.0872
.689	.067	.0648	.0674	.0597	.0882
.668	.0657	.0666	.0678	.0579	.0897
.648	.067	.0673	.0712	.0577	.0829
.628	.0669	.0652	.0708	.0547	.0896
.608	.0648	.0644	.0737	.0612	.0819
.587	.0663	.0662	.0709	.0631	.0891
.567	.0673	.0667	.0711	.0624	.0773
.547	.068	.0634	.069	.0669	.0873
.527	.0653	.0653	.0672	.0663	.0852
.506	.0654	.0655	.0688	.0669	.0877
.486	.0643	.0644	.067	.0665	.0779
.466	.066	.0653	.0675	.0653	.0769
.446	.0666	.0666	.0695	.0657	.0865
.425	.0661	.0658	.0713	.0652	.0852
.405	.066	.0666	.0717	.0693	.0825
.385	.0667	.0668	.0708	.0711	.0873
.365	.0652	.0693	.0755	.07	.079
.344	.0655	.0676	.0723	.07	.0766
.324	.069	.0685	.0711	.071	.0765
.304	.0672	.0687	.0728	.0698	.0868
.284	.0667	.069	.0715	.0664	.0777
.263	.0656	.0688	.0704	.0694	.0928
.243	.0678	.0702	.0705	.0662	.0823
.223	.0663	.0706	.071	.0683	.0805
.203	.0675	.0708	.0726	.0648	.0788
.182	.0669	.0692	.0747	.0705	.0824
.162	.0672	.073	.0736	.0721	.0831
.142	.0647	.072	.0727	.072	.0784
.122	.0657	.0698	.0729	.0736	.0782
.101	.0645	.0704	.0732	.0741	.0783
.081	.0715	.0746	.0798	.077	.0749
.061	.1268	.1194	.1317	.0929	.0963
.041	.2248	.2189	.2349	.1561	.1509
.02	.285	.29	.3038	.2544	.2706
0	.2411	.2532	.2727	.3563	.3912

***** TOTAL PRESSURE MAP AT 1.25 INCHES BEHIND BLADES 4 AND 5 *****
 POROUS WALLS INSTALLED

Nominal Flow Turning Angle= 18 Deg., Exit Wall Divergence Angle= .95 Deg
 Inlet Reynolds Number Per Foot= 2.67 Million

CHANNEL POSITION	SPANWISE POSITION IN INCHES				
	1.00	0.75	0.50	0.25	0.125
.992	.1166	.1347	.1454	.0991	.0517
.972	.1669	.1963	.2073	.1697	.1007
.952	.1879	.2049	.2231	.2065	.1719
.932	.1537	.1609	.174	.2691	.2446
.911	.0894	.0734	.0962	.289	.2946
.891	.0337	.0212	.0317	.2567	.3191
.871	.0105	.0061	.008	.2231	.3208
.851	.0078	.0087	.0089	.1807	.2599
.83	.0097	.01	.0067	.1109	.2038
.81	.0135	.0098	.0105	.058	.104
.79	.0108	.0114	.0065	.0225	.077
.77	.0139	.0117	.0096	.0024	.0323
.749	.0123	.0118	.0103	.0024	.0181
.729	.0124	.0115	.0083	.0078	.0155
.709	.0127	.0136	.0099	.0023	.0181
.689	.0115	.0132	.0126	.0076	.0354
.668	.0136	.0125	.0158	.0056	.0129
.648	.0127	.011	.0163	.006	.012
.628	.0114	.0164	.0191	.0102	.0132
.608	.0147	.0156	.0182	.0098	.0136
.587	.0157	.0151	.0169	.0121	.0089
.567	.0152	.0159	.0174	.0108	.0058
.547	.0133	.0163	.0141	.0118	.0115
.527	.0137	.0151	.0159	.0104	.0161
.506	.0161	.0158	.0162	.0163	.021
.486	.0154	.0164	.0183	.0146	.0171
.466	.0133	.017	.0176	.0183	.0243
.446	.0169	.02	.0198	.0162	.0157
.425	.0142	.0208	.0184	.0152	.0225
.405	.0159	.02	.0202	.0171	.0175
.385	.0185	.0187	.021	.0171	.0182
.365	.0166	.0194	.0226	.018	.0224
.344	.0203	.021	.0229	.0165	.0183
.324	.0198	.0209	.0249	.0202	.0202
.304	.0204	.0217	.0228	.0217	.0261
.284	.0188	.0215	.0237	.0207	.0226
.263	.0191	.0244	.0245	.0202	.0245
.243	.0191	.0237	.0213	.0185	.0256
.223	.0201	.0231	.0245	.016	.0298
.203	.0194	.0225	.0258	.0182	.0291
.182	.0224	.0207	.025	.0167	.0289
.162	.0206	.0233	.0269	.0202	.0281
.142	.0198	.026	.0314	.0225	.0271
.122	.0212	.0219	.029	.0242	.025
.101	.0196	.024	.0282	.0268	.0242
.081	.0184	.0231	.0281	.0261	.0281
.061	.0287	.0265	.0369	.027	.0233
.041	.0488	.0466	.0778	.0442	.035
.02	.0968	.122	.1481	.1135	.0752
0	.1433	.155	.1747	.1925	.1316

APPENDIX D: Velocity and Turbulence Intensity Profiles

VANE WAKE: CONF. NO.1, EVAL. NO.11
TRAVERSE NO. 1.00 AT .25 INCHES

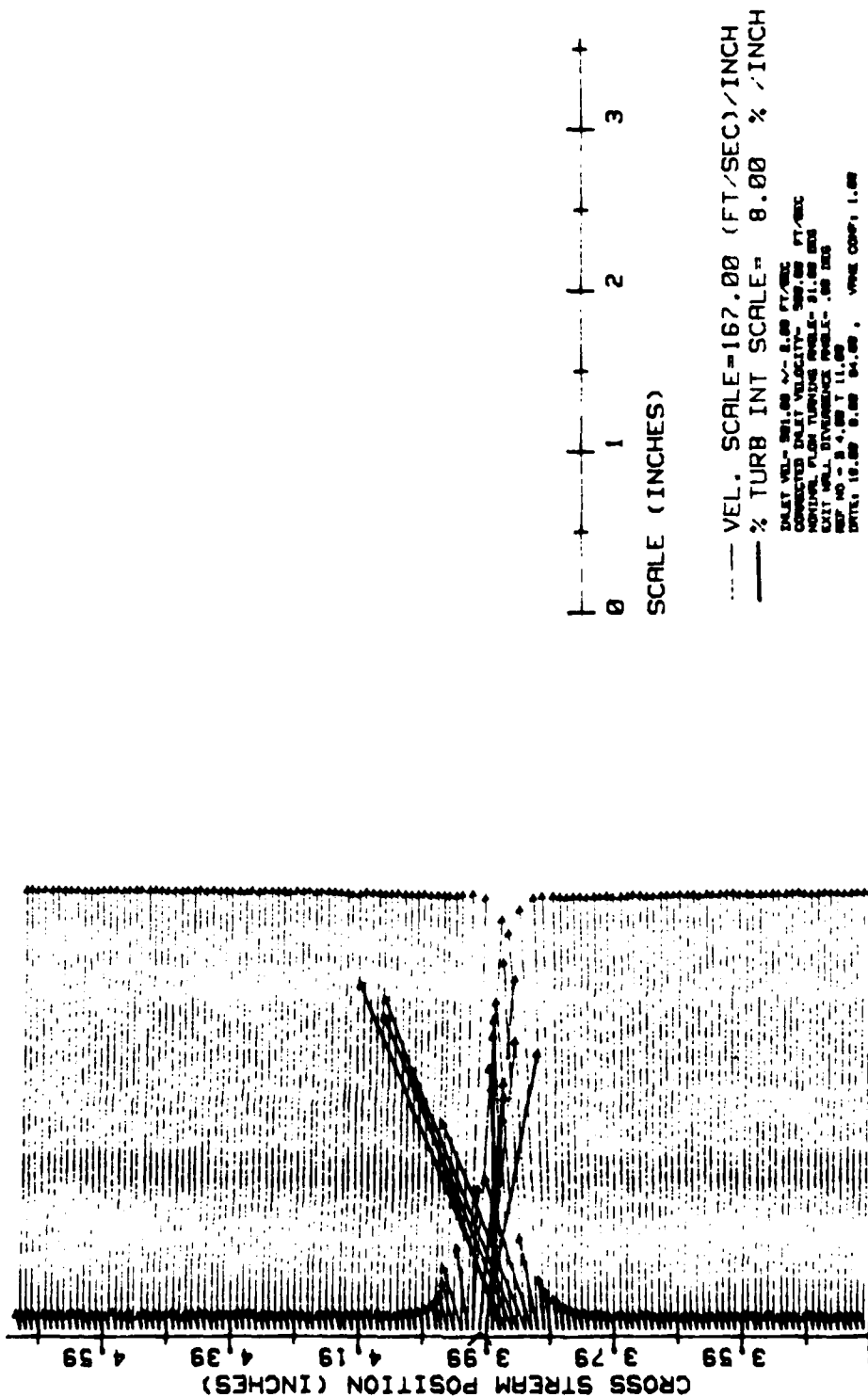
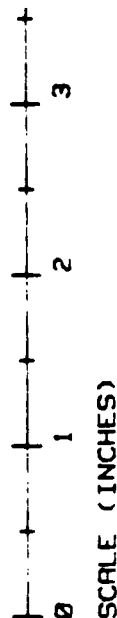
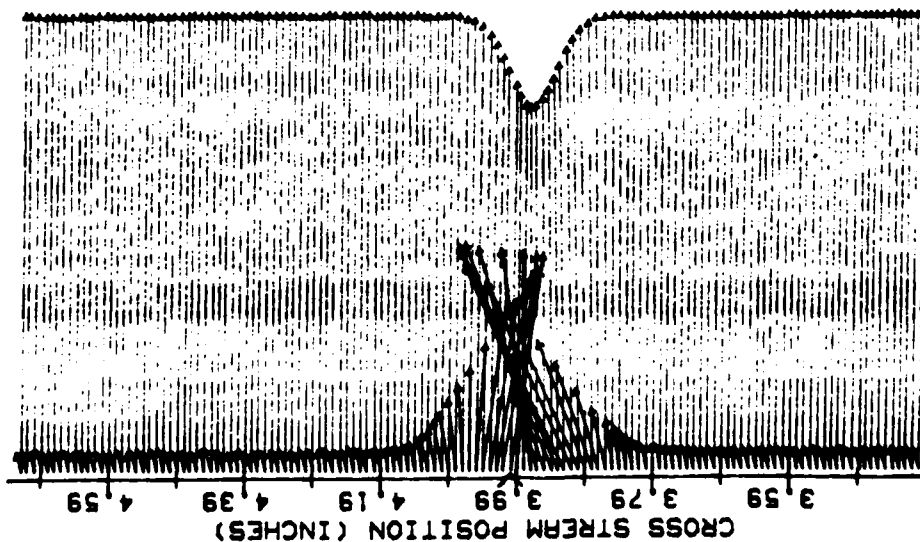


Figure 19a. Velocity and Turbulence Intensity Profile Conf No. 1, Traverse No. 1

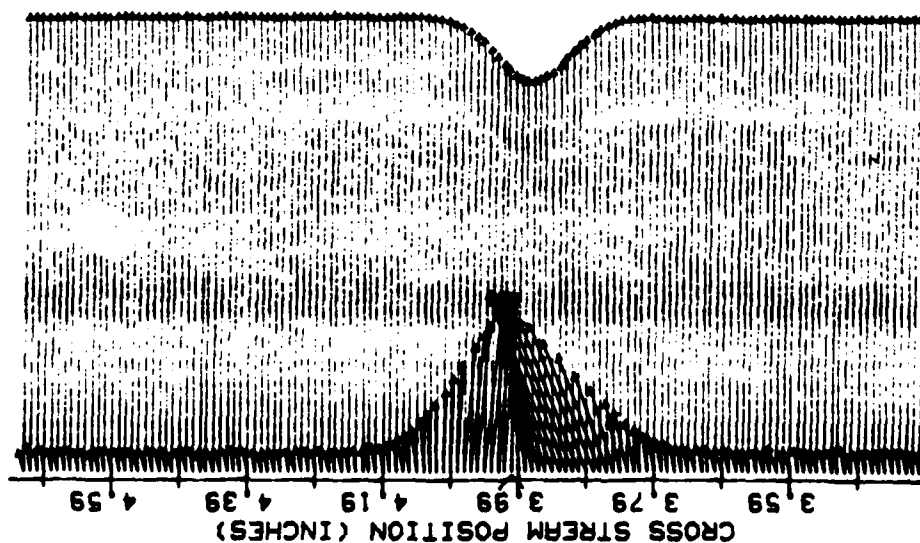
VANE WAKE: CONF. NO.1, EVAL. NO.11
 TRAVERSE NO. 2.00 AT 1.25 INCHES



— VEL. SCALE=167.00 (FT/SEC)/INCH
 — % TURB INT SCALE= 8.00 % /INCH
 INLET VEL= 281.00 +/- 2.00 FT/SEC
 CORRECTED INLET VELOCITY= 589.00 FT/SEC
 NOMINAL PLAN TURNING ANGLE= 91.00 DEG
 EXIT WHEEL TURNING ANGLE= .00 DEG
 REF NO= 9.4.00 T 11.00
 DATE: 10.00 0.00 04.00, VANE CONF: 1.00

Figure 19b. Velocity and Turbulence Intensity Profile Conf No. 1, Traverse No. 2

VANE WAKE: CONF. NO.1, EVAL.. NO.11
 TRAVERSE NO. 3.00 AT 2.25 INCHES



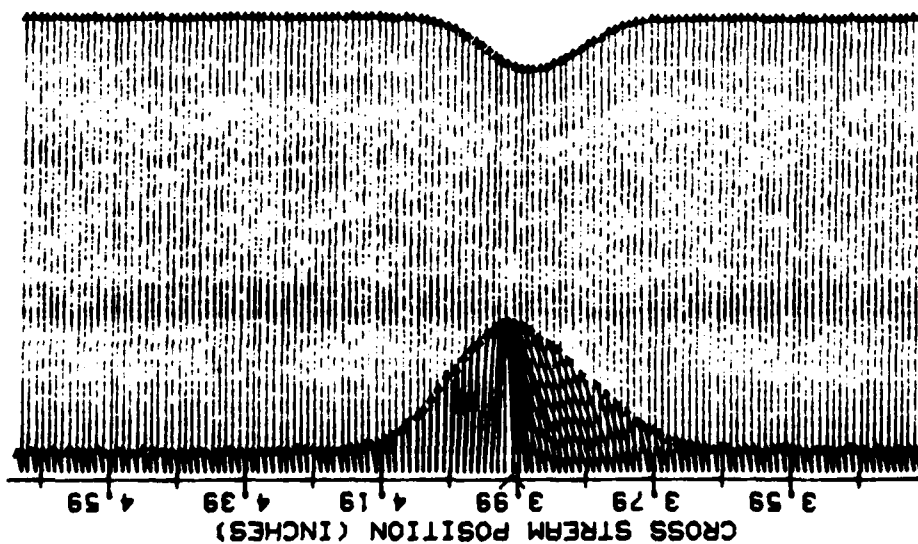
0 1 2 3
 SCALE (INCHES)

— VEL. SCALE=167.00 (FT/SEC)/INCH
 — % TURB INT SCALE= 8.00 % /INCH

INLET VEL= 501.00 +/- 2.00 FT/SEC
 CORRECTED INLET VELOCITY= 500.00 FT/SEC
 NOMINAL PLUM TUNING PEEK= 31.00 DEG
 EXIT WELL DISTANCE= 11.00 DEG
 INLET 10.00 0.00 0.00, VANE CONF. 1.00

Figure 19c. Velocity and Turbulence Intensity Profile Conf No. 1, Traverse No. 3

VARNE WAKE: CONF. NO. 1, EVRL. NO. 11
 TRAVERSE NO. 4.00 AT 3.25 INCHES



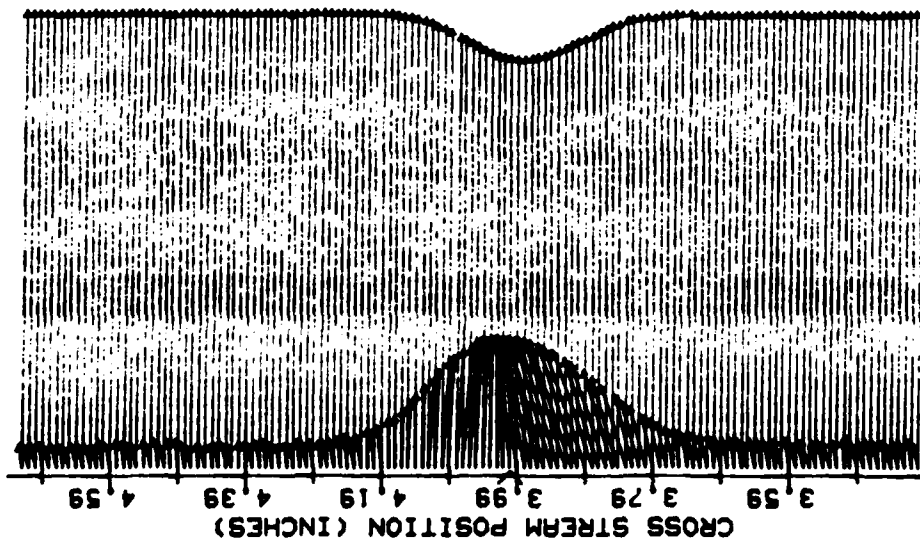
0 1 2 3
 SCALE (INCHES)

--- VEL. SCALE=167.00 (FT/SEC)/INCH
 --- % TURB INT SCALE= 8.00 % /INCH

INLET VEL= 591.00 +/- 2.00 FT/SEC
 CORRECTED INLET VELOCITY= 589.00 FT/SEC
 NOMINAL FLUX TURBIDITY= 21.00 DEG
 EXIT WALL TURBIDITY= 21.00 DEG
 EXIT NO. 9.00 +/- 11.00
 INLET 18.00 9.00 91.00, VARNE CONF. 1.00

Figure 19d. Velocity and Turbulence Intensity Profile Conf No. 1, Traverse No. 4

VANE WAKE: CONF. NO.1, EVAL. NO.11
TRAVERSE NO. 5.00 AT 4.25 INCHES



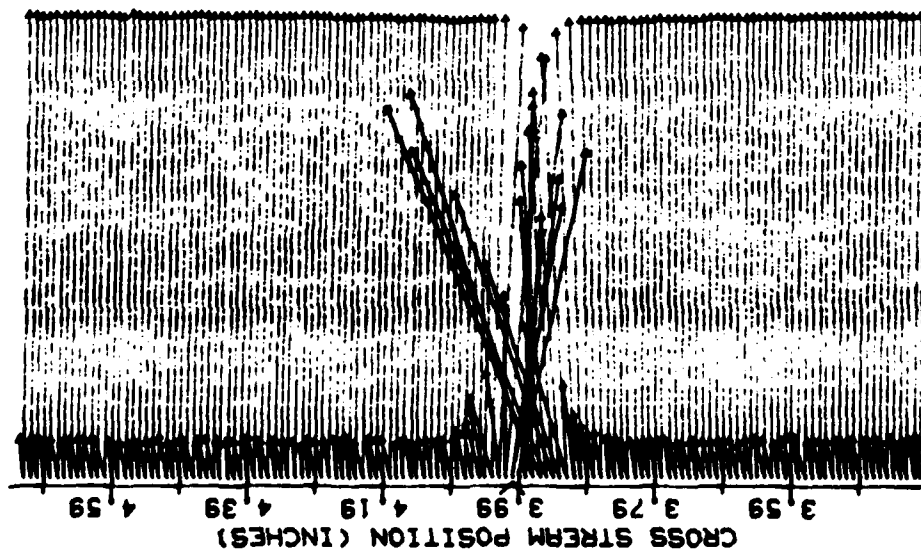
0 1 2 3
SCALE (INCHES)

— VEL. SCALE=167.00 (FT/SEC)/INCH
--- % TURB INT SCALE= 8.00 % /INCH

INLET VEL= 201.00 +/- 2.00 FT/SEC
CORRECTED INLET VELOCITY= 200.00 FT/SEC
NOMINAL FLOW TURNING ANGLE= 21.00 DEG
EXIT WALL STRESS= 0.00 LBS
REF NO = 3 4.00 T 11.00
DATE: 10.00 0.00 04.00 , VANE CONF: 1.00

Figure 19e. Velocity and Turbulence Intensity Profile Conf No. 1, Traverse No. 5

VANE WAKE: CONF. NO.2, EVAL. NO.1, SANDED BLADE
TRAVERSE NO. 1.00 AT .25 INCHES



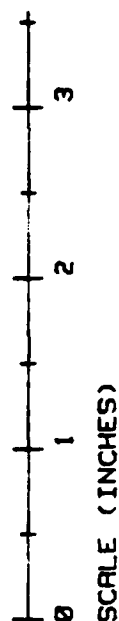
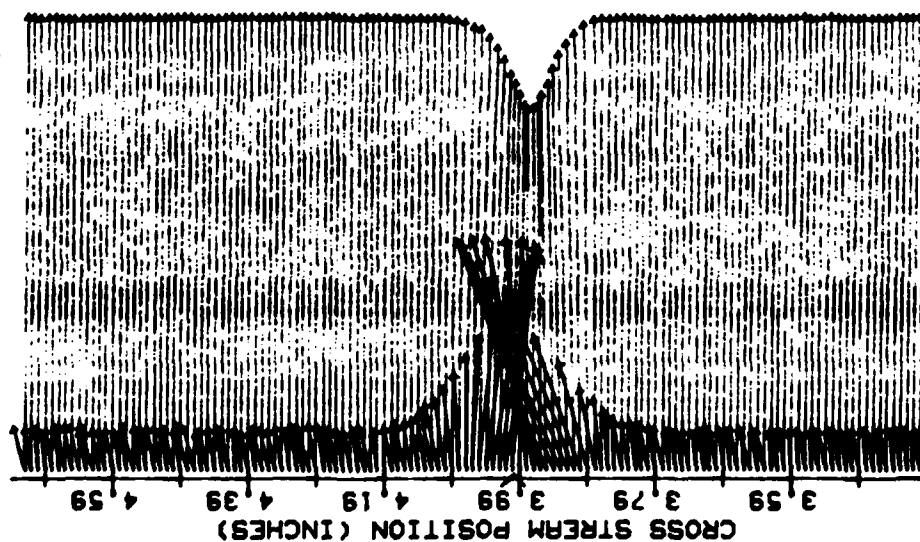
0 1 2 3
SCALE (INCHES)

--- VEL. SCALE=167.00 (FT/SEC)/INCH
--- % TURB INT SCALE= 8.00 %/INCH

INLET VEL= 501.01 +/- 2.00 FT/SEC
CORRECTED INLET VELOCITY= 500 FT/SEC
NOMINAL FLUX TURBINE MODEL= 90.0 DEG
NOMINAL FLUX TURBINE MODEL= 90.0 DEG
REF NO. 0 1 17 VANE CONF. 2
DATE: 08 08 84

Figure 20a. Velocity and Turbulence Intensity Profile Conf No. 2, Traverse No. 1

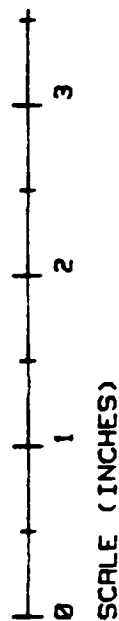
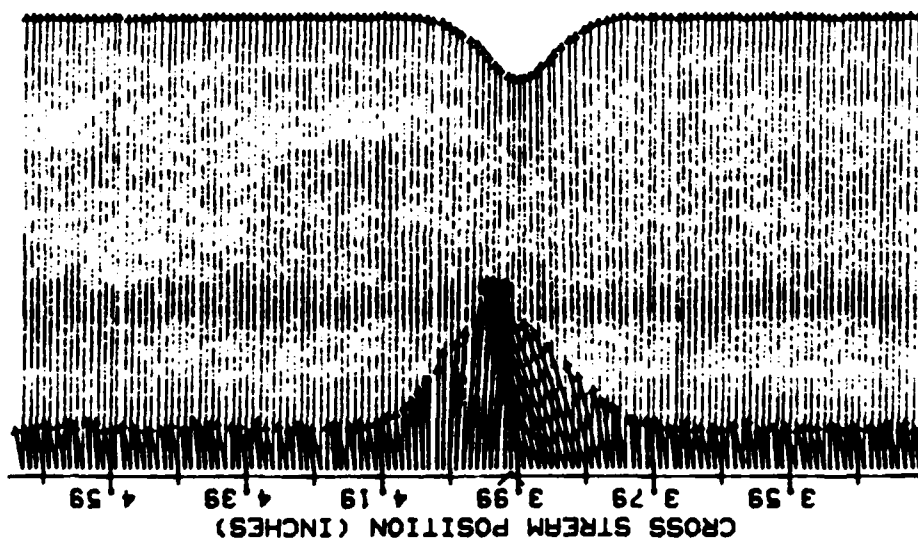
VANE WAKE: CONF. NO.2, EVAL. NO.1, SANDED BLADE
TRAVERSE NO. 2.00 AT 1.25 INCHES



--- VEL. SCALE=167.00 (FT/SEC)/INCH
 --- % TURB INT SCALE= 8.00 %/INCH
 INLET VEL= 201.81 +/- 8.00 FT/SEC
 CORRECTOR INLET VELOCITY= 500 FT/SEC
 HORIZONTAL FLUX TURNING ANGLE= 89.8 DEG
 EXIT WALL DISTANCE ANGLE= .00 DEG
 REF NO= 05117
 DATE: 08 04 1984 VANE CONF: 2

Figure 20b. Velocity and Turbulence Intensity Profile Conf No. 2, Traverse No. 2

VANE WAKE: CONF. NO.2, EVAL. NO.1, SANDED BLADE
TRAVERSE NO. 3.00 AT 2.25 INCHES

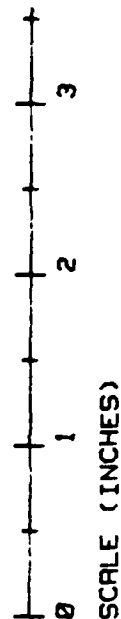
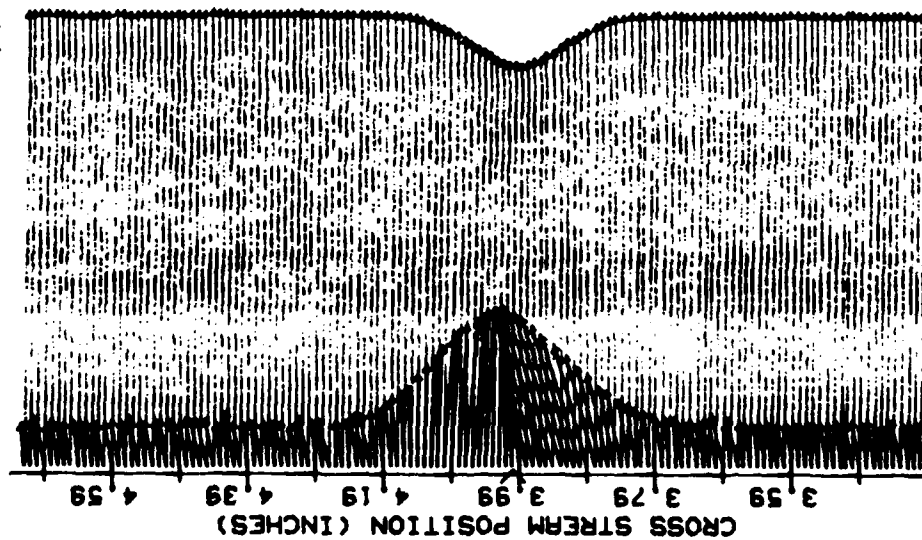


— VEL. SCALE=167.00 (FT/SEC)/INCH
— % TURB INT SCALE= 8.00 % /INCH

INLET VEL= 50.00 FT/SEC
CORRECTED INLET VELOCITY= 50.00 FT/SEC
MONITOR FLUX TUNING RANGE= 50.00 Hz
EXIT WALL DIVERGENCE RANGE= 50.00 Hz
REF NO= 3 5 1 17
DATE: 20 0 84 VANE CONF. 2

Figure 20c. Velocity and Turbulence Intensity Profile Conf No. 2, Traverse No. 3

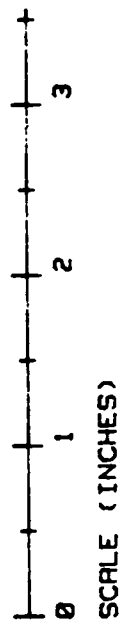
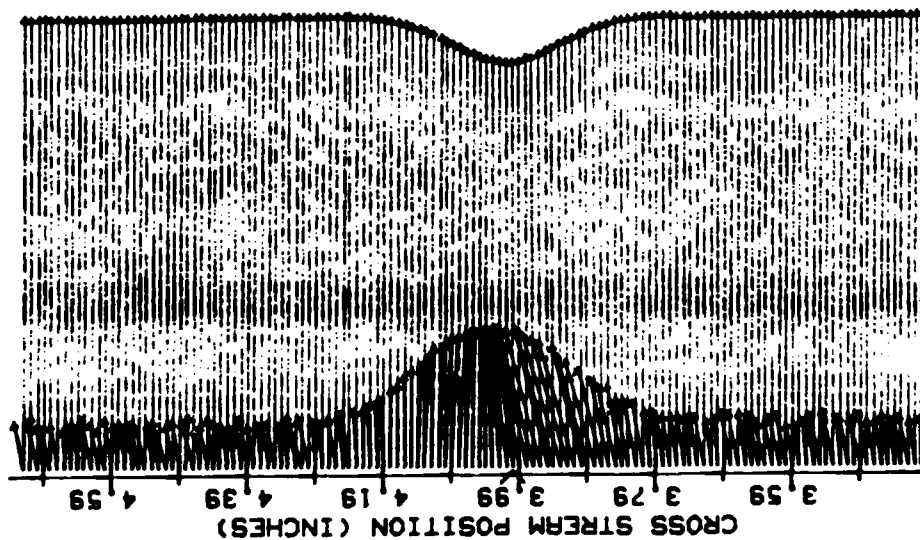
VANE WAKE: CONF. NO.2, EVAL. NO.1, SANDED BLADE
 TRAVERSE NO. 4.00 AT 3.25 INCHES



--- VEL. SCALE=167.00 (FT/SEC)/INCH
 --- % TURB INT SCALE= 8.00 %/INCH
 INLET VEL= 301.81 +/- 2.00 FT/SEC
 CORRECTED INLET VELOCITY= 300 FT/SEC
 NOMINAL FLAN TURNING ANGLE= 20.0 DEG
 EXIT WALL DISTANCE INLET= .00 INCH
 REF NO= 0 5 1 17
 UNTIL 20 0 04. VANE CONF: 2

Figure 20d. Velocity and Turbulence Intensity Profile Conf No. 2, Traverse No. 4

VANE WAKE: CONF. NO.2, EVAL. NO.1, SANDED BLADE
TRAVERSE NO. 5.00 AT 4.25 INCHES



— VEL. SCALE=167.00 (FT/SEC)/INCH
— % TURB INT SCALE= 8.00 % /INCH

INLET VEL= 201.81 +/- 2.00 FT/SEC
CORRECTED INLET VELOCITY= 500 FT/SEC
MONITOR PLUM TURNING ANGLE= 75.0 DEG
EXIT WHEEL STRESS/SEC ANGLE= .00 DEG
REF NO= 5 5 7 17
DATE: 25 8 84, VANE CONF. 2

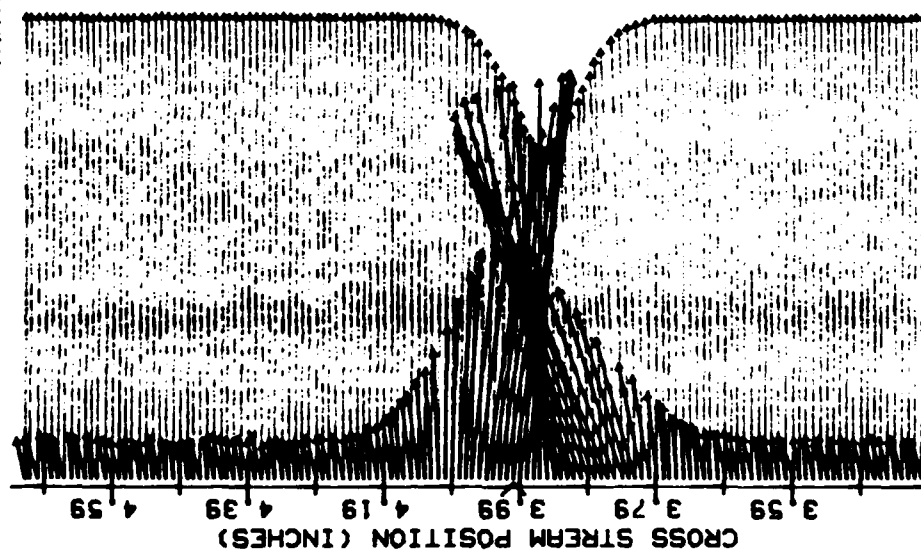
Figure 20e. Velocity and Turbulence Intensity Profile Conf No. 2, Traverse No. 5

- - - VEL. SCALE=167.00 (FT/SEC)/INCH
 — % TURB INT SCALE= 8.00 % /INCH

INLET VEL= 404.40 4.72 1.00 FT/SEC
 CORRECTION INLET VELOCITY= 500 FT/SEC
 CORRECTION FLUX TURBIDITY= 80.5 DEG
 EXIT HELL DIVERGENCE ANGLE= .74 DEG
 REF NO= 0.0 1.0 WAVE CORF= 0
 INTEL 27 0.04

Figure 21a. Velocity and Turbulence Intensity Profile Conf No. 3, Traverse No. 1

VANE WAKE: CONF. NO.3, EVAL. NO.1 Ra=19.8 micrometers
TRAVERSE NO. 2.00 AT 1.25 INCHES



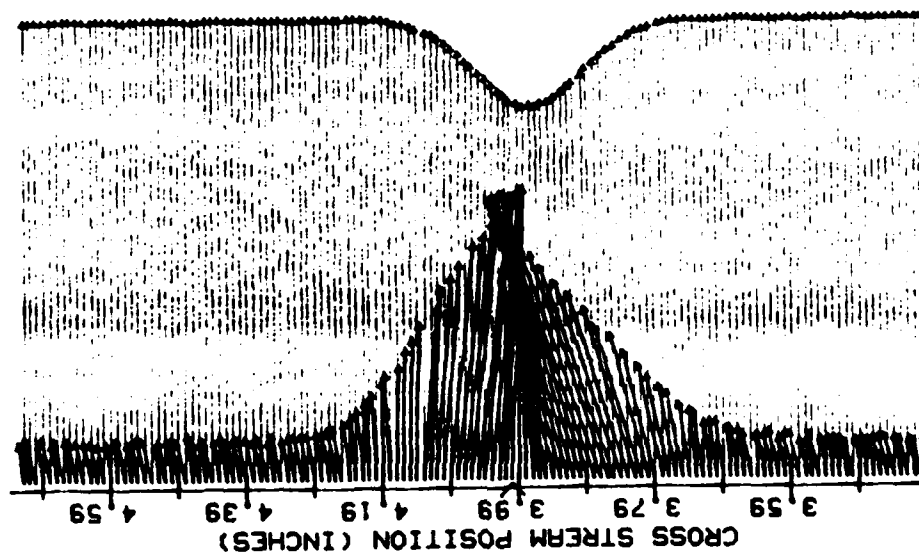
SCALE (INCHES)

— VEL. SCALE=167.00 (FT/SEC)/INCH
- - - % TURB INT SCALE= 8.00 % /INCH

INLET VEL= 494.48 +/- 1.00 FT/SEC
CORRECTED INLET VELOCITY= 500 FT/SEC
NOMINAL FLOW TURNING ANGLE= 20.3 DEG
EXIT WALL DIVERGENCE ANGLE= .74 DEG
REF NO= 00110
INLET: 27 0 04, VANE CONF: 3

Figure 21b. Velocity and Turbulence Intensity Profile Conf No. 3, Traverse No. 2

VANE WAKE: CONF. NO.3, EVAL. NO.1 Ra=19.8 micrometers
TRAVERSE NO. 3.00 AT 2.25 INCHES



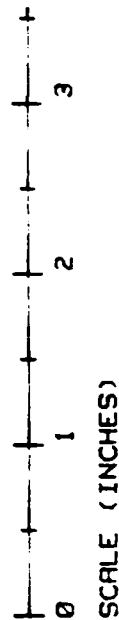
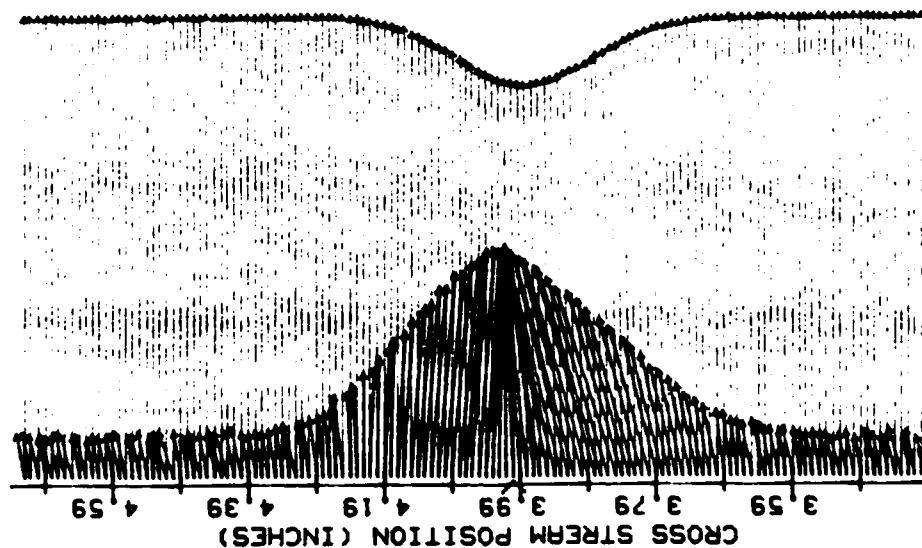
0 1 2 3
SCALE (INCHES)

— VEL. SCALE=167.00 (FT/SEC)/INCH
- - - % TURB INT SCALE= 8.00 %/INCH

INLET VEL= 400-45 +/- 1.00 FT/SEC
CORRECTED INLET VELOCITY= 380 FT/SEC
NOMINAL FLOW TURNING ANGLE= 80.5 DEG
EXIT WALL DIVERGENCE ANGLE= .74 DEG
REF NO= 000718
DATE: 07 0 04, VANE CONF: 0

Figure 21c. Velocity and Turbulence Intensity Profile Conf No. 3, Traverse No. 3

VANE WAKE: CONF. NO.3, EVAL. NO.1 Ra=19.8 micrometers
 TRAVERSE NO. 4.00 AT 3.25 INCHES

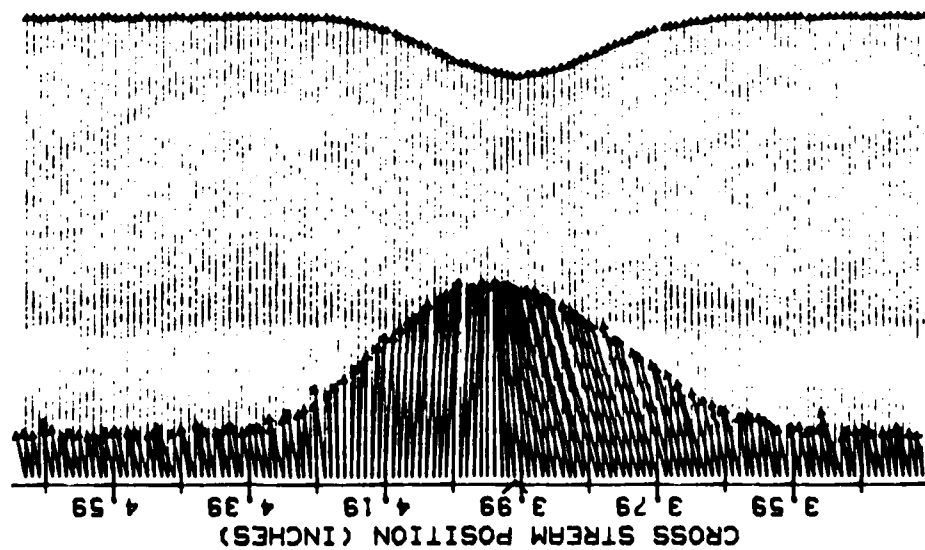


--- VEL. SCALE=167.00 (FT/SEC)/INCH
 --- % TURB INT SCALE= 8.00 %/INCH

INLET VEL=494.48 +/- 1.00 FT/SEC
 CORRECTED INLET VELOCITY= 500 FT/SEC
 NOMINAL FLUX TURNING ANGLE= 20.5 DEG
 EXIT MALL DIVERGENCE ANGLE= .74 DEG
 REF NO= 0 0 1 10
 DATE: 27 9 84, VANE CONF: 3

Figure 21d. Velocity and Turbulence Intensity Profile Conf No. 3, Traverse No. 4

VANE WAKE: CONF. NO.3, EVAL. NO.1 Ra=19.8 micrometers
 TRAVERSE NO. 5.00 AT 4.25 INCHES



0 1 2 3

SCALE (INCHES)

--- VEL. SCALE=167.00 (FT/SEC)/INCH
 --- % TURB INT SCALE= 8.00 % / INCH

INLET VEL= 404.43 +/- 1.00 FT/SEC
 CORRECTED INLET VELOCITY= 500 FT/SEC
 ADVANCE PLUM TURNING ANGLE= 20.5 DEG
 EXIT WALL DIVERGENCE ANGLE= .74 DEG
 REF NO= 9 0 T 18
 DATE, 27 8 84, VANE CONF, 3

Figure 21e. Velocity and Turbulence Intensity Profile Conf No. 3, Traverse No. 5

VANE WAKE: CONF. NO. 4, EVAL. NO. 1 Ra=26.9 micrometers
 TRAVERSE NO. 1.00 AT .25 INCHES

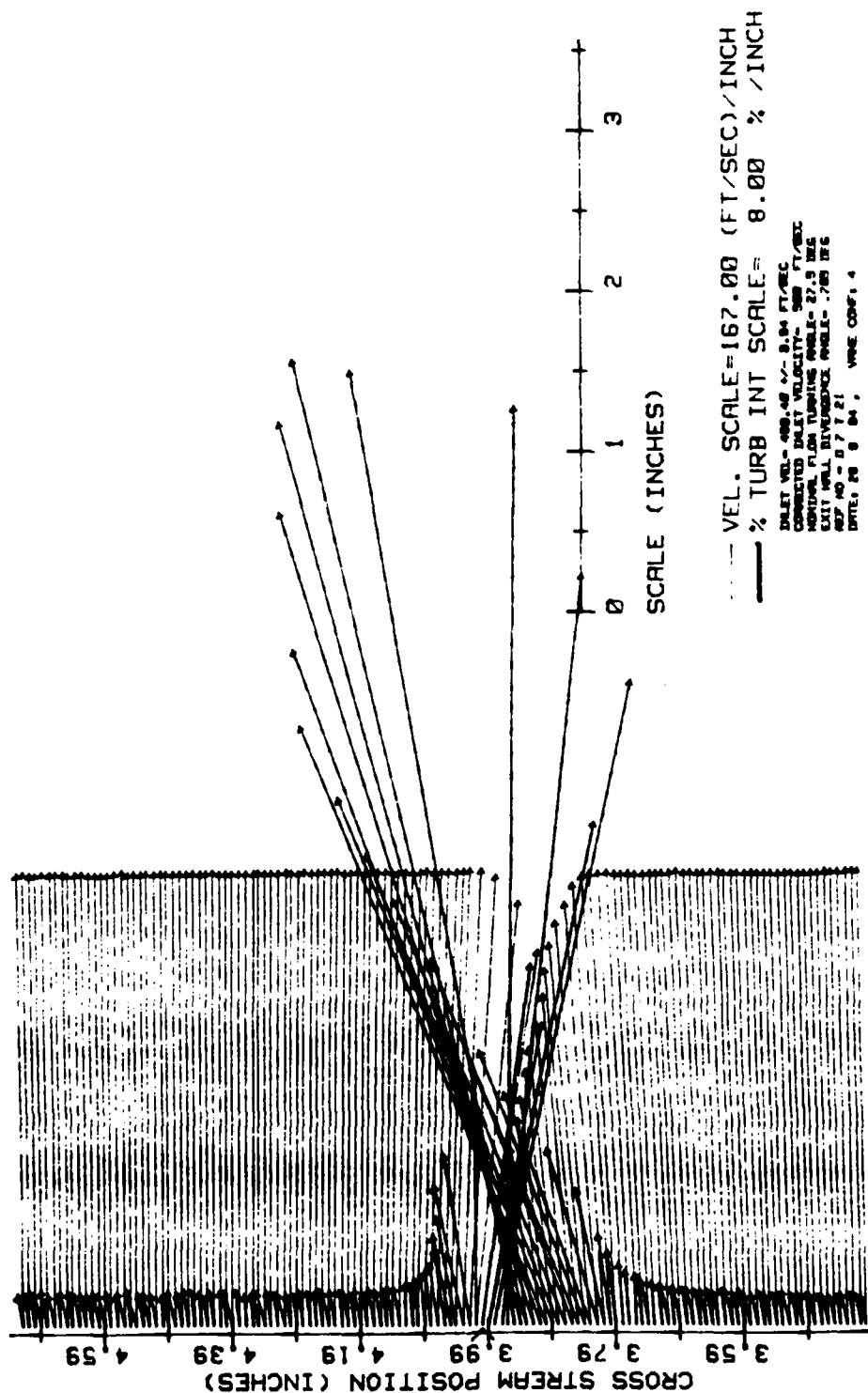
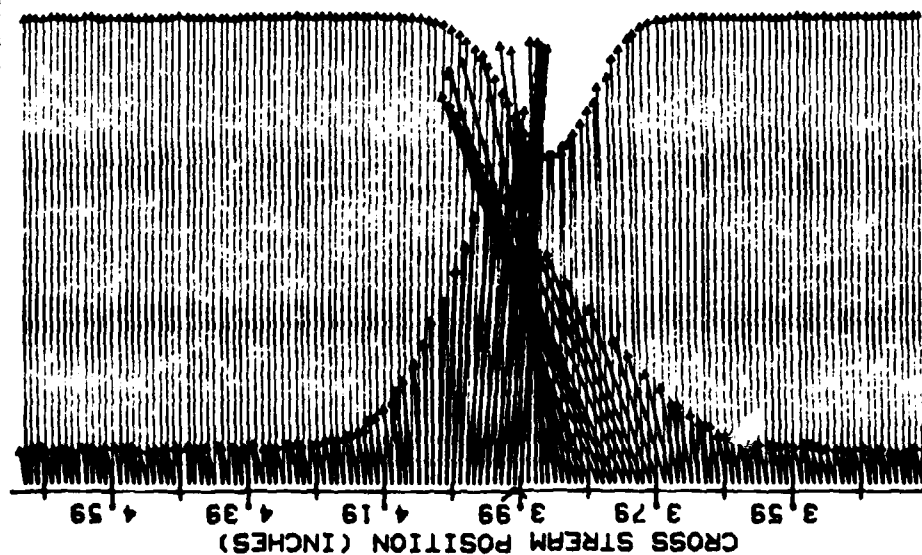


Figure 22a. Velocity and Turbulence Intensity Profile Conf No. 4, Traverse No. 1

VANE WAKE: CONF. NO. 4, EVAL. NO. 1 Ra=26.9 micrometers
TRAVERSE NO. 2.00 AT 1.25 INCHES



SCALE (INCHES)

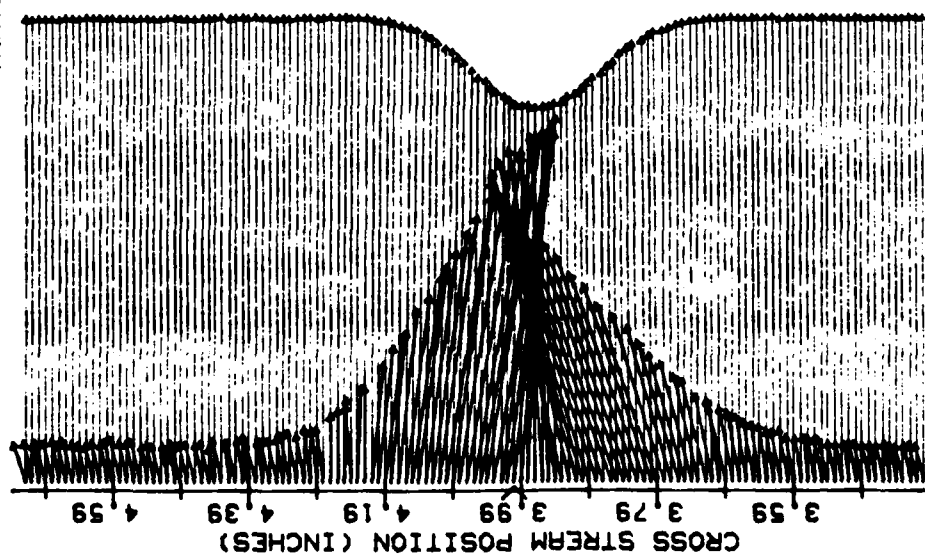
0 1 2 3

--- VEL. SCALE=167.00 (FT/SEC)/INCH
--- % TURB INT SCALE= 8.00 %/INCH

INLET VEL= 400.00 +/- 0.04 FT/SEC
CORRECTED INLET VELOCITY= 380 FT/SEC
HORIZONTAL FLASH TURNING ANGLE= 27.5 DEG
EXIT WALL DIVERGENCE ANGLE= .765 DEG
REF NO= 0 7 1 21
INLET NO 0 04, VANE CONF, 4

Figure 22b. Velocity and Turbulence Intensity Profile Conf No. 4, Traverse No. 2

VANE WAKE: CONF. NO. 4, EVAL. NO. 1 Ra=26.9 micrometers
TRAVERSE NO. 3.00 AT 2.25 INCHES



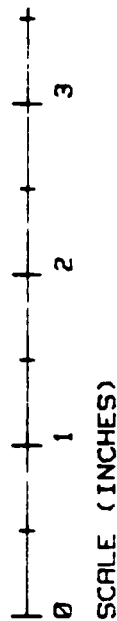
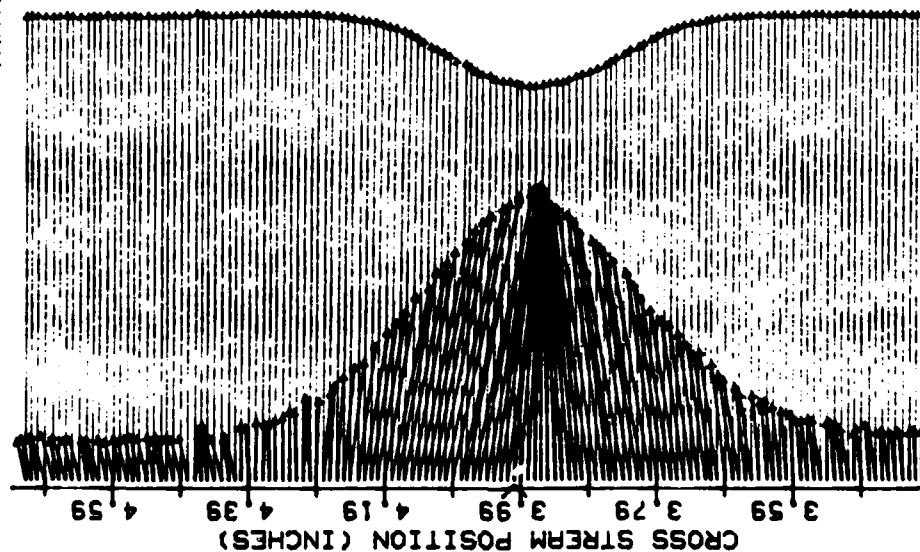
0 1 2 3
SCALE (INCHES)

--- VEL. SCALE=167.00 (FT/SEC)/INCH
--- % TURB INT SCALE= 8.00 % / INCH

INLET VEL= 400.00 FT/SEC
CORRECTED INLET VELOCITY= 500 FT/SEC
NOMINAL FLUX TURNING ANGLE= 27.5 DEG
EXIT WALL DIVERGENCE ANGLE= 1.70 DEG
REF NO - 0.7 T 21
DATE: 28 8 84, VANE CONF: 4

Figure 22c. Velocity and Turbulence Intensity Profile Conf No. 4, Traverse No. 3

VANE WAKE: CONF. NO. 4, EVAL. NO. 1 Ra=26.9 micrometers
 TRAVERSE NO. 4.00 AT 3.25 INCHES

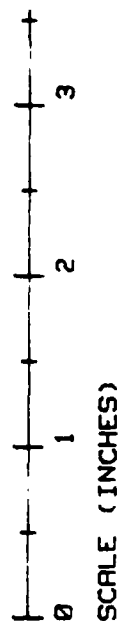
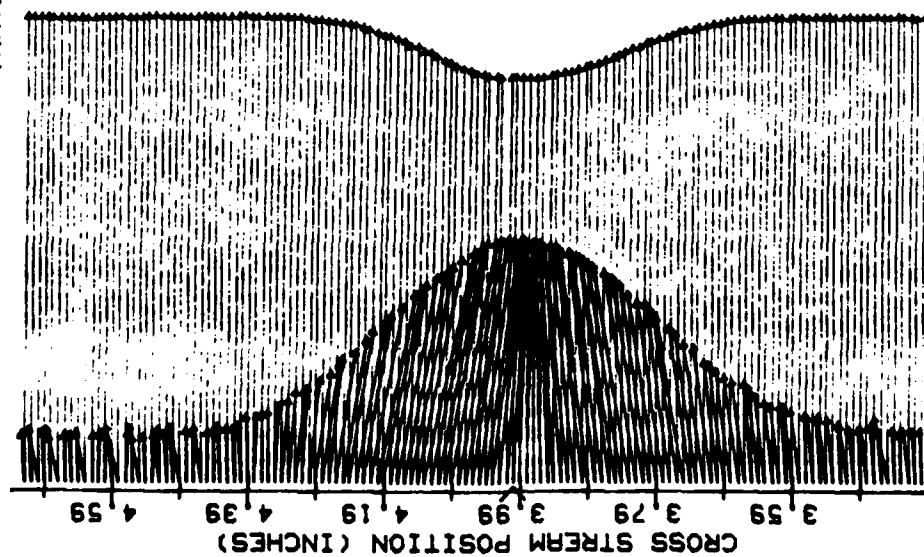


--- VEL. SCALE=167.00 (FT/SEC)/INCH
 --- % TURB INT SCALE= 8.00 % /INCH

INLET VEL= 489.40 +/- 0.04 FT/SEC
 CORRECTED INLET VELOCITY= 489.40 FT/SEC
 INLET TURBULENCE INTENSITY= 0.04 %
 EXISTING FLUID TURBULENCE= 0.04 %
 EXISTING WALL TURBULENCE= 0.04 %
 REF NO= 0.04, VANE CONF= 4
 DATE: 00 0 04

Figure 22d. Velocity and Turbulence Intensity Profile Conf No. 4, Traverse No. 4

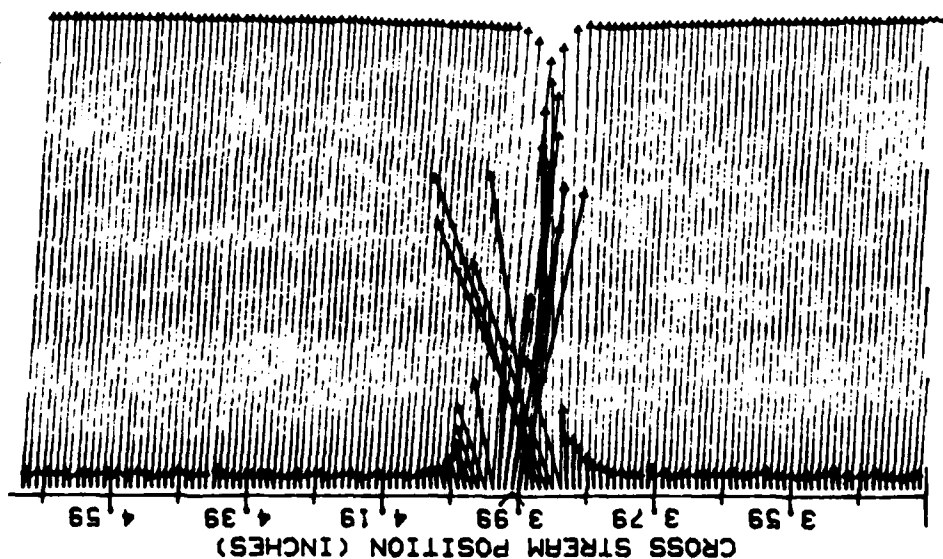
VANE WAKE: CONF. NO. 4, EVAL. NO. 1 Ra=26.9 micrometers
 TRAVERSE NO. 5.00 AT 4.25 INCHES



--- VEL. SCALE=167.00 (FT/SEC)/INCH
 --- % TURB INT SCALE= 8.00 % /INCH
 INLET VEL= 400.00 +/- 0.04 FT/SEC
 CORRECTED INLET VELOCITY= 389 FT/SEC
 NOMINAL FLUX TURNING ANGLE= 27.5 DEG
 EXIT WALL DISTANCE FROM INLET= 1.00 INCH
 REF NO= 0.7 1.21
 DATED 20 0 04, VANE CONF. 4

Figure 22e. Velocity and Turbulence Intensity Profile Conf No. 4, Traverse No. 5

VANE WAKE: CONF. NO. 11, EVAL. NO. 2 $Ra = .09$ micrometers
 TRAVERSE NO. 1.00 AT .25 INCHES

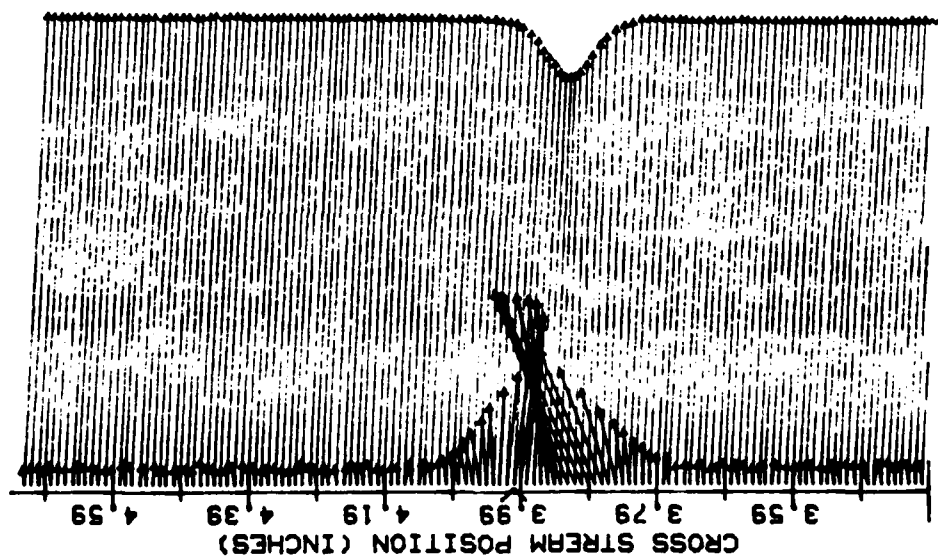


0 1 2 3
 SCALE (INCHES)

--- VEL. SCALE = 167.00 (FT/SEC)/INCH
 --- % TURB INT SCALE = 8.00 %/INCH
 INLET VEL = 400.00 +/- 1.04 FT/SEC
 CORRECTED INLET VELOCITY = 500 FT/SEC
 INITIAL FLUX TURBIDITY PAIR = 10 DEG
 INITIAL FLUX TURBIDITY PAIR = 10 DEG
 REF NO = 0.0 1.0 1.0 1.0
 DATE: 12 0 04 VANE COMP: 11

Figure 23a. Velocity and Turbulence Intensity Profile Conf No. 11, Traverse No. 1

VANE MAKE: CONF. NO.11, EVAL. NO.2 $Ra=09$ micrometers
 TRAVERSE NO. 2.00 AT 1.25 INCHES



0 1 2 3
 SCALE (INCHES)

--- VEL. SCALE=167.00 (FT/SEC)/INCH
 --- % TURB INT SCALE= 8.00 %/INCH

INLET VEL= 400.50 +/- 1.44 FT/SEC
 CORRECTED INLET VELOCITY= 500 FT/SEC
 NOMINAL FLOW TURNING ANGLE= 15 DEG
 EXIT WALL DIVERGENCE ANGLE= .05 DEG
 REF NO = 0 0 1 27
 DATE: 12 0 84 VANE CONF. 11

Figure 23b. Velocity and Turbulence Intensity Profile Conf No. 11, Traverse No. 2

VANE WAKE: CONF. NO. 11, EVAL. NO. 2 Ra=.09 micrometers
TRAVERSE NO. 3.00 AT 2.25 INCHES

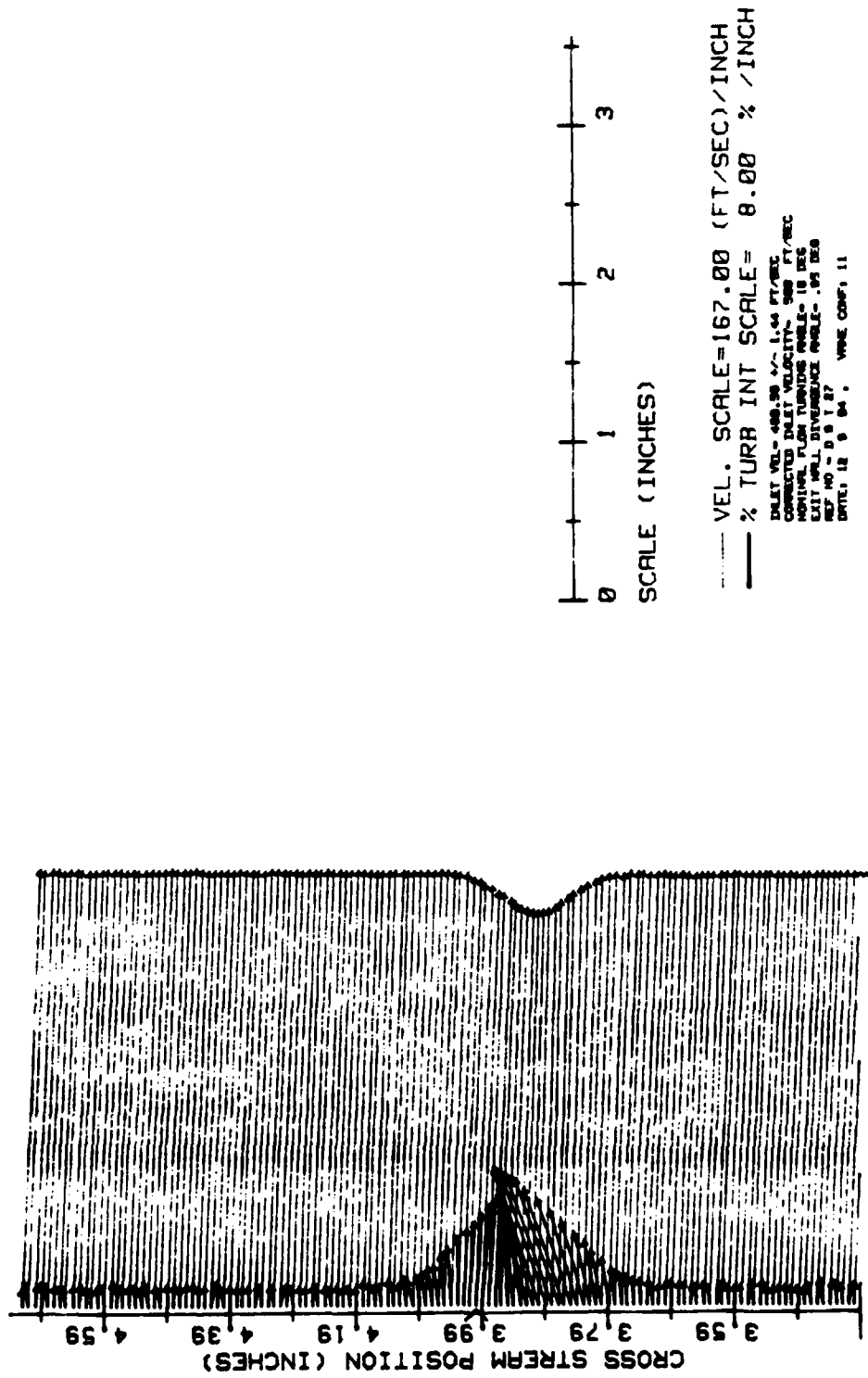
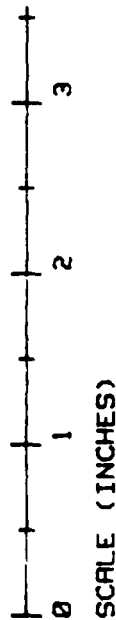
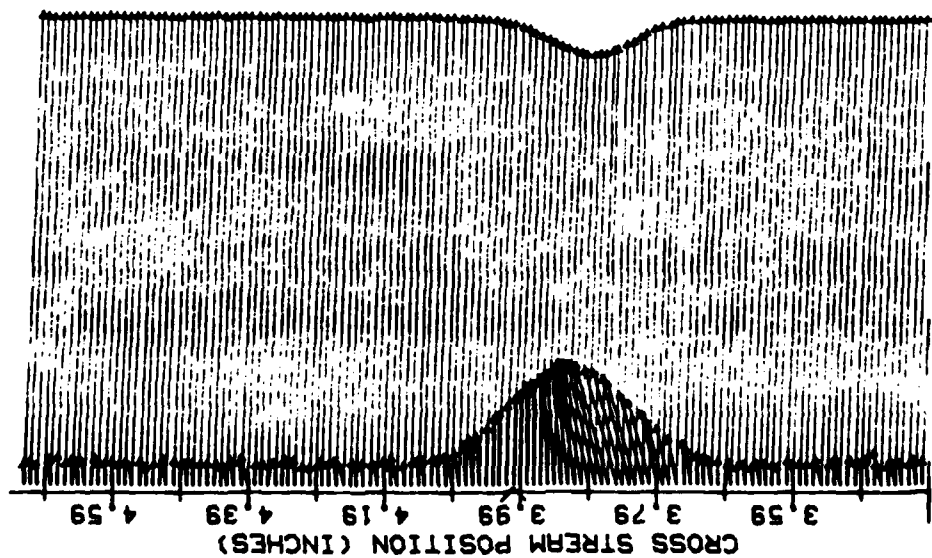


Figure 23c. Velocity and Turbulence Intensity Profile Conf No. 11, Traverse No. 3

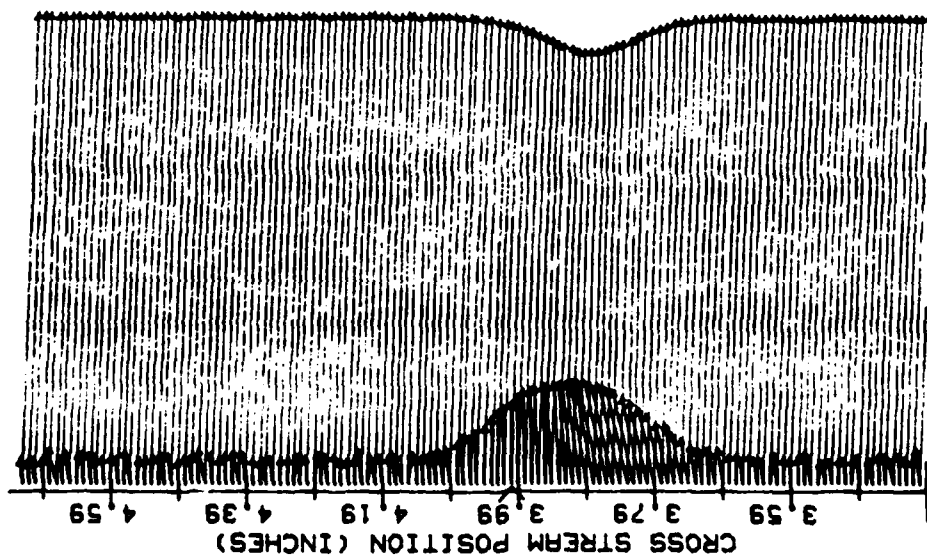
VRANE WAKE: CONF. NO. 11, EVAL. NO. 2 $Ra = 0.9$ micrometers
 TRAVERSE NO. 4.00 AT 3.25 INCHES



--- VEL. SCALE = 167.00 (FT/SEC)/INCH
 --- % TURB INT SCALE = 8.00 %/INCH
 INLET VEL = 400.00 +/- 1.44 FT/SEC
 CORRECTED INLET VELOCITY = 500 FT/SEC
 NOMINAL FLUX TURNING ANGLE = 10 DEG
 EXIT WALL DIVERGENCE ANGLE = .94 DEG
 REF NO = D 8 T 27
 DATED 12 9 84, VRANE CONF. 11

Figure 23d. Velocity and Turbulence Intensity Profile Conf No. 11, Traverse No. 4

VANE MAKE: CONF. NO. 11, EVAL. NO. 2 Ra=.09 micrometers
 TRAVERSE NO. 5.00 AT 4.25 INCHES



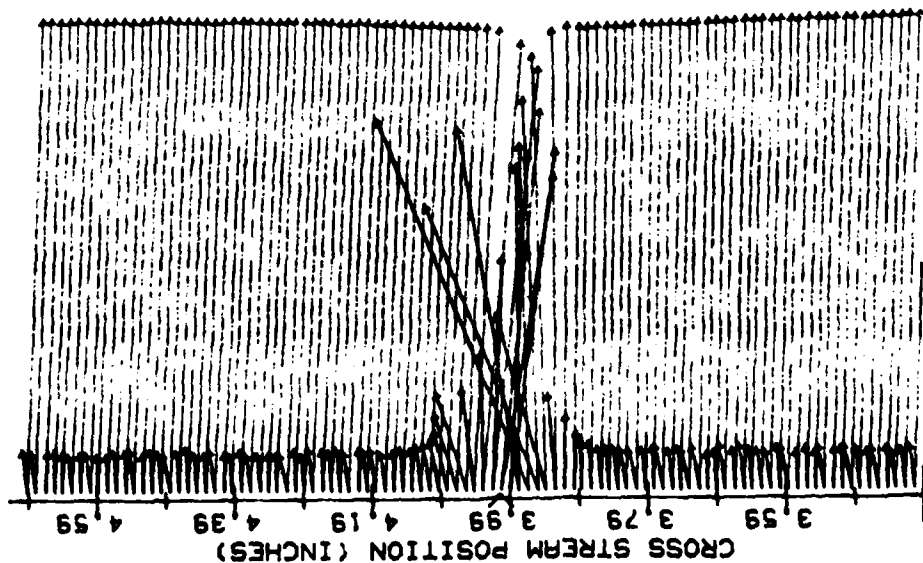
SCALE (INCHES)

--- VEL. SCALE=167.00 (FT./SEC.)/INCH
 --- % TURB INT SCALE= 8.00 %/INCH

INLET VEL= 400.00 +/- 1.44 FT/SEC
 CORRECTED INLET VELOCITY= 500 FT/SEC
 MONITOR FLUX TURBIDITY= 18.00
 EXIT WALL DIVERGENCE ANGLE= .00 DEG
 REF NO= 0.0 T. 27
 DATED 12 9 84, VANE CONF. 11

Figure 23e. Velocity and Turbulence Intensity Profile Conf No. 11, Traverse No. 5

VANE WAKE: CONF. NO.12 EVAL. NO.2 Sandblasted Blades
 TRAVERSE NO. 1.00 AT .25 INCHES



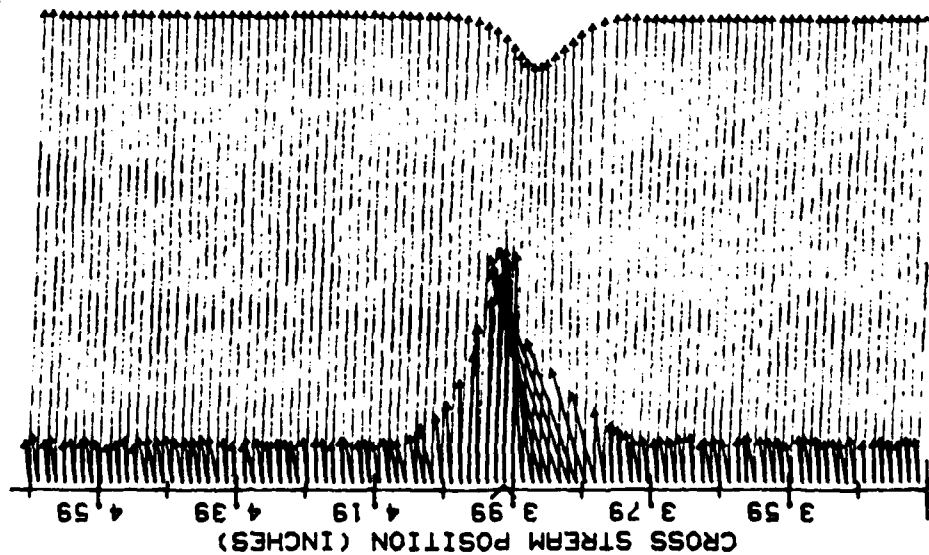
SCALE (INCHES)

--- VEL. SCALE=167.00 (FT/SEC)/INCH
 --- % TURB INT SCALE= 8.00 % /INCH

INLET VEL= 400.00 FT/SEC
 CORRECTED INLET VELOCITY= 380.00 FT/SEC
 CORRECTED TURBULENCE INTENSITY= 1.00 %
 CORRECTED TURBULENCE INTENSITY= 1.00 %
 DATE: 08 01 12 27 WAVE CONF. 12

Figure 24a. Velocity and Turbulence Intensity Profile Conf No. 12, Traverse No. 1

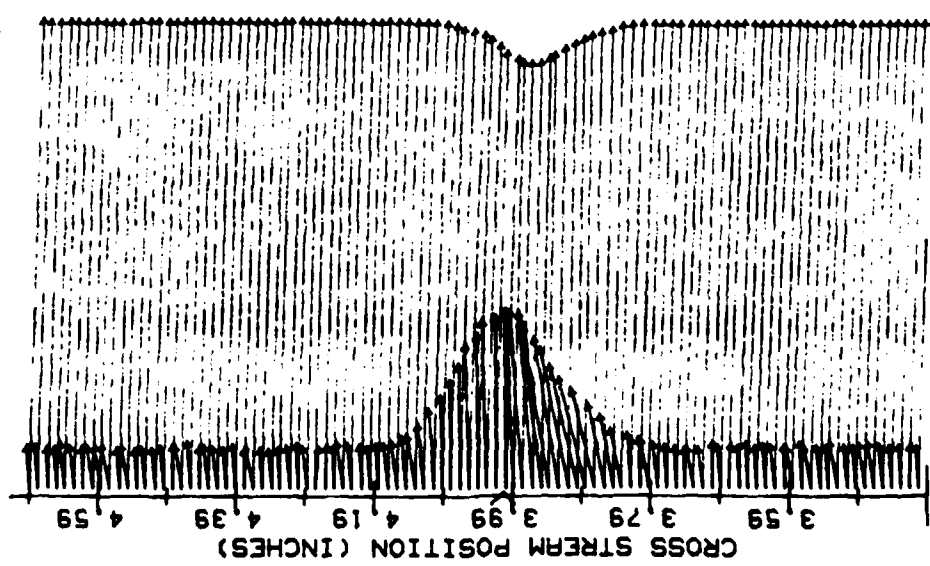
VANE WAKE: CONF. NO.12 EVRL. NO.2 Sandblasted Blades
 TRAVERSE NO. 2.00 AT 1.25 INCHES



--- VEL. SCALE=167.00 (FT/SEC)/INCH
 --- % TURB INT SCALE= 8.00 % /INCH
 INLET VEL= 498.87 +/- 1.48 FT/SEC
 CORRECTED INLET VELOCITY= 500 FT/SEC
 NOMINAL FLAM TURNING ANGLE= 12.5 DEG
 EXIT WALL DIVERGENCE ANGLE= .00 DEG
 REF NO = 5 11 1 27
 DATE: 20 9 84 , VANE CONF: 12

Figure 24b. Velocity and Turbulence Intensity Profile Conf No. 12, Traverse No. 2

VANE WAKE: CONF. NO. 12 EVRL. NO. 2 Sandblasted Blades
TRAVERSE NO. 3.00 AT 2.25 INCHES



SCALE (INCHES)

--- VEL. SCALE=167.00 (FT/SEC)/INCH
 --- % TURB INT SCALE= 8.00 %/INCH

INLET VEL= 400.07 +/- 1.40 FT/SEC
 CORRECTED INLET VELOCITY= 389 FT/SEC
 NOMINAL FLOW TURNING ANGLE= 17.5 DEG
 EXIT WALL DIVERGENCE ANGLE= .00 DEG
 REF NO= D 11 T 27
 DATED 20 9 84 VANE CONF: 12

Figure 24c. Velocity and Turbulence Intensity Profile Conf No. 12, Traverse No. 3

AD-A151 855

INFLUENCE OF SURFACE ROUGHNESS ON COMPRESSOR BLADES AT
HIGH REYNOLDS NUMB. (U) AIR FORCE INST OF TECH
WRIGHT-PATTERSON AFB OH SCHOOL OF ENGI.. G P MOE

2/2

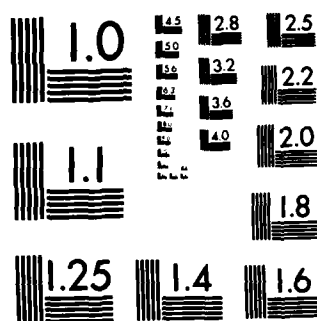
UNCLASSIFIED

DEC 84 AFIT/GAE/AA/84D-19

F/G 20/4

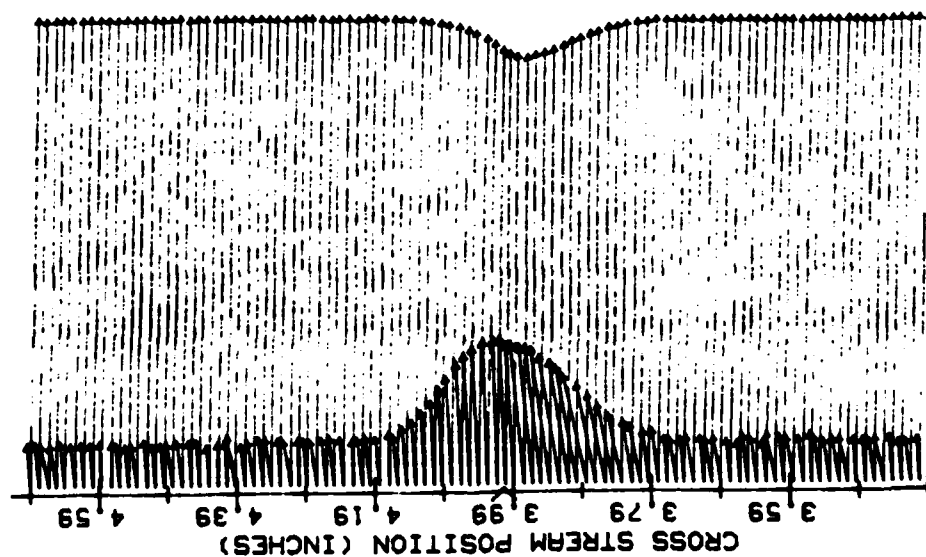
NL





MICROCOPY RESOLUTION TEST CHART
NATIONAL BUREAU OF STANDARDS-1963-A

VRNE WAKE: CONF. NO.12 EVRL. NO.2 Sandblasted Blades
 TRAVERSE NO. 4.00 AT 3.25 INCHES



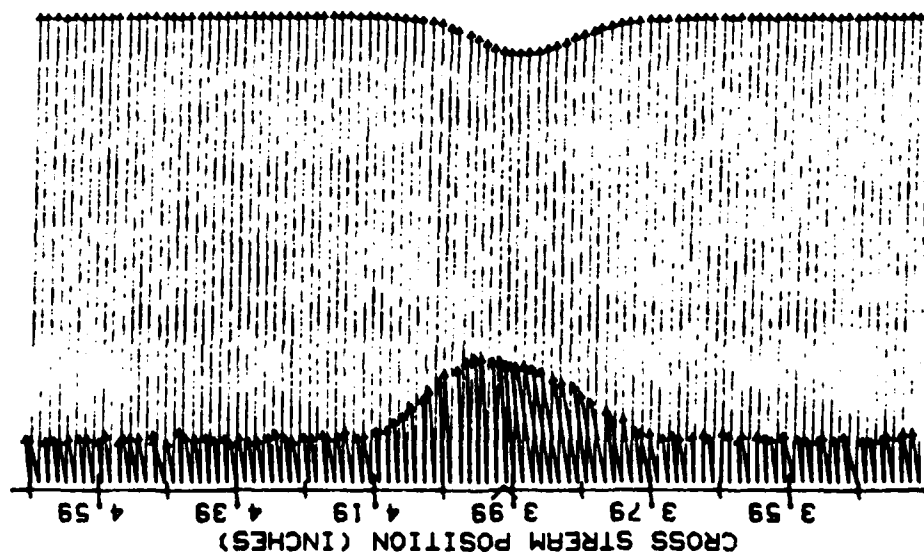
SCALE (INCHES)

--- VEL. SCALE=167.00 (FT/SEC)/INCH
 --- % TURB INT SCALE= 8.00 % /INCH

INLET VEL= 400.00 FT/SEC
 CORRECTED INLET VELOCITY= 500 FT/SEC
 WINDING FLUX TURNING POLE= 12.5 DEG
 EXIT WLL BIVERTICE POLE= .00 DEG
 REF NO= 5.11.1.27
 DATE: 00 0 04, VRNE CONF. 12

Figure 24d. Velocity and Turbulence Intensity Profile Conf No. 12, Traverse No. 4

VANE WAKE: CONF. NO.12 EVAL. NO.2 Sandblasted Blades
 TRAVERSE NO. 5.00 AT 4.25 INCHES



0 1 2 3
 SCALE (INCHES)

— VEL. SCALE=167.00 (FT/SEC)/INCH
 --- % TURB INT SCALE= 8.00 % /INCH

DELTA VEL= 499.87 +/- 1.46 FT/SEC
 CORRECTED DELTA VELOCITY= 500 FT/SEC
 HORIZONTAL FLASH TURBULENCE WAKE= 12.5 DEG
 EXIT WALL STRESS WAKE= .00 DEG
 REF NO = 8 11 7 27
 DATE: 28 9 84 , VANE CONF: 12

Figure 24e. Velocity and Turbulence Intensity Profile Conf No. 12, Traverse No. 5

VANE MAKE: CONF. NO.13, EVAL. NO.1 Ra=17.9 micrometers
 TRAVERSE NO. 1.00 AT .25 INCHES

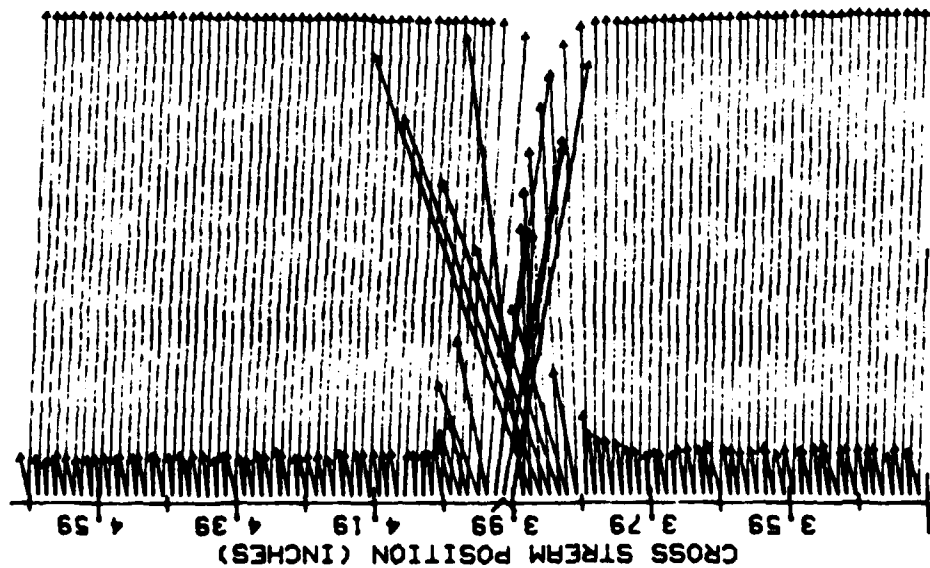
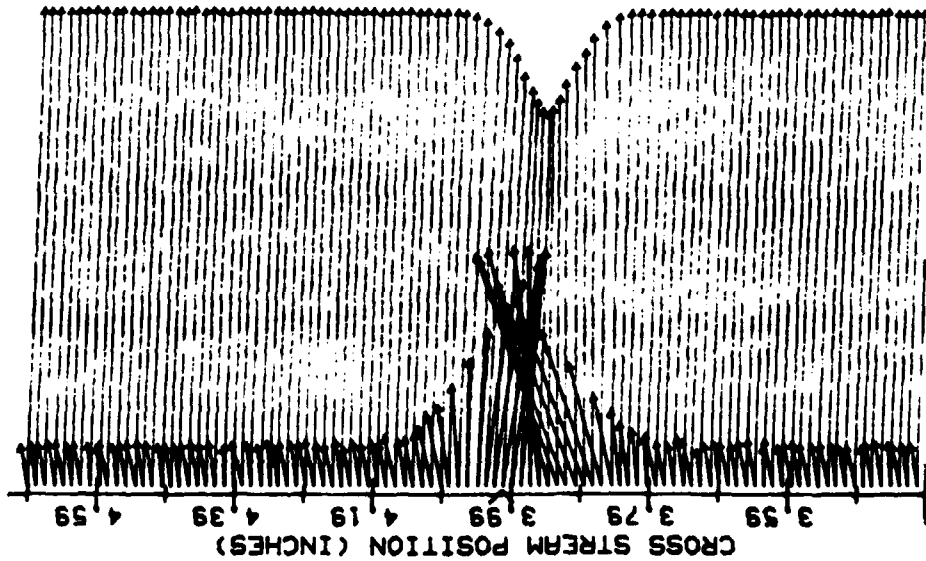


Figure 25a. Velocity and Turbulence Intensity Profile Conf No. 13, Traverse No. 1

VRANE WAKE: CONF. NO.13, EVAL. NO.1 Ra=17.9 micrometers
TRAVERSE NO. 2.00 AT 1.25 INCHES



--- VEL. SCALE=167.00 (FT/SEC)/INCH
--- % TURB INT SCALE= 8.00 % /INCH

INLET VEL= 400.00 +/- 1.79 FT/SEC
CORRECTED INLET VELOCITY= 399 FT/SEC
ADDITIONAL PLAIN TURBULENCE PROFILE= 17.9 MIC
EXIT WALL DISTURBANCE PROFILE= .57 SEC
REF NO = 9.9 1.20
DATES 18 9 84, VRANE CONF: 18

Figure 25b. Velocity and Turbulence Intensity Profile Conf No. 13, Traverse No. 2

A vertical number line with tick marks labeled 0, 1, 2, and 3.

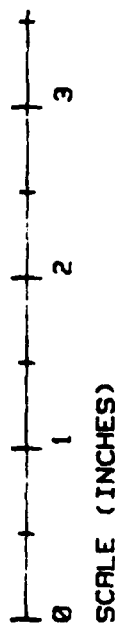
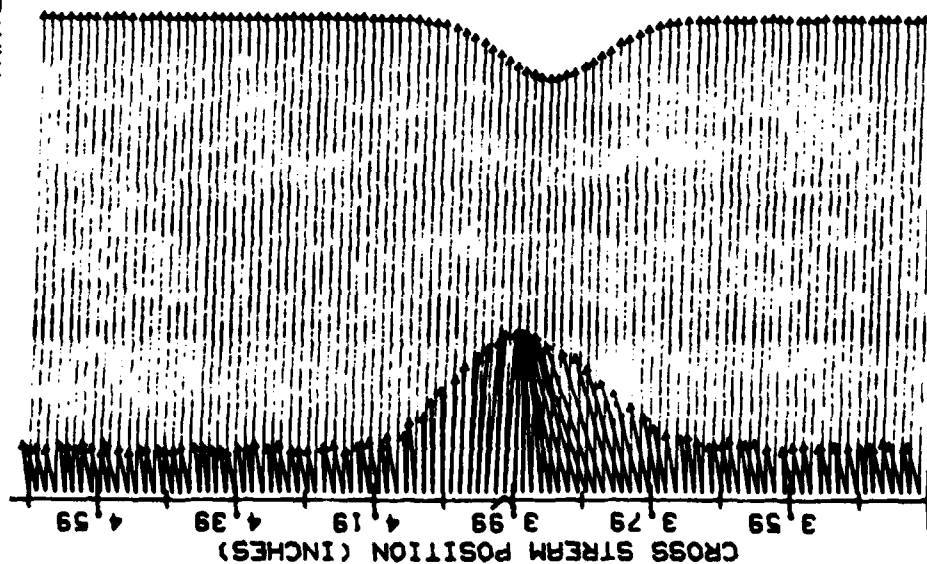
SCALE (INCHES)

--- VEL. SCALE=167.00 (FT/SEC)/INCH
----- % TURB INT SCALE= 8.00 % /INCH

INLET VEL. = 400.00 ~ 1.70 FT/SEC
CONNECTED INLET VELOCITY = 500 FT/SEC
WASHING FLAM TUNING NOBLE = 17.9 SEC
EXIT WALL SPRINGBACK NOBLE = .57 SEC
EXIT NO. = 50 FT/SEC
DATE: 10 9 84, WAVE CONF: 10

Figure 25c. Velocity and Turbulence Intensity Profile Conf No. 13, Traverse No. 3

VANE WAKE: CONF. NO.13, EVRL. NO.1 Ra=17.9 micrometers
TRAVERSE NO. 4.00 RT 3.25 INCHES

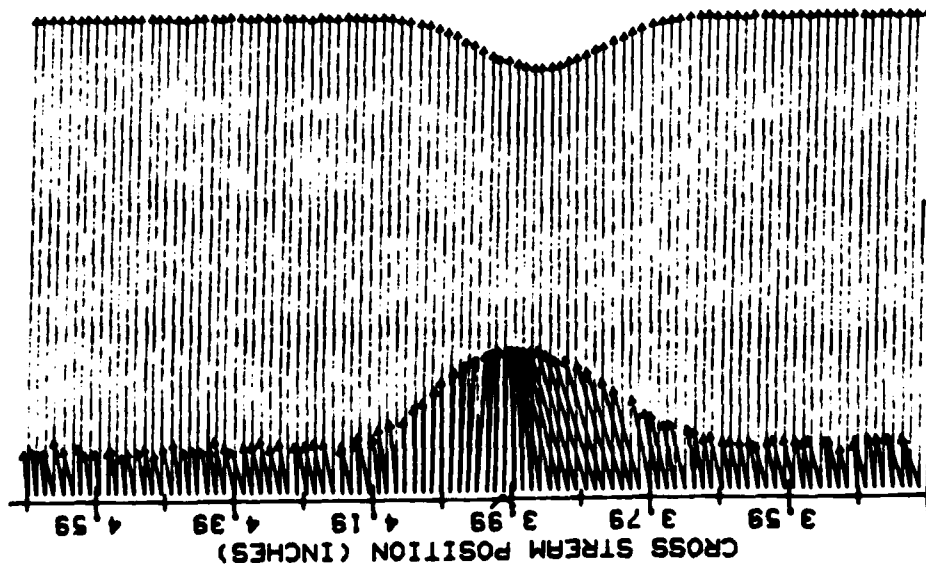


— VEL. SCALE=167.00 (FT/SEC)/INCH
— % TURB INT SCALE= 8.00 % /INCH

DALET VEL= 400.00 IN= 1.70 FT/SEC
CORRELATED DALET VELOCITY= 500 FT/SEC
MINORAL PLAIN TURBULENCE= 17.5 DEG
DALET WALL STRESS= 0.57 DEG
REF NO= 9.9 T.00
DALET 10 0 04. VANE CONF. 10

Figure 25d. Velocity and Turbulence Intensity Profile Conf No. 13, Traverse No. 4

VRNE WAKE: CONF. NO.13, EVAL. NO.1 Ra=17.9 micrometers
TRAVERSE NO. 5.00 AT 4.25 INCHES



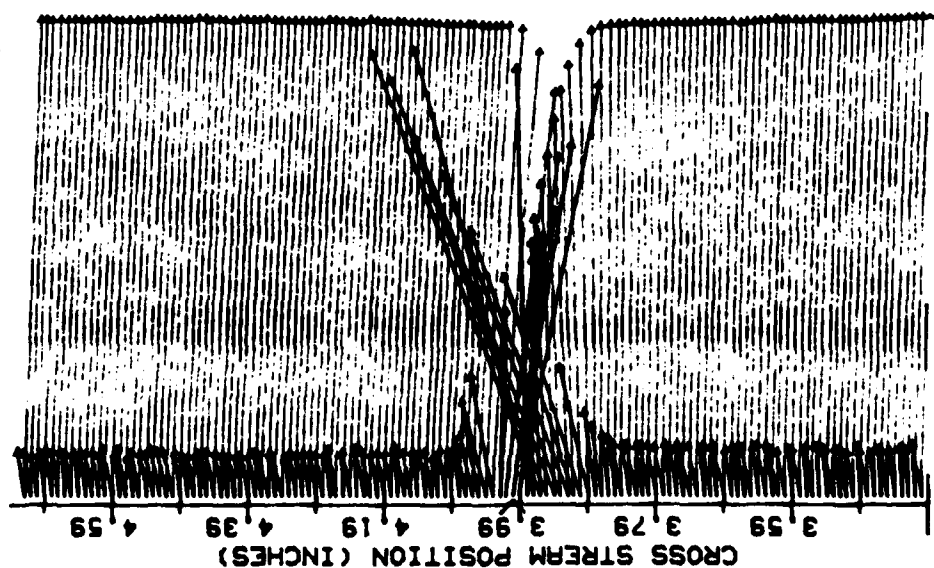
SCALE (INCHES)

--- VEL. SCALE=167.00 (FT/SEC)/INCH
— % TURB INT SCALE= 8.00 % /INCH

INLET VEL= 400.00 +/- 1.79 FT/SEC
CORRECTED INLET VELOCITY= 389 FT/SEC
HORIZONTAL PLAIN TURBULENCE= 17.5 %
EXIT WALL DISTURBANCE= 17.5 %
REF NO= 00000000
DATE= 10 0 04, VRNE CONF: 10

Figure 25e. Velocity and Turbulence Intensity Profile Conf No. 13, Traverse No. 5

VANE WAKE: CONF. NO.14, EVAL. NO.1 Ra=25.5 micrometers
TRAVERSE NO. 1.00 AT .25 INCHES



SCALE (INCHES)

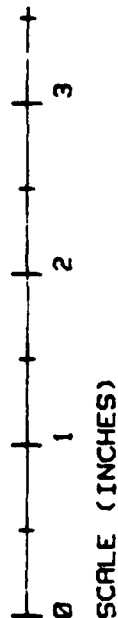
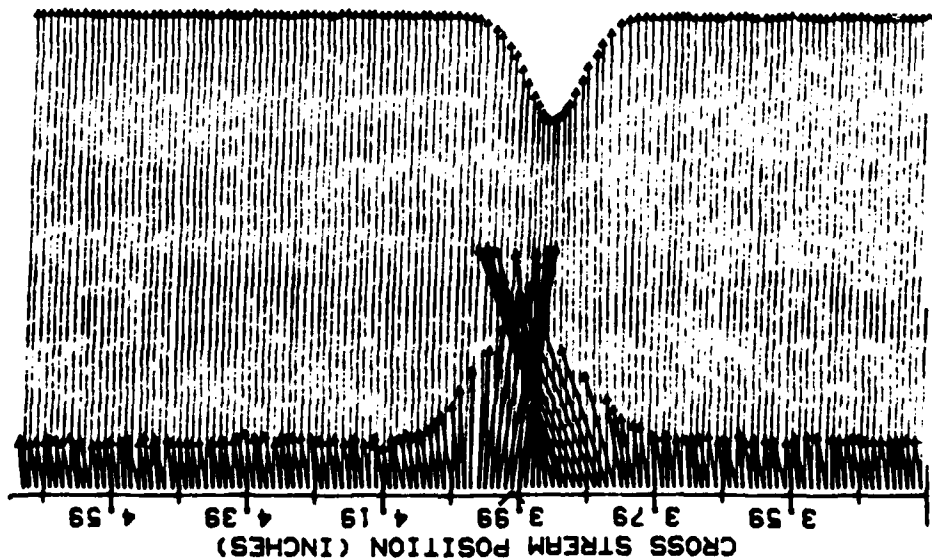
0 1 2 3

--- VEL. SCALE=167.00 (FT/SEC)/INCH
--- % TURB INT SCALE= 8.00 %/INCH

INLET VEL= 400.00 +/- 0.00 FT/SEC
CORRECTION FOR WALL EFFECTS= 0.00 FT/SEC
CORRECTION FOR TURBULENCE= 0.00 FT/SEC
EXIT WALL DISTANCE= 17.5 INCH
REF NO= 0.0 7.00
DATE: 14 0 04, VANE CONF: 14

Figure 26a. Velocity and Turbulence Intensity Profile Conf No. 14, Traverse No. 1

VANE WAKE: CONF. NO. 14, EVAL. NO. 1 Ra=25.5 micrometers
 TRAVERSE NO. 2.00 AT 1.25 INCHES

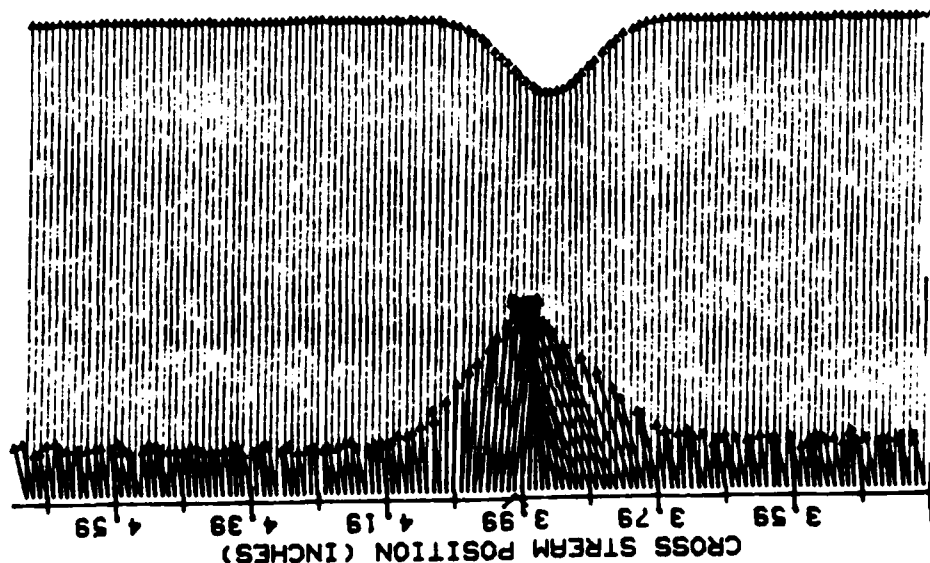


--- VEL. SCALE=167.00 (FT/SEC)/INCH
 --- % TURB INT SCALE= 8.00 %/INCH

DALEY VEL= 482.00 +/- 2.00 FT/SEC
 CORRECTED DALEY VELOCITY= 500 FT/SEC
 HORIZONTAL PLUM TURNING ANGLE= 17.5 DEG
 EXIT WALL STRESS/INCH= .05 DEG
 REF NO= 9.0 1.25
 DATE: 14 9 84, VANE CONF. 14

Figure 26b. Velocity and Turbulence Intensity Profile Conf No. 14, Traverse No. 2

VRNE WAKE: CONF. NO.14, EVAL. NO.1 Ra=25.5 micrometers
 TRAVERSE NO. 3.00 AT 2.25 INCHES



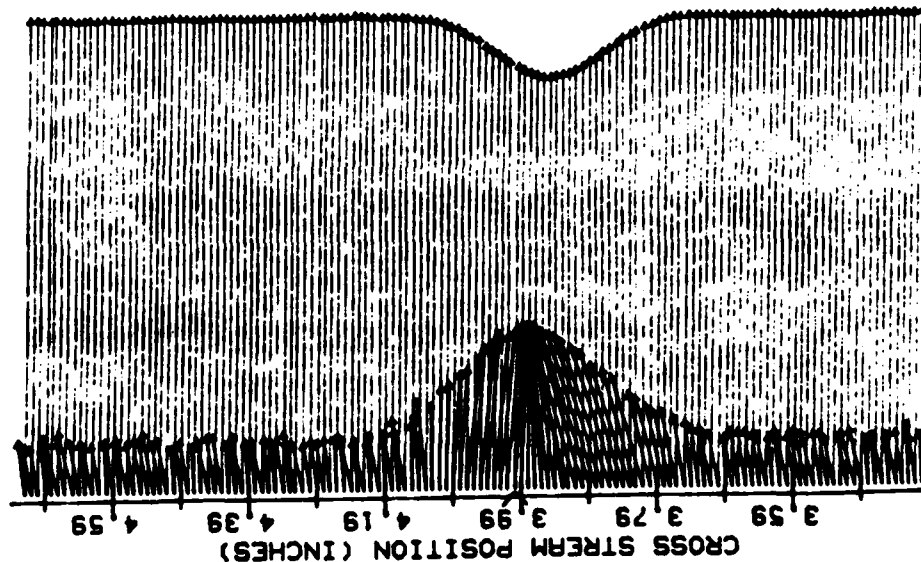
0 1 2 3
 SCALE (INCHES)

--- VEL. SCALE=167.00 (FT/SEC)/INCH
 --- % TURB INT SCALE= 8.00 % /INCH

DALET VEL= 488.24 +/- 9.08 FT/SEC
 CORRECTED DALET VELOCITY= 509 FT/SEC
 NOMINAL PLUM TURNING ANGLE= 17.5 DEG
 DALET WALL STRESSANCE PAIR= .05 INCH
 REF NO = 9 9 1 28
 DATE: 14 9 84 VRNE CONF: 14

Figure 26c. Velocity and Turbulence Intensity Profile Conf No. 14, Traverse No. 3

VANE WAKE: CONF. NO. 14, EVAL. NO. 1 Ra=25.5 micrometers
 TRAVERSE NO. 4.00 AT 3.25 INCHES



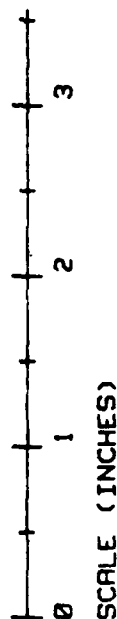
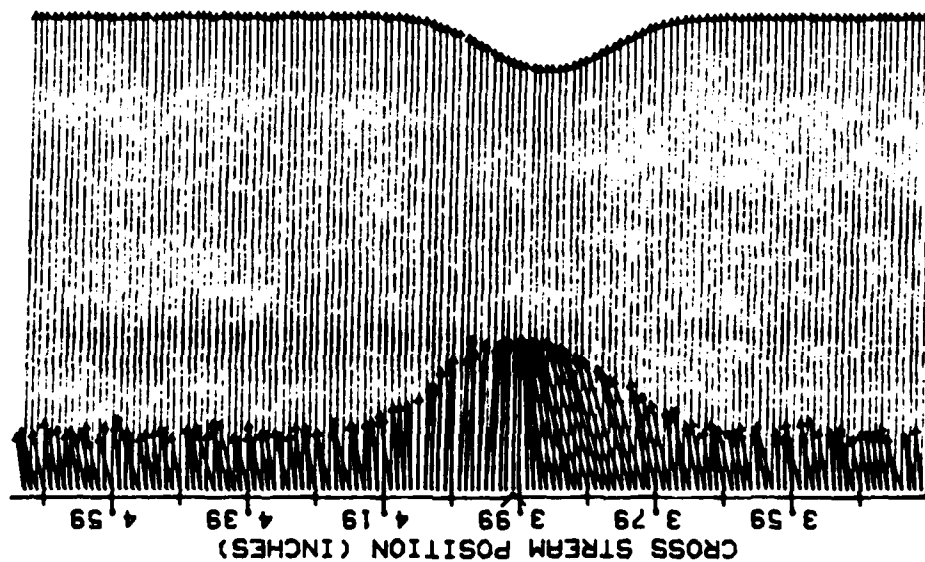
0 1 2 3
 SCALE (INCHES)

--- VEL. SCALE=167.00 (FT/SEC)/INCH
 --- % TURB INT SCALE= 8.00 % / INCH

INLET VEL. = 400.00 FT/SEC
 CORRECTED INLET VELOCITY = 17.5 FT/SEC
 NOMINAL PLUM TURBULENCE INT. = 17.5 %
 EXIT INLET VELOCITY = 17.5 FT/SEC
 EXIT INLET TURBULENCE INT. = 17.5 %
 DATE: 10 30 84, VANE CONF: 14

Figure 26d. Velocity and Turbulence Intensity Profile Conf No. 14, Traverse No. 4

VANE WAKE: CONF. NO.14, EVAL. NO.1 Ra=25.5 micrometers
 TRAVERSE NO. 5.00 AT 4.25 INCHES



— VEL. SCALE=167.00 (FT/SEC)/INCH
 --- % TURB INT SCALE= 8.00 %/INCH

INLET VEL= 489.84 +/- 0.00 FT/SEC
 CORRECTED INLET VELOCITY= 589 FT/SEC
 INITIAL FLUX TUBE NO. 17.5 SEC
 INITIAL FLUX TUBE NO. 17.5 SEC
 INITIAL FLUX TUBE NO. 17.5 SEC
 INITIAL FLUX TUBE NO. 17.5 SEC
 INITIAL FLUX TUBE NO. 17.5 SEC
 INITIAL FLUX TUBE NO. 17.5 SEC

Figure 26e. Velocity and Turbulence Intensity Profile Conf No. 14, Traverse No. 5

Bibliography

1. Allison, Dennis M. Design and Evaluation of a Cascade Test Facility, Unpublished MS Thesis, Wright-Patterson AFB, Ohio: Air Force Institute of Technology, June 1982.
- 2. Briggs, William R. Effect of Mach Number on the Flow and Application of Compressibility Effects in A Two-Dimensional Subsonic-Transonic Compressor Cascade Having Varied Porous-Wall Suction at the Blade Tips, Technical Note No. 2649, National Advisory Committee on Aeronautics.
3. Bullock, R. O. Analysis of Reynolds number and Scale Effects on Performance of Turbo machinery, ASME Series A Journal of Engineering for Power, 86:247, July 1964.
4. Erwin, John R., Emery, James C. "Effect of Tunnel Configuration and Testing Technique on Cascade Performance," Report No. 1016 National Advisory Committee on Aeronautics, 263-277, 1951.
5. Fottner, L., Schaffler, A. AGARD 175, Neuilly sur Seine, France; AGARD 1976.
6. Genovese, David T. Roughness Effects on Compressor Outlet Guide Vanes at High Reynolds Number and High Angle of Attack, Unpublished MS Thesis. Wright-Patterson AFB, Ohio: Air Force Institute of Technology, December 1982.
7. Keenan, Joseph H., Kay, Joseph. Gas Tables, New York; John Wiley & Sons, Inc., 1948.
8. Koch, C. C., Smith, L. H. Jr. "Loss Sources and Magnitudes in Axial Flow Compressors," Journal of Engineering for Power, 411-424, July 1976.
9. Lieblein, Seymor, Roudebush, William H. Low Speed Wake Characteristics of Two-Dimensional Cascade and Isolated Airfoil Sections, Technical Note 3771, National Advisory Committee on Aeronautics, October 1956.
10. Nikuradse, J. Turbulente Reibungsschichten an der Platte, Munchen and Berlin; ZWB, 1942.
11. Peacock, R. E. Boundary Layer Suction to Eliminate Corner Separation in Cascades of Aerofoils, A.R.C. R.&M. No. 3663, University Engineering Department, Cambridge, October 1965, (AD 90037).

12. Schaffler, A. "Experimental and Analytical Investigation of the Effects of Reynolds Number and Blade Surface Roughness on Multistage Axial Flow Compressors," ASME Journal of Engineering for Power, 102:5-13 January 1980.
13. Schlichting, Hermann. Boundary Layer Theory, Seventh Edition, New York; McGraw-Hill, 1979.
14. Scholz, Norbert. Aerodynamics of Cascades, AG220, Neuilly sur Seine, France; AGARD, 1977.
15. Tanis, Frederick J. Roughness Effect on Compressor Blade Performance in Cascade at High Reynolds Number, Unpublished MS Thesis. Wright-Patterson AFB, Ohio: Air Force Institute of Technology, November 1983.
16. Taylor, Hobson. Surtronic 3 Operating Instructions. Leichester, England: Rank Taylor Hobson, (undated).
17. Vincent, Edward T. The Theory and Design of Gas Turbines and Jet Engines, New York; McGraw-hill, 1950.
18. Vonada, John A. and Elrod, William C., Allison, Dennis M. Wake Mixing Investigation of Crenelated Trailing Edge Blades in Cascade, Proceedings, AIAA Ninth Annual Mini-Symposium on Aerospace Science and Technology. Wright-Patterson AFB, Ohio: Air Force Institute of Technology, 22 March 1983.
19. Wassell, A. B., "Reynolds Number Effects in Axial Compressors," ASME Journal of Engineering for Power, 149-156, April 1968.
20. -----, The Pall Porous Metal Filter Guide, Pall Corporation, 1982.
21. Wennerstrom, A. J. Personal interview, AFWAL, Wright-Patterson AFB, Ohio, 1 Nov 1984.

VITA

Captain Gary P. Moe was born on 9 March 1955 in North Hollywood, California. In 1972 he attended the University of California, Berkeley from which he received the degree of Bachelor of Science in Mechanical Engineering in June 1976. Upon graduation, he received a commission in the USAF through the ROTC program. He was employed as a research assistant for the Electrical Engineering Department, Texas Tech University, Lubbock, Texas until called to active duty in May 1977. He completed pilot training and received his wings in May 1978. Captain Moe then served as a KC-135 copilot and aircraft commander in the 97th Air Refueling Squadron, Blytheville AFB, Arkansas, until entering the School of Engineering, Air Force Institute of Technology, in June 1983. He is a member of Tau Beta Pi.

Permanent address:

4325 Sonoma Mtn. Road
Santa Rosa, CA 95404

UNCLASSIFIED

SECURITY CLASSIFICATION OF THIS PAGE

REPORT DOCUMENTATION PAGE

1a. REPORT SECURITY CLASSIFICATION UNCLASSIFIED			1b. RESTRICTIVE MARKINGS										
2a. SECURITY CLASSIFICATION AUTHORITY			3. DISTRIBUTION/AVAILABILITY OF REPORT Approved for public release; distribution unlimited.										
2b. DECLASSIFICATION/DOWNGRADING SCHEDULE													
4. PERFORMING ORGANIZATION REPORT NUMBER(S) AFIT/GAE/AA/84D-19			5. MONITORING ORGANIZATION REPORT NUMBER(S)										
6a. NAME OF PERFORMING ORGANIZATION School of Engineering		6b. OFFICE SYMBOL (If applicable) AFIT/ENY		7a. NAME OF MONITORING ORGANIZATION									
6c. ADDRESS (City, State and ZIP Code) Air Force Institute of Technology Wright-Patterson AFB, OH 45433		7b. ADDRESS (City, State and ZIP Code)											
8a. NAME OF FUNDING/SPONSORING ORGANIZATION		8b. OFFICE SYMBOL (If applicable)		9. PROCUREMENT INSTRUMENT IDENTIFICATION NUMBER									
8c. ADDRESS (City, State and ZIP Code)		10. SOURCE OF FUNDING NOS. <table border="1"><tr><td>PROGRAM ELEMENT NO.</td><td>PROJECT NO.</td><td>TASK NO.</td><td>WORK UNIT NO.</td></tr><tr><td></td><td></td><td></td><td></td></tr></table>				PROGRAM ELEMENT NO.	PROJECT NO.	TASK NO.	WORK UNIT NO.				
PROGRAM ELEMENT NO.	PROJECT NO.	TASK NO.	WORK UNIT NO.										
11. TITLE (Include Security Classification) See Box 19													
12. PERSONAL AUTHOR(S) Moe, Gary Patrick, B.S., Capt, USAF													
13a. TYPE OF REPORT MS Thesis		13b. TIME COVERED FROM _____ TO _____		14. DATE OF REPORT (Yr., Mo., Day) 1984 December									
15. PAGE COUNT 112													
16. SUPPLEMENTARY NOTATION													
17. COSATI CODES <table border="1"><tr><th>FIELD</th><th>GROUP</th><th>SUB. GR.</th></tr><tr><td>21</td><td>05</td><td></td></tr></table>			FIELD	GROUP	SUB. GR.	21	05		18. SUBJECT TERMS (Continue on reverse if necessary and identify by block number) Cascade Testing, Two-Dimensional Flow Compressor Blades, Roughness Effects, Boundary Layer				
FIELD	GROUP	SUB. GR.											
21	05												
19. ABSTRACT (Continue on reverse if necessary and identify by block number) Thesis Title: INFLUENCE OF SURFACE ROUGHNESS ON COMPRESSOR BLADES AT HIGH REYNOLDS NUMBER IN A TWO-DIMENSIONAL CASCADE Advisor: Dr. William C. Elrod <div style="text-align: right;"><i>Approved for public release</i> <i>under AFR 130-17</i> <i>LYNN E. WOLLAVER</i> <i>21 Feb 85</i> Dean for Research and Professional Development Air Force Institute of Technology (AFIT) Wright-Patterson AFB OH 45433</div>													
20. DISTRIBUTION/AVAILABILITY OF ABSTRACT UNCLASSIFIED/UNLIMITED <input checked="" type="checkbox"/> SAME AS RPT. <input type="checkbox"/> DTIC USERS <input type="checkbox"/>			21. ABSTRACT SECURITY CLASSIFICATION UNCLASSIFIED										
22a. NAME OF RESPONSIBLE INDIVIDUAL William C. Elrod		22b. TELEPHONE NUMBER (Include Area Code) 513-255-3517		22c. OFFICE SYMBOL AFIT/ENY									

DD FORM 1473, 83 APR

EDITION OF 1 JAN 73 IS OBSOLETE.

UNCLASSIFIED

SECURITY CLASSIFICATION OF THIS PAGE

A cascade test facility has been established which incorporates sidewall boundary layer control, permitting two-dimensional flow investigation over the center span (about $2/3$ the width of the blade) of an airfoil in cascade, and an investigation has been conducted to determine the influence of roughness on the airfoil. Two representative compressor profiles, the NACA 64-A905 and 65-A506, with two inch chords and aspect ratios of one were tested at airflow inlet velocities comparable to those in axial flow compressors. An Axial Velocity Density Ratio of unity was the criterion used to determine when two-dimensional flow was achieved.

Test results indicate that initial small increases of roughness have a much greater effect on blade total pressure loss than do subsequent larger roughness values. A small increase in roughness produces a substantial increase in free stream turbulence with practically no effect on the wake. Further increase in roughness produces a substantial effect on the wake but little effect on the free stream turbulence. Surface roughness is shown to have a much greater influence on blade wake turbulence intensity for the higher camber airfoils tested than for lower camber airfoils.

END

FILMED

4-85

DTIC